AMAP Technical Report No. 4 (2011)

The Impact of Black Carbon on Arctic Climate

P.K. Quinn, A. Stohl, A. Arneth, T. Berntsen, J. F. Burkhart, J. Christensen, M. Flanner, K. Kupiainen, H. Lihavainen, M. Shepherd, V. Shevchenko, H. Skov, and V. Vestreng

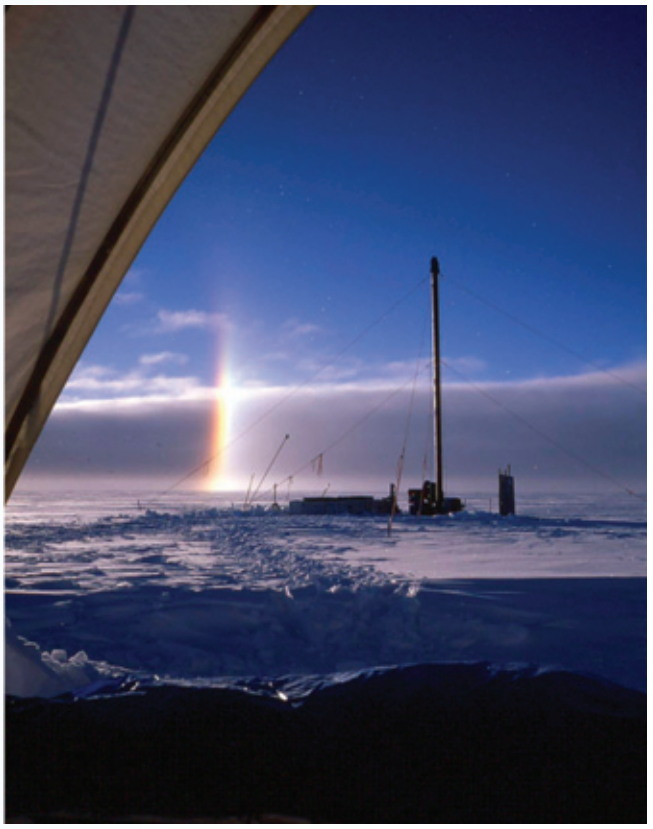

AMAP
Arctic Monitoring and Assessment Programme

Citation: AMAP, 2011. The Impact of Black Carbon on Arctic Climate (2011). By: P.K. Quinn, A. Stohl, A. Arneth, T. Berntsen, J. F. Burkhart, J. Christensen, M. Flanner, K. Kupiainen, H. Lihavainen, M. Shepherd, V. Shevchenko, H. Skov, and V. Vestreng. Arctic Monitoring and Assessment Programme (AMAP), Oslo. 72 pp.

ISBN – 978-82-7971-069-1

Available as an electronic document from www.amap.no

Authors/AMAP Short-lived Climate Forcers Expert Group
P.K. Quinn[1], A. Stohl[2], A. Arneth[3], T. Berntsen[4], J. Burkhart[2], J. Christensen[5], M. Flanner[6], K. Kupiainen[7,8], H. Lihavainen[9], M. Shepherd[10], V. Shevchenko[11], H. Skov[5], and V. Vestreng[12]

[1]NOAA Pacific Marine Environmental Laboratory, Seattle, WA, USA
[2]Norwegian Institute for Air Research, Kjeller, Norway
[3]Lund University, Lund, Sweden
[4]University of Oslo, Oslo, Norway
[5]Aarhus University, Roskilde, Denmark
[6]University of Michigan, Ann Arbor, Michigan, USA
[7]Finnish Environment Institute, Helsinki, Finland
[8]International Institute for Applied Systems Analysis, Vienna, Austria
[9]Finnish Meteorological Institute, Helsinki, Finland
[10]Environment Canada, Toronto, Canada
[11]P.P. Shirshov Insitute of Oceanology of the Russian Academy of Sciences, Moscow, Russia
[12]Norwegian Pollution Control Authorities, Oslo, Norway

AMAP Short-lived Climate Forcers Expert Group
Chairs: Patricia K. Quinn (USA), Andreas Stohl (Norway)
Scientific Secretary: John F Burkhart

Editing: Kristine Aasarød, Ann-Christine Engvall Stjernberg

Production: Carolyn Symon (carolyn.symon@btinternet.com), John Bellamy (johnbellamy@swipnet.se)

Printing: Narayana Press, Denmark (a swan-labelled printing company, 541 562)

Cover photo: Collecting the 'Summit 99' ice core at Summit, Greenland

The Arctic Monitoring and Assessment Programme (AMAP) was established in June 1991 by the eight Arctic countries (Canada, Denmark, Finland, Iceland, Norway, Russia, Sweden and the United States) to implement parts of the Arctic Environmental Protection Strategy (AEPS). AMAP is now one of six working groups of the Arctic Council, members of which include the eight Arctic countries, the six Arctic Council Permanent Participants (indigenous peoples' organizations), together with observing countries and organizations.

AMAP's objective is to provide 'reliable and sufficient information on the status of, and threats to, the Arctic environment, and to provide scientific advice on actions to be taken in order to support Arctic governments in their efforts to take remedial and preventive actions to reduce adverse effects of contaminants and climate change'.

AMAP produces, at regular intervals, assessment reports that address a range of Arctic pollution and climate change issues, including effects on health of Arctic human populations. These are presented to Arctic Council Ministers in 'State of the Arctic Environment' reports that form a basis for necessary steps to be taken to protect the Arctic and its inhabitants.

AMAP technical reports are intended to communicate the results of scientific work that contributes to the AMAP assessment process. This report has been subject to a formal and comprehensive peer review process. The results and any views expressed in this series are the responsibility of those scientists and experts engaged in the preparation of the reports and have not been approved by either the AMAP working group or the Arctic Council.

AMAP would like to express its appreciation to the Nordic Council of Ministers, Norway, Canada and the USA for their financial support and to sponsors of projects that have delivered data for use in this technical assessment.

The AMAP Secretariat is located in Oslo, Norway. For further information regarding AMAP or ordering of reports, please contact the AMAP Secretariat (PO Box 8100 Dep., N-0032 Oslo, Norway) or visit the AMAP website at www.amap.no.

Contents

1. Introduction

The Arctic Monitoring and Assessment Programme (AMAP) established an Expert Group on Short-Lived Climate Forcers (SLCFs) in 2009 with the goal of reviewing the state of science surrounding SLCFs in the Arctic and recommending the science tasks that AMAP should conduct or promote to improve the state of knowledge and its application to policy-making. In addition, the Expert Group was charged with providing scientific advice regarding the assessment of Arctic climate benefits of the mitigation strategies investigated by the Task Force on SLCFs established by the Arctic Council. This document is a result of the work completed by the AMAP Expert Group on SLCFs. It focuses on black carbon (BC) but also considers the impact of co-emitted organic carbon (OC). The analyses are focused on Arctic impacts with the Arctic defined as all regions north of 60° N. This limited perspective is not meant to downplay the importance of the other SLCFs, including methane (CH_4) and ozone (O_3), but reflects the limited time line provided by AMAP and the expertise of the membership of the Expert Group. Future efforts that detail impacts of CH_4 and O_3 on Arctic climate are recommended.

Arctic temperatures have increased at almost twice the global average rate over the past 100 years (IPCC, 2007; AMAP, 2011). From 1954 to 2003, annual average surface air temperatures increased from 2 to 3 °C in Alaska and Siberia. The increase during the winter months has been up to 4 °C (ACIA, 2004). In the period since the completion of the Arctic Climate Impact Assessment in 2004 (ACIA, 2004), the Arctic has experienced its highest surface air temperatures of the instrumental record (AMAP, 2011). Warming in the Arctic has been accompanied by an earlier onset of spring melt, a lengthening of the melt season, and changes in the mass balance of the Greenland Ice Sheet (Zwally et al., 2002; Stroeve et al., 2006, AMAP, 2011). In addition, Arctic sea-ice extent decreased in every month between 1979 and 2006 (Serreze et al., 2007a). During the 2007 melt season, Arctic sea-ice extent fell to the lowest levels observed since satellite measurements began in 1979, resulting in the first recorded complete opening of the Northwest Passage (NSIDC, 2007). Arctic sea-ice extent for September 2010 was the third lowest in the satellite record for the month behind 2007 (lowest) and 2008 (second lowest) (NSIDC, 2010) (Figure 1.1). Both the Northwest Passage and the Northern Sea Route were open for a period during September 2010. The Norwegian trimaran *Northern Passage* and the Russian yacht *Peter I* each successfully navigated both passages and circumnavigated the Arctic in a single season.

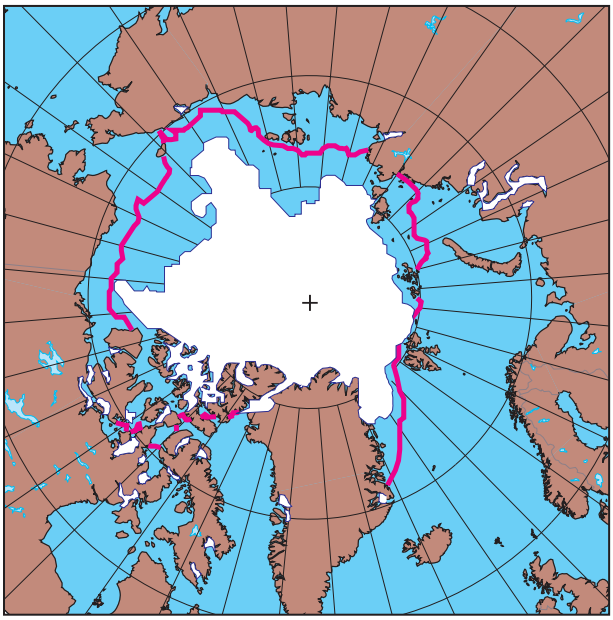

Figure 1.1. Arctic sea-ice extent for September 2010. The magenta line shows the 1979 to 2000 median extent for that month. The black cross indicates the geographic North Pole. Source: National Snow and Ice Data Center.

Overall, the 2001–2010 average September monthly sea-ice extent is 5.56 million km^2; 21.0% below the 1979–2000 average of 7.04 million km^2. The trend over the ten-year period is -201 000 km^2 per year (-28.5% per decade relative to the 1979–2000 average) (AMAP, 2011).

Impacts of ice loss include reduction in the Earth's albedo; a positive feedback that leads to further warming. As the sun rises in the spring, temperatures increase, and snow on the surface begins to melt leading to the exposure of bare sea ice, melting ponds and, with continued melting, ocean water. Exposing the underlying dark surfaces leads to a decrease in albedo, an increase in the absorption of solar energy, and further warming. The result, a snow-albedo feedback, is one of the reasons that the Arctic is highly sensitive to changes in temperature. The earlier onset of spring melt observed in recent years is of particular concern as this is the season of maximum snow-albedo feedback (e.g., Hall and Qu, 2006).

Timescales for a collapse of the Greenland Ice Sheet and a transition to a seasonally ice-free Arctic are highly uncertain, as are the regional and global impacts. However, clear ecological signals of significant and rapid response to these changes within the Arctic are already present. For example, paleolimnological data from across the Arctic have recorded striking changes in diatoms and other bioindicators corresponding to conditions of

decreased ice cover and warming (Smol et al., 2005). Circumpolar vegetation is also showing signs of rapid change, including an expansion of shrub and tree coverage (Chapin et al., 2005). An earlier snowmelt on land in Arctic and alpine tundra will have direct and substantial impacts on plant primary production. A two-week prolongation of the growing season in May (when global radiation influx is at maximum) will potentially result in a 15–25% increase in productivity (whereas a similar prolongation in September/October has no effect as light quality is inferior for photosynthesis) (Björk and Molau, 2007). However, the major proportion of that increase in tundra plant biomass will be accounted for by invasive boreal species (e.g., birch, willow, blueberry, certain grasses), outcompeting the resident Arctic specialist species (Sundqvist et al., 2008). This shift in plant biodiversity will have immediate negative impacts on animal biodiversity, which, in turn, implies large shifts in the lifestyle of indigenous peoples and for activities such as tourism and reindeer husbandry. This ongoing 'shrubbification' has already been documented to occur in the Arctic and subarctic parts of Alaska and Scandinavia (Walker et al., 2006). Reduction in sea ice is also likely to be devastating for polar bears, ice-dependent seals, and people who depend on these animals for food (ACIA, 2004). Warming of the Arctic will also impact the planet as a whole (ACIA, 2004) as melting of Arctic glaciers is one of the factors contributing to sea-level rise around the world and weakening of the thermohaline circulation. Recent research has suggested that loss of Arctic sea ice can also impact atmospheric circulation patterns over much of the Northern Hemisphere (Overland and Wang, 2010).

Arctic warming is a manifestation of global warming, such that reducing global-average warming will reduce Arctic warming and the rate of melting (IPCC, 2007). Reductions in the atmospheric burden of carbon dioxide (CO_2) are the backbone of any meaningful effort to mitigate climate forcing. But even if swift and deep reductions were made, given the long lifetime of CO_2 in the atmosphere, the reductions may not be achieved in time to delay a rapid thawing of the Arctic. Hence, the goal of constraining the length of the melt season and, in particular, delaying the onset of spring melt, may best be achieved by also targeting shorter-lived climate forcing agents; especially those that impose a surface forcing that may trigger regional scale climate feedbacks pertaining to the melting of sea ice.

CH_4, O_3, and BC-containing aerosols are the species commonly identified as being short-lived climate forcers. With a lifetime of about nine years (Prinn et al., 1995), CH_4 is much shorter lived than CO_2 but is still globally well-mixed. On a per molecule basis, CH_4 is a more effective greenhouse gas (GHG) than CO_2 (IPCC, 2001). Radiative forcing by CH_4 results directly from the absorption of longwave radiation and indirectly through chemical reactions that lead to the formation of other radiatively important gases (Wuebbles and Hayhoe, 2002). Tropospheric O_3 is also a GHG and can affect Arctic climate by altering local radiation fluxes and modulating the transport of heat to the polar region (Shindell, 2007).

BC is the most efficient atmospheric particulate species at absorbing visible light. As a result, it exerts a warming effect that contrasts with the cooling effect of purely scattering aerosol components. Pure BC particles rarely occur in the atmosphere, however. Soon after emission, BC becomes mixed with other aerosol chemical components such as sulfate and organics. BC-containing aerosols can have either a warming effect or a cooling effect on climate depending on the albedo of the underlying surface relative to the albedo of the BC haze itself. The albedo of the haze depends on what other chemical species are present, their relative amounts, and whether they primarily scatter or absorb light. As a result, when determining the climate impact of BC and the effectiveness of a given mitigation strategy, species co-emitted with BC (e.g., OC and SO_2) must be taken into account.

BC-containing aerosols in the Arctic can perturb the radiation balance in a number of ways (see Figure 1.2). Direct aerosol forcing (rightmost column in Figure 1.2) occurs through absorption or scattering of solar (shortwave) radiation by aerosols. An absorbing aerosol, such as one containing BC, over a highly reflective surface will result in a warming at altitudes above and within the haze layer (Shaw and Stamnes, 1980). The added atmospheric heating will subsequently increase the downward longwave radiation to the surface, warming the surface. With the highly reflective surfaces typical of the Arctic springtime, even a moderately absorbing aerosol can lead to a heating of the surface-atmosphere-aerosol column.

Radiative forcing by BC can also result from aerosol-cloud interactions. The aerosol first indirect effect in the shortwave (middle right column in Figure 1.2) occurs when pollution particles lead to an increase in cloud droplet number concentration, a decrease in the size of the droplets, a corresponding increase in shortwave cloud albedo, and a cooling at the surface (Twomey, 1977). Measurements made at Barrow, Alaska over a four-year period indicate that pollution transported to the Arctic produces high cloud drop number concentrations and small cloud drop effective radii in low-level cloud microstructures (Garrett

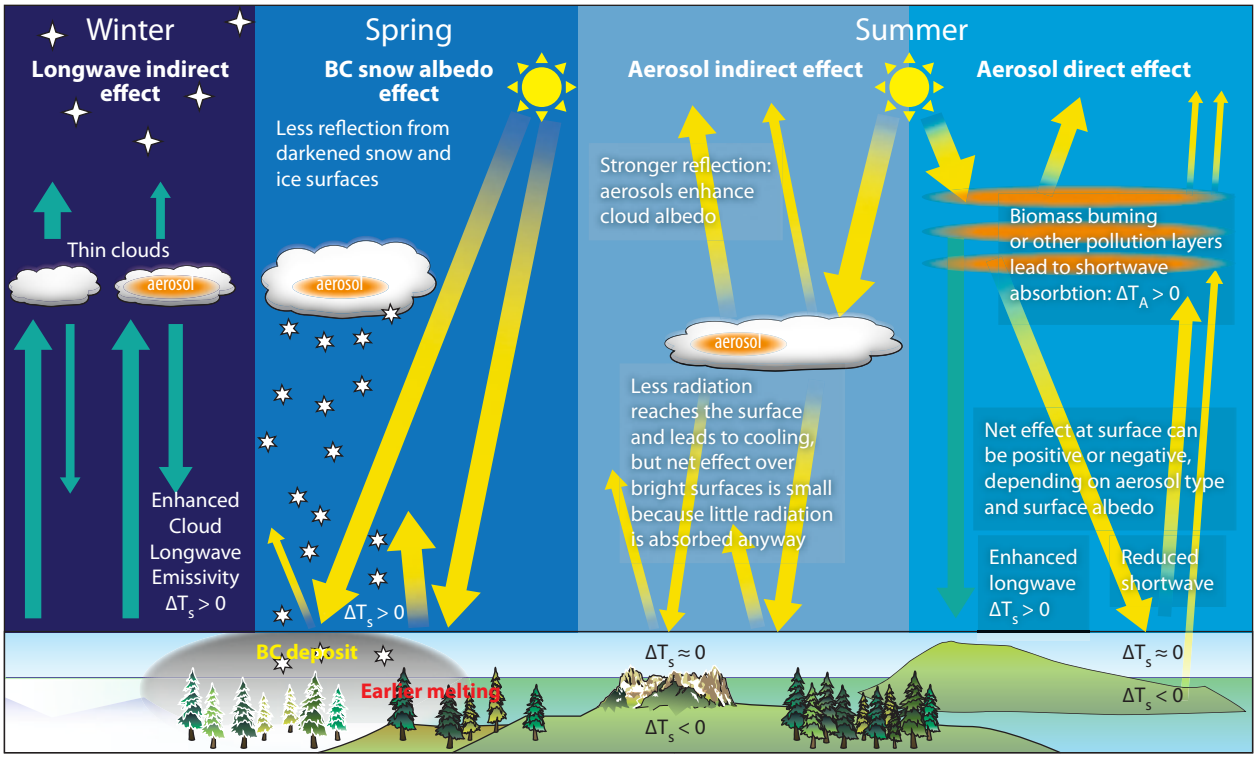

Figure 1.2. Forcing mechanisms in the Arctic due to short-lived pollutants. ΔT_s indicates the surface temperature response.

et al., 2004). Measurements and global modeling studies indicate that carbonaceous aerosols have a significantly larger impact on cloud albedo than sulfate aerosols (Lohmann et al., 2000; Chuang et al., 2002; Leaitch et al., 2010). Aerosol-cloud interactions can also lead to a significant longwave forcing and warming at the surface (leftmost column in Figure 1.2). When the cloud drop number concentration of thin Arctic liquid-phase clouds is increased through interaction with anthropogenic aerosols, the clouds become more efficient at trapping and re-emitting longwave radiation (Garrett and Zhao, 2006).

BC-containing aerosol has an additional forcing mechanism when it is deposited to snow and ice surfaces (Clarke and Noone, 1985). Such deposition enhances absorption of solar radiation at the surface which can warm the lower atmosphere and induce snow and ice melting (middle left column in Figure 1.2). The BC snow/ice forcing mechanism is *in addition* to the stronger snow-albedo feedback process. Snow-albedo feedback is driven by the melting of snow and loss of sea ice exposing darker surfaces and enhancing absorption of radiation and surface warming. Surface temperature responses are strongly linked to surface radiative forcings in the Arctic because the stable atmosphere of the region prevents rapid heat exchange with the upper troposphere (Hansen and Nazarenko, 2004).

In light of the many atmospheric processes altering the properties and lifetime of BC, the potential for transport of BC to the Arctic and deposition to reflective surfaces, and the multiple forcing mechanisms, it is necessary to consider the entire source-climate response spectrum in order to establish the impact of changing emissions and the effectiveness of mitigation action. Figure 1.3 illustrates the opportunities and challenges in characterizing BC impacts on Arctic climate. The figure makes clear the need to quantify how changes in emissions affect atmospheric concentrations and surface albedo, and how these changes relate to the specific climate response (changing temperature, snow/ice cover and precipitation) using models. There is no single BC indicator that directly relates to the climate response.

The remaining parts of this report include a review of the most recent literature as well as results of model calculations undertaken for this assessment. Section 2 reviews the chemical, physical, and optical properties of BC that make it a short-lived climate forcer. The methods used for measuring BC and modeling its transport to the Arctic and radiative forcing are reviewed in Section 3. Emissions of BC as a function of energy sector and geographical region are addressed in Section 4. Transport of BC to the Arctic is reviewed in Section 5 and seasonality and trends of Arctic BC concentrations are reviewed in Section 6. Estimates of the radiative forcing due to specific sources (by energy sector and geographical region) are presented in the latter half of the report

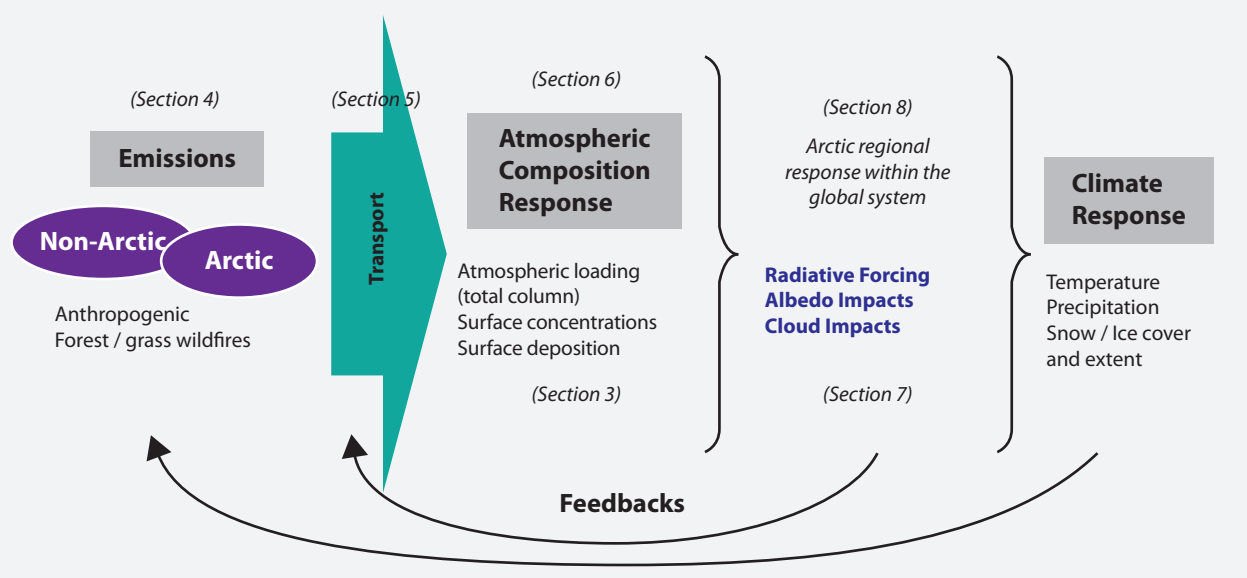

Figure 1.3. Conceptual model of the links between BC emissions and Arctic climate response. The sections in the text that describe each part of the figure are indicated.

(Sections 7 and 8). This analysis takes into account BC and co-emitted OC with the goal of identifying the sources that have the largest potential impact on Arctic climate. The report concludes with two sections addressing knowledge gaps and recommendations for future research.

2. Formation and properties of black carbon

Black carbon is uniquely identifiable among all particulate phase species due to its morphology, strong absorption of solar radiation, refractory nature (stability at high temperatures), and insolubility in water. BC is a product of the combustion of hydrocarbon-based fuels when there is not enough oxygen to yield a complete conversion of the fuel into CO_2 and water. Through the combustion process, small graphitic particles of the order of tens of nanometers in size are formed (Slowik et al., 2004). These particles change rapidly after emission as they collapse into densely packed clusters (Martins et al., 1998) and take up water and other gas phase species also emitted during combustion.

Size distributions of BC-containing aerosol are a function of the production mechanism of the aerosol and atmospheric processing that has occurred since emission. Newly emitted BC particles resulting from combustion are found primarily in the submicrometer size range. Measurements of aircraft exhaust immediately after emission reveal a primary BC mode with a diameter around 30 nm and a larger mode of BC particles with a diameter of ~150 nm (Petzold et al., 1999). Schwarz et al. (2008) reported measurements of BC cores in fresh urban and biomass burning plumes using a single particle soot photometer or SP2. As described in Section 3, the SP2 is able to measure the size of BC cores in the 90 to 600 nm size range as well as the fraction of the number of BC particles with associated coatings. Shiraiwa et al. (2008) made similar measurements in aged plumes in Asian outflow. BC cores in urban plumes were found to have mass geometric diameters of 170 nm while BC cores in aged Asian plumes were larger in size at 200 to 220 nm. The larger size in aged plumes suggests growth via coagulation during transport away from the source region. BC cores in biomass burning plumes were similar to those in aged urban plumes with a size of 210 nm.

Coal piles, such as have been reported to exist in Svalbard (Myhr, 2003) may also provide a local source of BC-containing particles to the Arctic. The wind-driven production of coal dust results in considerably larger particles than combustion (Ghose and Majee, 2007). Sedimentation rates increase with particle size so that particles larger than about 10 μm in diameter have much shorter lifetimes than submicrometer particles (hours versus

days). In addition, the absorption coefficient per unit mass decreases with particle size for diameters larger than about 200 nm (Bergstrom, 1973). From a climate perspective, these large coal dust particles are expected to have a localized effect on climate through the BC-snow albedo forcing mechanism. Their short lifetime limits their impact through atmospheric forcing. Hence, the following discussion focuses on BC particles derived from combustion.

After emission, combustion particles coagulate with each other and react with particles and gases in the surrounding atmosphere. Measurements indicate that the uptake of gas phase species, coagulation, and atmospheric reactions occur of the order of hours after emission. For example, measurements made downwind of Japan showed that BC particles became internally mixed with other aerosol components (e.g., sulfate and OC) on a time scale of 10 hours in an urban plume (Moteki et al., 2007). As a result, pure BC particles are rarely observed in the atmosphere. The impact of the rapid processing of BC after emission on the composition of the resulting BC-containing particles, their optical and cloud nucleating properties, and their lifetime are described below.

The composition of combustion particles depends, in part, on the fuel burned. Fossil fuel combustion results in emissions of BC and OC with a relatively high ratio of BC to OC mass concentration. Sulfate is also emitted. Combustion of biomass (wood, solid waste, forest, grass) also results in the emission of BC and OC but with a lower ratio of BC to OC mass concentration. Other particulate species such as potassium and ammonium are also emitted. Combustion of fossil fuel and biomass also results in the emission of gas phase species including SO_2, NOx, CO, and volatile organic carbon species. The composition of the co-emitted species as well as the air masses the combustion particles encounter during transport affect the way in which the BC ages, including its degree of hygroscopicity (i.e., ability to take up water), its ability to nucleate cloud droplets, and its absorption and scattering of solar radiation. The properties acquired during the aging process determine the atmospheric lifetime of the BC-containing aerosol.

BC is hydrophobic upon emission but becomes increasingly hydrophilic, or hygroscopic, as it takes up gases, coagulates with nearby particles, and undergoes atmospheric reactions with species in the surrounding atmosphere (e.g., Abel et al., 2003). A recent review of observations of aerosol hygroscopicity from remote and urban regions showed that hydrophobic particles are found only near emission sources (Swietlicki et al., 2008). These results confirm that the lifetime of hydrophobic particles (which are indicative of BC) is of the order of hours. As BC-containing aerosol becomes more hydrophilic, its chances of removal from the atmosphere through in-cloud scavenging and precipitation increase (Stier et al., 2006). Hence, the conversion of BC-containing particles from hydrophobic to more hydrophilic changes the lifetime of BC. At the same time, the BC-containing particles may alter cloud properties.

The ability of an aerosol particle to take up water to the point that it activates and forms a cloud droplet depends on its size and composition (or hygroscopicity) and the supersaturation within the cloud. At high supersaturations, most particles will activate droplet formation regardless of size or composition. For the relatively low supersaturations of Arctic stratiform clouds, small hydrophobic particles will not form cloud droplets (Shaw, 1986). Hence, freshly emitted BC particles, which are both small and hydrophobic, will make very poor nucleation sites for cloud droplets. In contrast, aged BC particles, which have grown in size and become more soluble since emission, will have an increased ability to nucleate cloud droplets. Measurements of BC particles in Tokyo showed that the number of BC particles able to nucleate cloud droplets increased as the amount of soluble material condensed upon the BC increased (Kuwata et al., 2007). Hence, the aging of BC during transport to the Arctic (Figure 2.1) is expected to affect its ability to form cloud droplets and influence cloud properties and aerosol indirect forcing.

As will be discussed in more detail in Section 5, the time for transport of BC from extra-Arctic source regions to the Arctic is typically of the order of several days to weeks (e.g., Heidam et al., 2004). This timeframe can be appreciably longer than the time for 'aging' or conversion to a hydrophilic particle. Whether BC emitted in lower latitudes is transported to and deposited within the Arctic depends, in part, on atmospheric processing en route and whether it is removed from the atmosphere before it reaches the Arctic, as well as cloud conditions in the Arctic itself. Accurately modeling the transport of BC to the Arctic is difficult as there is considerable uncertainty associated with the timescales of atmospheric processes that transform freshly emitted, near hydrophobic particles into less hydrophobic and eventually more hygroscopic aerosol particles (Swietlicki et al., 2008). The prescribed time for

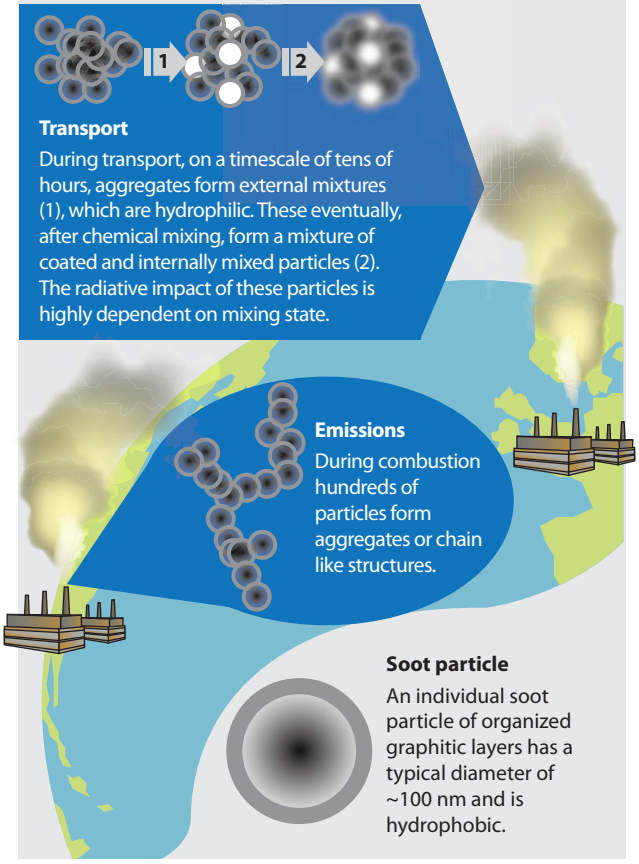

Figure 2.1. Conceptual overview of the evolution of BC particles during transport to the Arctic.

conversion of BC particles from hydrophobic to hydrophilic varies between models but is typically a day or less (e.g., Park et al., 2005). This timescale agrees with recent measurements but a uniform value or even values that are allowed to vary within a model based on coincident concentrations of soluble species cannot account for all processes affecting hygroscopicity.

The transformations undergone by BC after emission also have implications for the magnitude of light absorption by the resulting internally mixed aerosol. It has been shown theoretically that light absorption by an absorbing core is enhanced when coated with scattering material (Fuller et al., 1999). The scattering shell serves to amplify the amount of solar radiation hitting the BC core. Calculations indicate that the core-shell configuration enhances light absorption by the particles by up to 50–100% (e.g., Bond et al., 2006; Shiraiwa et al., 2008). Absorption enhancements due to coating of BC cores have also been observed experimentally (e.g., Schnaiter et al., 2005; Zhang et al., 2008).

Methods for measuring mass concentrations of BC and OC and the light absorption due to BC are described in Section 3. The section also includes a description of methods for modeling the transport of BC to the Arctic and the resulting distributions of BC in the Arctic environment.

3. Measurement and modeling of black carbon concentrations

3.1. Overview of BC measurements

Measurements of BC in the Arctic and in its source regions are needed to characterize BC as it is transformed from a hydrophobic, single component aerosol to an internally mixed, hydrophilic aerosol. In addition, observations of BC are required to develop, assess, and improve emission inventories, transport models, and mitigation strategies designed to reduce the warming of the Arctic. The systematic observation of aerosols, including BC, is expanding globally through a host of national and international sampling networks. Parts of the mid-latitude source regions for the Arctic are well monitored, particularly in regions where there are public health concerns. It is anticipated that monitoring in these regions will continue to expand as mitigation policies for both air quality and climate focus on BC. In contrast, there are only a few long-term observations of BC in the Arctic. These are confined to the North American and European sectors of the Arctic and, as a result, do not give a full picture of BC atmospheric burdens in the Arctic or long-term trends.

Long-term monitoring observations and short-term intensive field campaigns have both provided information on the sources, transport, and properties of Arctic BC. A small number of atmospheric monitoring sites have provided the majority of long-term information on BC and other aerosol chemical components in the Arctic atmosphere. These include Alert (82.46° N) in the Canadian Arctic, Barrow in Alaska (71.3° N), Station Nord in Greenland (81.4° N),

both Ny Alesund and Zeppelin (79° N) on the island of Svalbard, and recently Summit, Greenland (78° N). Table 3.1 gives a complete listing of aerosol monitoring sites and measurements in the Arctic. Historically, there has been a lack of published, long-term observations of BC in the eastern Arctic. Intensive field campaigns that have provided snapshot, detailed pictures of BC transported to the Arctic include the AGASP (Arctic Gas and Aerosol Sampling Programs) series (e.g., Schnell, 1984) conducted in the western Arctic in the 1980s and the many international experiments conducted under the umbrella of POLARCAT (Polar Study using Aircraft, Remote Sensing, Surface Measurements and Models of Climate, Chemistry, Aerosols, and Transport) (e.g., Spackman et al., 2010) during the International Polar Year (IPY) in 2008. Over this same span of years, a few studies have also been conducted on BC deposited to Arctic snow and ice. In the early 1980s, Clarke and Noone (1985) focused on BC deposited to the western Arctic. Recently, Doherty et al. (2010) reported measurements that updated and expanded the initial survey of Clarke and Noone. This more recent study was conducted from 2005 to 2009 with snow collection in Alaska, Canada, Greenland, Svalbard, Norway, Russia, and the Arctic Ocean (Figure 3.1). However, while visually the spatial coverage of these data appears broad, the number of samples is quite

Table 3.1. Long-term systematic observations in the Arctic, north of 60° N.

Country/site	Location	MSL	Physical properties		Optical properties		Chemical inorganic speciation		
			No. concentration	No. size distribution	Light absorption	Light scattering	Integrated filter	Continuous	Direct carbon[a]
United States									
Barrow	71.32°N, 156.6°W	11	✓	✓	✓	✓	Fine Coarse		
Summit, Greenland	78.36°N, 38.5°W	3802			✓		DRUM Sampling		
Canada									
Alert	82.45°N, 62.52°W	210	✓		✓	✓	Elements SO_4^{2-}; NO_3^-; NH_4^+		Weekly EC/OC
Denmark									
Thule	76.52°N, 68.77°W	200				✓			
Kangerlussusaq	67.00°N, 50.98°W	150				✓			
St. Nord	81°36′ N, 16°39′ W	25	✓	✓	✓		Elements SO_4^{2-}; NO_3^-; NH_4^+;	GEM; O_3; NOx; CO, CO_2; H_2	Weekly EC/OC
Norway									
Kårvatn / Kaarvatn	62.78°N, 8.88°E	210					SO_4^{2-}		
Zeppelin Mt. (Ny Ålesund)	78.91°N, 11.88°E	474	✓	✓	✓	✓	SO_4^{2-}		
Tustervatn	65.83°N, 13.92°E	439					SO_4^{2-}		
Sweden									
Bredkälen	63.84°N, 15.32°E	410					SO_4^{2-}		
Finland									
Pallas	67.97°N, 24.12°E	560	✓	✓	✓	✓			
Matorova	68.00°N, 24.24°E	340		✓					
Virolahti	60.53°N, 27.68°E	4	✓		✓				
Oulanka	66.32°N, 29.40°E	310					SO_4^{2-}		
Russia									
Terski									
Janiskoski	68.93°N, 28.85°E	118					SO_4^{2-}		
Pinega	64.70°N, 43.40°E	28					SO_4^{2-}		

[a] A direct carbon measurement would be the use of integrated filter measurements for BC and OC (e.g., thermal evolution techniques) or optical methods (e.g., SP2 or ACMS).

low. Furthermore, as the sampling is not synoptic, the samples do not represent a 'pan-Arctic' snapshot. Owing to these factors, it is a challenge to generalize findings from these campaigns.

With a few exceptions, concentrations of BC reported in Arctic aerosol and snow are not based on direct measurement of BC. Methods that have been used rely on the measurement of an aerosol property assumed to be relatable to BC (e.g., light absorption or lack of volatility at a given temperature). BC concentrations derived from the different methods can disagree by a factor of two or more. The different methods and their associated uncertainties are discussed in Sections 3.2 and 3.3. Methods for modeling the transport of BC to the Arctic and its spatial and temporal distribution are described in Section 3.4.

3.2. Atmospheric measurement of BC

3.2.1. Measurement of absorption

3.2.1.1. Filter-based absorption photometer

Owing to ease of remote operation, filter-based absorption has been the most commonly used technique in the Arctic for deriving atmospheric BC concentrations. In this method, aerosol is collected on a filter and light absorption is calculated from the change in transmission through the filter over time. Filter-based absorption instruments include the Particle Soot Absorption Photometer (PSAP) (Bond et al., 1999; Virkkula et al., 2005), currently in use at Barrow, and the Aethalometer (Hansen et al., 1982) which is currently in use at Alert and Summit and has been used at Barrow. At Zeppelin, both a PSAP and an aethalometer are currently in use. This method yields an aerosol light absorption coefficient that is converted to a BC mass concentration through the use of a mass absorption cross section (MAC). The mass absorption cross section of BC is defined as the amount of light absorption per unit mass of BC and has units of m^2/g. The resulting BC concentration is often termed an 'equivalent BC concentration' as it is not based on a direct measurement of BC.

The MAC for BC can be derived from simultaneous measurements of light absorption (such as from the PSAP or aethalometer) and elemental carbon (EC) mass concentrations (from methods that are described in Section 3.2.2). The MAC for newly emitted BC has been found to have a fairly narrow range of 7.5 ± 1.2 m^2/g (Clarke et al., 2004; Bond and Bergstrom, 2006).

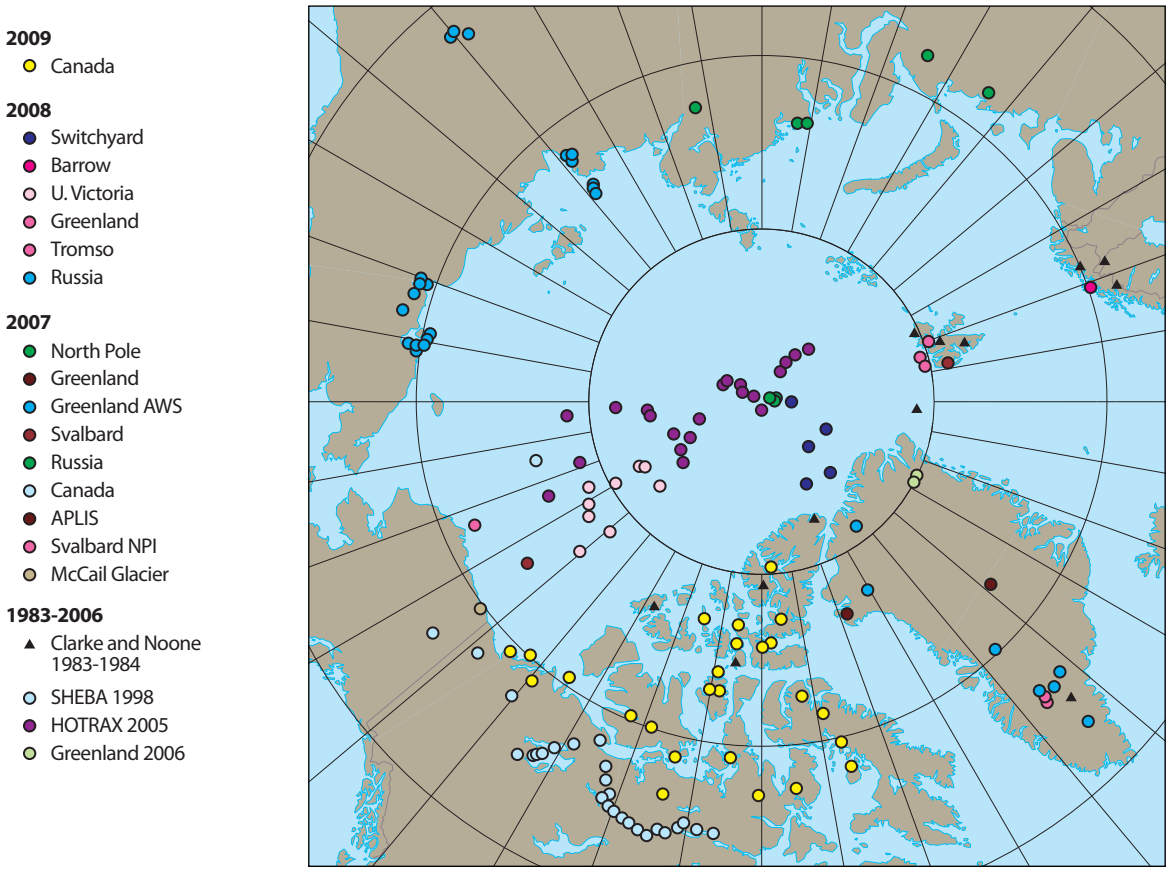

Figure 3.1. Location of BC snow sampling campaigns across the Arctic. Source: Doherty et al. (2010).

The MAC for BC measured downwind of sources is generally larger and has a much wider range of values (Quinn and Bates, 2005) due to the enhancement in absorption for internally mixed aerosol and measurement of non-BC light absorbing species (e.g., OC and dust). If the absorption due to other species is significant compared to that for BC, the MAC value will be overestimated and the resulting concentration of BC will be underestimated. Sharma et al. (2004) derived winter/spring and summer BC MAC values for Alert based on three years of measurements of light absorption with an aethalometer and EC mass concentration using a thermal-optical method (see Section 3.2.2.1). The resulting values, 19 m^2/g for winter/spring and 29 m^2/g for summer, were used to calculate BC mass concentrations at Alert and Barrow (Sharma et al., 2004, 2006). Since long-term uncertainty in the seasonally adjusted MAC values could not be assessed, it was assumed they were valid for a trend analysis of BC concentrations that covered a span of 13 years. This assumption will not be valid if aerosol sources and composition that impact light absorption during the 13-year period were not well represented by the three years of simultaneous measurements of light absorption and EC mass concentrations that were used to derive the MAC.

Filter-based absorption methods can suffer from interferences that result in artificially high absorption values. If the light transmission is reduced by scattering aerosol that has been collected on the filter, the absorption coefficient will be overestimated (Bond et al., 1999). The empirical schemes that are available to correct for the influence from scattering yield accuracies of the PSAP between 20% and 30% (Bond et al., 1999; Virkkula et al., 2005). However, these correction schemes are based on laboratory-generated aerosols which may limit their application and accuracy for the measurement of atmospheric aerosols. In addition, PSAP absorption coefficients can be biased high (50–80%) when the ratio of organic aerosol to light absorbing carbon (LAC) is high (15–20%). Lack et al. (2008) postulated that this high bias was due to the redistribution of liquid-like OC which affected either light scattering or absorption. Other filter based techniques including the aethalometer may suffer from the same bias.

3.2.1.2. Photoacoustic spectrometer

The photoacoustic spectrometer (PAS) is a non-filter based method for measuring aerosol light absorption that was recently used in the Arctic during several of the intensive field campaigns associated with POLARCAT. In the PAS (e.g., Arnott et al., 1997; Lack et al., 2006), particles are drawn into a cavity and irradiated by laser light. The heat that is produced when the particles absorb the light is transferred to the surrounding gas creating an increase in pressure. Sensitive microphones are used to detect the standing acoustic wave that results from the pressure change. The detected signal and instrument parameters are used to calculate the absorption coefficient. The overall uncertainty of the PAS with respect to aerosol absorption has been reported at about 5% (Lack et al., 2006). The uncertainty of the PAS is low, in part, because it is not subjected to the sampling artifacts associated with collecting aerosol on a filter. At present, the PAS is too expensive to routinely deploy at multiple monitoring sites.

3.2.2. Measurement of BC mass

3.2.2.1. Filter-based thermal-optical carbon analyzer

In many monitoring networks, BC concentrations are determined by collecting aerosol on a filter and then heating the filter to discriminate between organic (volatile) and elemental (non-volatile) carbon. Elemental carbon (EC) is defined as the non-volatile or refractory portion of the total carbon (TC = OC + EC) measured. Frequently, the sample filter is first heated in inert gas to volatilize OC, cooled, and then heated again with oxygen to combust the EC (e.g., Chow et al., 1993; Birch and Cary, 1996). A complication is 'charring' of OC at high temperatures, which reduces its volatility and causes it to become an artifact in the EC/OC determination. Variations of this method include different temperature ramping schemes, and correcting for the charring of OC during pyrolysis by monitoring the optical reflectance (Huntzicker et al., 1982) or light transmission (Turpin et al., 1990). Comparisons between different thermal evolution protocols reveal that EC concentrations can differ by more than an order of magnitude (Schmid et al., 2001), and that much of this difference is caused by the lack of correction for charring, which leads to considerable overestimates of EC. In addition, there are significant differences in EC concentrations depending on the method used to correct for charring (Chow et al., 2004). Methods are comparable if the filter contains a shallow surface deposit of EC or if OC is uniformly distributed through the filter. If EC and OC both exist at the surface and are distributed throughout the filter, the different corrections yield different concentrations of EC. Hence, the level of agreement depends, in part, on the OC/EC ratio in the sample. As a result, the different correction schemes yield similar results for diesel exhaust, which is dominated by EC, but can differ widely for complex atmospheric mixtures.

3.2.2.2. Single particle soot photometer

The Single Particle Soot Photometer (SP2) is a newly developed instrument that is used to quantify refractory BC mass (the mass remaining after heating to ~3500 K) and optical size of individual BC cores in the 90 to 600 nm diameter size range (Schwarz et al., 2006, 2008). In addition, the instrument is able to detect coatings on the BC aerosol and the thickness of those coatings. The SP2 was used on several of the platforms involved in the recent POLARCAT campaigns. In the instrument, particles are heated by a laser and raised to their vaporization temperature thereby emitting thermal radiation. Refractory BC is identified by its unique temperature signal and the intensity of the thermal radiation is linearly related to the mass of the BC core. Internal mixtures with BC cores are identified by the laser light that is scattered as the particle is heated. The uncertainty associated with BC mass loadings has been reported at 25% (Schwarz et al., 2006). Like the PAS, the instrument is relatively new, expensive, and not suited for long-term remote operation.

3.3. Measurement of BC in snow

BC-snow/ice forcing peaks during the spring when solar energy is increasing, there is maximum snow/ice cover, and rapid meridional transport of BC-containing aerosol from the northern hemisphere mid-latitudes is frequent. In addition, the snowpack is at its deepest and melting has not yet occurred. Snow can be collected at the surface to characterize recent deposition events and in layers below the surface to sample deposition that occurred throughout the winter and spring. Collected snow is melted and, depending on the analysis method, either analyzed directly or filtered with the analysis performed on the BC collected on the filter. When filtering, care must be taken so as not to lose BC to the walls of the filtering apparatus or to lose a fraction of the BC through the filter (Doherty et al., 2010). Analysis methods used for the measurement of atmospheric BC absorption and mass concentration have been or could potentially be used for quantification of snow BC.

3.3.1. Measurement of BC mass in snow

Snowmelt that has been filtered through a quartz fiber filter can be analyzed with the thermal-optical techniques described in Section 3.2.2.1. It has been shown that a significant fraction of snowmelt BC will pass through a quartz fiber filter upon filtration, however (Hadley et al., 2010). If this method is to be used, the collection efficiency of the filters used should first be tested and quantified. Alternatively, an SP2 (described in Section 3.2.2.2) can be used to directly measure the BC mass concentration in snowmelt (McConnell et al., 2007).

3.3.2. Measurement of absorption due to BC in snow

As with the quantification of BC in the atmosphere, the absorption due to BC in snow can be determined and converted to a mass concentration. This method was used in the pan-Arctic survey of snow BC concentrations reported by Doherty et al. (2010). After filtering snowmelt through a Nuclepore filter, Doherty et al. (2010) used an Integrating-Sandwich/Integrating Sphere (ISSW) to quantify light-absorbing aerosol collected on the filter. Spectrally resolved absorption is measured (300 to 750 nm) and used to discriminate between BC and other light-absorbing species (e.g., dust and organics). An assumed MAC is then used to derive an equivalent BC mass concentration from the measured absorption.

3.4. Methods for modeling BC in the Arctic

Several types of models, which vary in their level of complexity, are used for modeling the transport of BC to the Arctic and its distribution in the atmosphere and on the underlying surface. The simplest are trajectory models (Stohl, 1998), which are often used to infer source regions for BC measured in the Arctic (e.g., Polissar et al., 1999, 2001; Sharma et al., 2004, 2006; Eleftheriadis et al., 2009; Huang et al., 2010a). Trajectory models are limited, however, because they have no emission information and do not account for atmospheric turbulence and convection, processes relevant for aerosol transformation and removal. Lagrangian particle dispersion models are similar to trajectory models but account for turbulence and convection. They can also incorporate emission information explicitly (Stohl, 2006) and have been used for statistical analyses of measured data to quantify source contributions throughout the Arctic (Hirdman et al., 2010a,b). However, Lagrangian models do not account for aerosol processing and, thus, assumptions on lifetimes need to be made, which may not necessarily be correct.

In order to explicitly simulate aerosol transport into the Arctic, Eulerian chemistry models are needed. These models use detailed emission information and explicitly treat chemical processes such as changes of BC hygroscopicity, its state of mixture (external vs. internal) with other aerosol components, and removal from the atmosphere. The level of detail in the treatment of these various

processes can be very different between models and can lead to large differences in atmospheric BC loadings, particularly in the Arctic (Huang et al., 2010b; Liu et al., 2011; Vignati et al., 2010). Two different types of Eulerian models are available: Chemistry Transport Models (CTMs) and Chemistry Climate Models (CCMs). CTMs are driven with derived meteorological fields (e.g., from re-analysis data), while CCMs generate their own climate. Both model types have advantages and disadvantages. CTMs can be used to simulate 'real' events if they are run on analyzed meteorological data, which can be compared directly to observations. If coupled with a radiative transfer model, they can also determine radiative forcing values. However, CTMs cannot be used to evaluate feedback processes in the climate system, such as the albedo feedback triggered by radiative forcing of BC. In contrast, CCMs simulate these feedback processes but cannot reproduce observed events as they generate their own 'model climate'. They can be 'nudged' toward observed meteorological data and, thus, be used in a manner similar to CTMs but in that case lose their ability to simulate feedback processes.

One important constraint on CTM and CCM simulations is computation time, which increases with the number of processes treated and the level of detail incorporated into the various process sub-modules. In practice, this limits the vertical and horizontal resolution of these model simulations, especially for CCMs. This is a critical problem especially in the Arctic where the high static stability produces fine-scale atmospheric structure, which is lost in the model simulations. Regional models can typically be run at higher resolution than global models and can be attractive tools for the Arctic. Another challenge models face in the Arctic is that available parameterizations of aerosol processes may not have been designed for the Arctic in particular. For example, dry deposition of aerosols over sea ice may not be adequately treated by the model's deposition schemes. In addition, aerosol processing and removal in Arctic mixed-phase clouds is inherently difficult to simulate because observations of these processes are lacking.

In this report, both a CCM and a CTM are used to calculate radiative forcing values due to the atmospheric direct effect and the BC-snow/ice effect. The CCM used is the National Center for Atmospheric Research (NCAR) Community Earth System Model, Version 1 (Gent et al., in press, http://www.cesm.ucar.edu/models/cesm1.0/), in a CCM configuration with bulk aerosol transport (Rasch et al., 2000). Although model-generated atmospheric fields introduce greater uncertainty in BC transport to the Arctic, 'active' atmosphere, land, and sea-ice modules are needed to treat particle processing, and hence radiative forcing, in each of these components. The CTM used is the OsloCTM2. Both models are described in more detail in Section 8.

4. Emissions of black carbon and organic carbon in the Arctic context

4.1. Overview

Black carbon and OC are formed and co-emitted from combustion processes. The ratio of OC to BC emitted per mass of particulate matter is a function of combustion conditions that depend on several factors (e.g., the combustion device and the way it is operated as well as the fuel that is burned). Diesel engines emit more BC than OC and, as a result, their emissions have high BC to OC ratios. Open biomass burning typically emits more OC than BC such that biomass burning emissions have relatively low BC to OC ratios. While combustion is the primary source of BC, OC can also be produced from gaseous precursors that undergo processing in the atmosphere to form secondary organic aerosol (SOA). BC has a lifetime of days to weeks and, as a result, is not globally well mixed. The main source sectors and regions of BC emissions and subsequent transport to the Arctic need to be identified and their climate impacts studied before developing effective reduction strategies (Law and Stohl, 2007; Quinn et al., 2008). Determining emissions from the source sectors and geographical regions that have an impact on Arctic climate is a major motivation for this assessment.

As discussed in detail in Section 5, recent research indicates that emissions from parts of Europe, East and Northern Asia, and North America contribute to Arctic surface and mid-troposphere BC concentrations to varying degrees (e.g., Stohl, 2006; Shindell et al., 2008; Hirdman et al., 2010b). There is further evidence that some of this emitted BC is deposited to snow- and ice-covered regions (Doherty et al., 2010) and, thus, has the potential to influence the radiative balance of the region through the BC-snow/ice forcing mechanism. In addition, Arctic BC concentrations are extremely sensitive

to emissions within the Arctic itself (Hirdman et al., 2010b). Changes in local activities that result in increased emission of BC in the Arctic may thus play an important role.

The relative contribution of individual emission sources to BC in the Arctic depends not only on their relative emission strength, but also on the relative efficiency of transport from source to receptor. Since the transport efficiency depends on season (see Section 5), seasonal differences in emissions also need to be considered. For instance, transport from Eurasia to the Arctic is more efficient in winter than in summer and, thus, emissions occurring in Eurasia in winter will have a greater impact on Arctic BC loadings than those occurring in summer.

Emissions of BC and OC are usually calculated by combining information on fuel use with emission characteristics of various combustion technologies and emission controls (Bond et al., 2004; Kupiainen and Klimont, 2007; Klimont et al., 2009). The databases consist of numerous fuel sector-technology combinations and emissions are usually presented as aggregated sectors or fuels. Combustion technology-specific emission factors are developed based on source measurements, using the same measurement techniques described in Section 3.2. The most used methods in source characterization have been the thermal optical techniques, which, as described in Section 3.2, quantify EC based on its thermal involatility. It is well known that the different measurement techniques can yield significantly different concentrations of BC (see discussion in Section 3.2 and Bond et al., 2004). However, not enough is known about the uncertainties of the measurements used to develop the inventories to account for them (Bond et al., 2004). As a result, they add to the uncertainties of the emission data. In addition to the measurement techniques, differences in fuel properties, combustion devices, and their operational practices are a major source of variability in the emission data.

Emission model results can be accessed from peer-reviewed scientific journals and through the internet. For example, emission information of carbonaceous aerosols is included in the following web resources:

- Greenhouse Gas and Air Pollution Interactions and Synergies model (GAINS) of the International Institute for Applied Systems Analysis (IIASA) can be operated at http://gains.iiasa.ac.at and results from the
- Special Pollutant Emission Wizard (SPEW) model of the University of Illinois can be accessed at www.hiwater.org/.

There are also web resources that give access to globally gridded (usually in regular latitude/longitude grids) emission data. Examples of these sources are:

- Representative Concentration Pathways (RCP) (www.iiasa.ac.at/web-apps/tnt/RcpDb/dsd?Action=htmlpage&page=about#). The RCPs are meant to serve as input for climate and atmospheric chemistry modeling, i.e., for the IPCC's Fifth Assessment Report.
- Global Emissions Inventory Activity (GEIA), www.geiacenter.org.
- Emission Database for Global Atmospheric Research (EDGAR) (http://edgar.jrc.ec.europa.eu/index.php).

4.1.1. Emissions of BC and OC

In this assessment, BC and OC emissions were taken from the RCP database (Lamarque et al., 2010) to determine the source sectors and regions which cause the largest radiative forcing in the Arctic. Emission data are represented separately for the Arctic Council nations, that is, Canada, Nordic countries (Denmark, Finland, Iceland, Norway and Sweden), Russia, United States, and the rest of the world (ROW). Emissions are aggregated into six source sectors:

1. **Domestic combustion**: Use of wood or coal, in heating stoves and boilers of different kinds. The size of installation spans from small room heaters to boilers providing heat for larger buildings such as malls and hospitals.
2. **Land transport**: On-road and off-road diesel and gasoline vehicles and machinery, with subcategories reflecting the different engine and vehicle types as well as levels of emission control.
3. **Shipping**: Different vessel types operating in Arctic waters. For more information see Corbett et al. (2010).
4. **Energy and industrial production and waste treatment:** Use of fossil and biofuels for power generation and process emissions from industrial production and combustion of wastes. This sector may include emissions from machinery operating within industrial facilities.
5. **Field burning**: Anthropogenic burning of agricultural wastes (crop residues).
6. **Forest and grass fires**: Biomass burning can be natural or anthropogenic. In northern latitudes these fires are generally considered 'natural',

yet there is evidence that anthropogenic activities are increasing their frequency.

In addition to these sectors, emissions from oil and gas flaring are discussed based on estimates from the IIASA GAINS model. These aggregated source sectors do not include aviation. Global BC and OC emissions from aircraft are small, about 0.1% of total emissions. However, the topic should receive more attention in future work as some of the major aviation routes go north of 60° N (Lee et al., 2009) and may have a significant contribution to the BC burden at high altitudes (Koch and Hansen, 2005). The aggregated emissions are discussed here for illustration and because they were used as input to the modeling runs to support this assessment. More detailed discussion of individual emission sources and mitigation potentials for Arctic BC and OC can be found in the Arctic Council Task Force on Short-Lived Climate Forcers report (ACTFSLCF, 2011).

Some countries have also developed their own emission estimates that are independent of the global datasets. However, a discussion of these national inventories is not included here because they are not available from all Arctic Council nations. Available datasets can be found from the Task Force report (ACTFSLCF, 2011). The emissions of some co-emitted species, specifically SO_2 and some of the O_3 precursors, are presented later in this section (see Section 4.4).

4.1.2. Anthropogenic emissions of BC and OC in 2000

Anthropogenic emissions in this assessment refer to the first five aggregated sectors and exclude forest and grassland fires, which are discussed separately in Section 4.1.6. Global anthropogenic BC emissions (Lamarque et al., 2010) by latitude for 2000 are shown in Figure 4.1. Most anthropogenic BC emissions take place in the northern mid-latitudes, with peak emissions around 35° N. In the context of the Arctic, 40° N is often considered a reasonable approximation for the southernmost boundary of the Arctic front during winter and early spring. By this definition, emissions north of 40° N are assumed to significantly affect the Arctic atmosphere. The extent to which this assumption is true depends on transport pathways and receptor location. The Arctic is defined in this assessment as the region between latitudes 60° N and 90° N, and therefore emissions within this area are also discussed separately.

BC emissions north of 40° N comprise 24% of the global anthropogenic total while emissions north of 50° N comprise 9% and those north of 60° N comprise less than 1%. Major sectors north of 40° N are domestic combustion and transport which together comprise about 70% of the anthropogenic total.

BC emissions in the high Arctic (north of 70° N) are negligible compared with the global total, and mostly originate from shipping. Flaring in the oil and gas industry is another potential source of BC, which may have significant emissions in the far north. Flaring is a way of discharging and disposing of gaseous and liquid hydrocarbons through combustion at offshore and onshore petroleum prospecting sites, production installations, and refineries. Currently there is no quantitative spatial estimate of flaring emissions available, but based on satellite image assessment by NOAA on the location of flares[1] it is possible to observe that there are flares in Prudhoe Bay, Alaska located around 70° N; that the majority of Russian flares are between 60° and 68° N in western Siberia; and that there is a significant number of flares along the coast of Norway between 60° and 66° N. Based on the NOAA data these coastal flares are mostly Norwegian but also include some from the United Kingdom.

OC emissions peak at 26° N (Figure 4.1), which is more southerly than the peak for BC. The shares of emissions north of 40°, 50°, and 60° N are 21%,

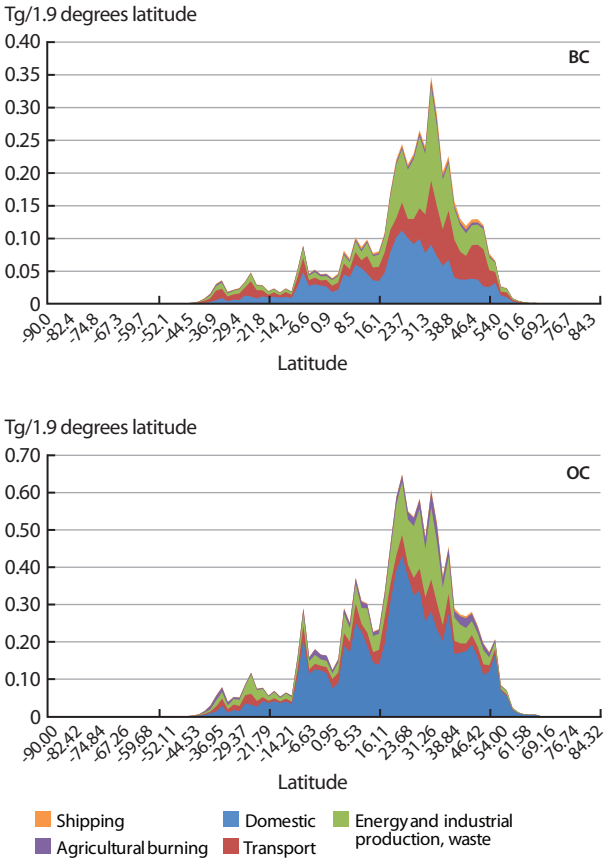

Figure 4.1. Emissions of BC and OC in 2000 by latitude. Source: Lamarque et al. (2010).

[1]See www.ngdc.noaa.gov/dmsp/interest/gas_flares.html (Elvidge et al., 2009).

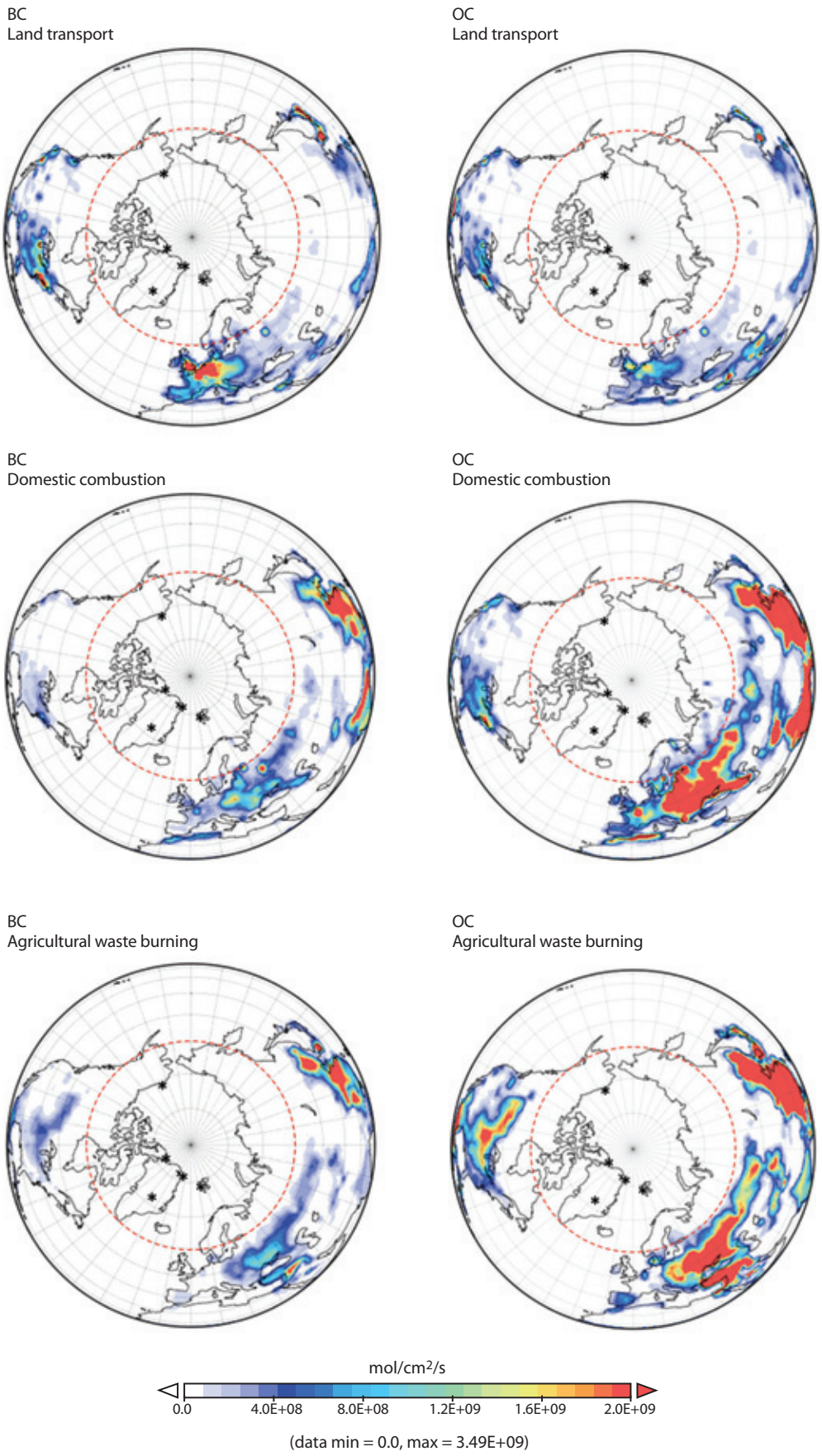

Figure 4.2. Spatial distribution of BC (left) and OC (right) emissions from land transport, domestic combustion and agricultural waste burning. Dashed line shows 60° N. Black asterisks depict measurement station locations.

8% and 1% of the global anthropogenic total, respectively. Comparison of BC and OC emissions in Figure 4.1 demonstrates the co-emission of BC and OC from some major source sectors. Variability in the OC to BC ratio between the aggregated sectors and the dependence on fuel burned and combustion characteristics can also be seen. For example, domestic combustion has a higher OC to BC ratio than the other major anthropogenic emission sectors and thus accounts for a higher share of OC than BC emissions (see also Figure 4.2). However, it is important to note that these aggregated sectoral OC to BC ratios reflect a mix of a vast number of combustion technologies and fuels. For example, land transport is dominated by diesel engines, which have a low OC to BC ratio, but this sector also includes gasoline vehicles with higher OC to BC ratios. In the case of OC, domestic combustion alone is responsible for about 67% of the anthropogenic emissions north of 40° N and 78% north of 60° N. For designing targeted mitigation strategies, it is necessary to have a finer breakdown of emission categories than the aggregated sectors discussed here. However, for impact analyses such as that within this assessment, this sectoral aggregation level is sufficient to provide important new insight into the influence of the different sources on the atmospheric burden of Arctic BC and OC.

Figure 4.2 shows the spatial distribution of BC and OC emission fluxes around the Arctic from the major anthropogenic emission sectors of land transport, domestic combustion, and agricultural burning. Major emission hot spots are Central and Eastern Europe, Western Russia, Eastern United States and Canada as well as East Asia. A closer look at countries contributing to the BC emissions north of 40° N (Figure 4.3) shows that the EU-27 countries, Russia, China and the United States are responsible for over 80% of the total emissions. Within the EU-27 countries, France, Germany, Poland and United Kingdom contribute each about 5–6% of total emissions north of 40° N. Emissions from Ukraine comprise 5% and those from the Nordic countries and Canada both make up 3%. Class 'Other N40' in Figure 4.3 consists of about 20 countries that have areas north of 40° N, each contributing about 1% or less to the total emission flux within the area, altogether totaling 8% (Figure 4.3).

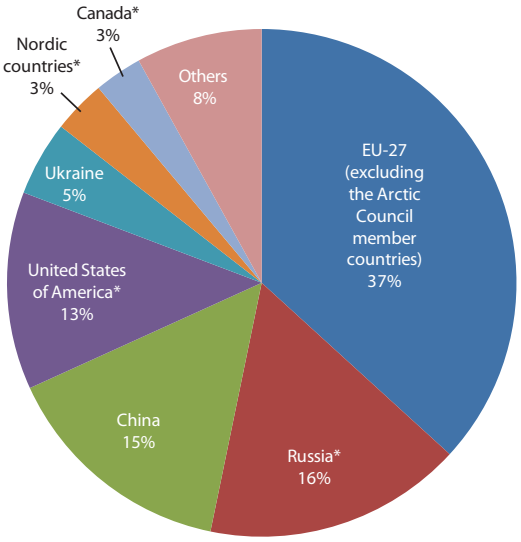

Figure 4.3. Country contributions to anthropogenic BC emission fluxes north of 40° N. Arctic Council nations are marked with an asterisk.

The Nordic countries and Russia are responsible for most of the anthropogenic emissions north of 60° N (dashed line in Figure 4.2). The RCP database does not include emissions from Greenland and these are discussed separately in Section 4.1.5. Land transport emissions are especially concentrated in population centers in Central Europe and North America. This feature shows up more clearly in the BC map as transport emissions are dominated by emissions from diesel vehicles, which have a low OC to BC ratio.

Domestic combustion has a similar distribution in North America to land transport but in Eurasia the emissions are concentrated more in Eastern Europe, Western Russia and East Asia. In the northern latitudes, including the Arctic Council nations, most of the domestic combustion takes place for heating purposes. Small domestic heating stoves that use solid fuels like wood and coal and have relatively poor combustion conditions are commonly used and, as a consequence, are a large source of BC and OC emissions (Bond et al., 2004; Cofala et al., 2007; Kupiainen and Klimont, 2007). Heating activity peaks during the winter months and so the BC and OC emissions from domestic combustion have more pronounced seasonal variation than other major emission sectors such as transport.

The spatial distribution of agricultural burning reflects the location of areas with high agricultural activity. Earlier studies identified North America, including the Canadian provinces of Alberta and Saskatchewan and the Great Plains of the United States; as well as agricultural areas of Eastern Europe, European Russia, Asiatic Russia and north-eastern Asia, as regions of significant agricultural fire activity (e.g., Korontzi et al., 2006; Roy et al., 2008; van der Werf et al., 2010). Emissions from these regions can be seen in the maps in Figure 4.2. Agricultural fires also have strong seasonal and interannual variability which varies across the regions depending on crop type and crop calendar (Korontzi et al., 2006; van der Werf et al., 2010). Figure 4.4 shows fire variability for source regions relevant to the Arctic in the period 2001 to 2003.

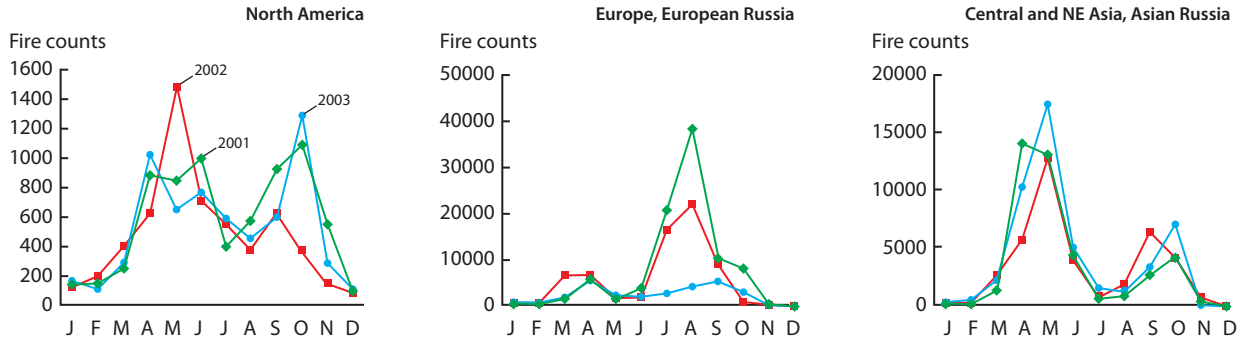

Figure 4.4. Monthly time series of MODIS TERRA agricultural fire detections in the period 2001 to 2003. Source: Korontzi et al. (2006).

4.1.3. BC and OC emissions in the Arctic Council nations

Global anthropogenic BC and OC emissions from the RCP database (Lamarque et al., 2010), by Arctic Council nations and the rest of the world, are shown in Figure 4.5. The figure also shows the anthropogenic BC and OC emissions split between the Arctic Council nations, with the Nordic countries (Denmark, Finland, Iceland, Norway, Sweden) aggregated into one region. The allocation of emissions to individual countries and regions was made based on 1.9° × 2.5° gridded global emissions. A finer resolution may lead to minor differences (less than 10% per sector) on a national basis, mostly due to re-allocation of emissions across borders.

The emissions from the Arctic Council nations comprise 12% and 7% of the global total anthropogenic BC and OC emissions, respectively. The United States and Russia are responsible for almost 90% of the roughly 600 Gg/y of BC and 850 Gg/y of OC emitted annually from the Arctic Council nations. In case of BC, the United States accounts for 61% and Russia 28% of emissions and Canada and the Nordic countries for the rest with roughly similar shares. In the case of OC the shares are 47%, 41%, 8% and 4%, respectively for the United States, Russia, Canada and the Nordic countries. The United States is the only country that has significant land areas south of 40° N. About 40% of the BC and OC from the United States is emitted north of 40° N.

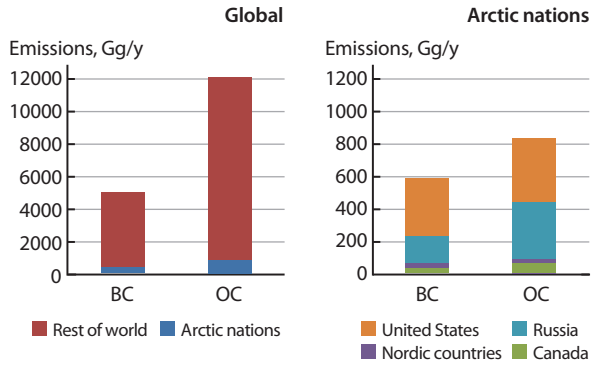

Figure 4.5. Global and Arctic nation BC and OC emissions in 2000. Source: data from Lamarque et al. (2010).

Figure 4.6 shows the anthropogenic BC and OC emissions in the Arctic Council nations in 2000 with sectoral distribution. This includes a comparison with other available inventories. The data shown are:

- 'Bond': BC and OC inventory based on Bond et al. (2004, 2007) as presented in the ACTFSLCF white paper (Sarofim et al., 2009).
- 'AMAP emission inputs': BC and OC emissions from the RCP database (www.iiasa.ac.at/web-apps/tnt/RcpDb/dsd?Action=htmlpage&page=about#) (Lamarque et al., 2010) as used in the model runs described in Section 8.
- 'GAINS': Emissions calculated with the IIASA GAINS model (http://gains.iiasa.ac.at) and reported to ACTFSLCF (ACTFSLCF, 2011).

The inventories identify the same top-emitting sectors, but demonstrate differences in total emissions and distribution of the sectors, arising from differences in the background data (i.e., characterization of combustion technologies and potential emission controls, emission factors as well as fuel use estimates underlying the inventories).

The emission sectors with the highest contributions of BC are the use of diesel fuel in transport and domestic combustion of solid fuels. Additional potentially important source sectors are agricultural burning and flaring in the oil and gas industries (the latter are not included in Bond and RCP databases). The class 'other' in the figures includes minor sources such as barbeques and cigarette smoking that could not be classified into the aggregated sectors included here.

The RCP database has higher emissions from the industry and power sector than the other two inventories. The probable reason is in the allocation

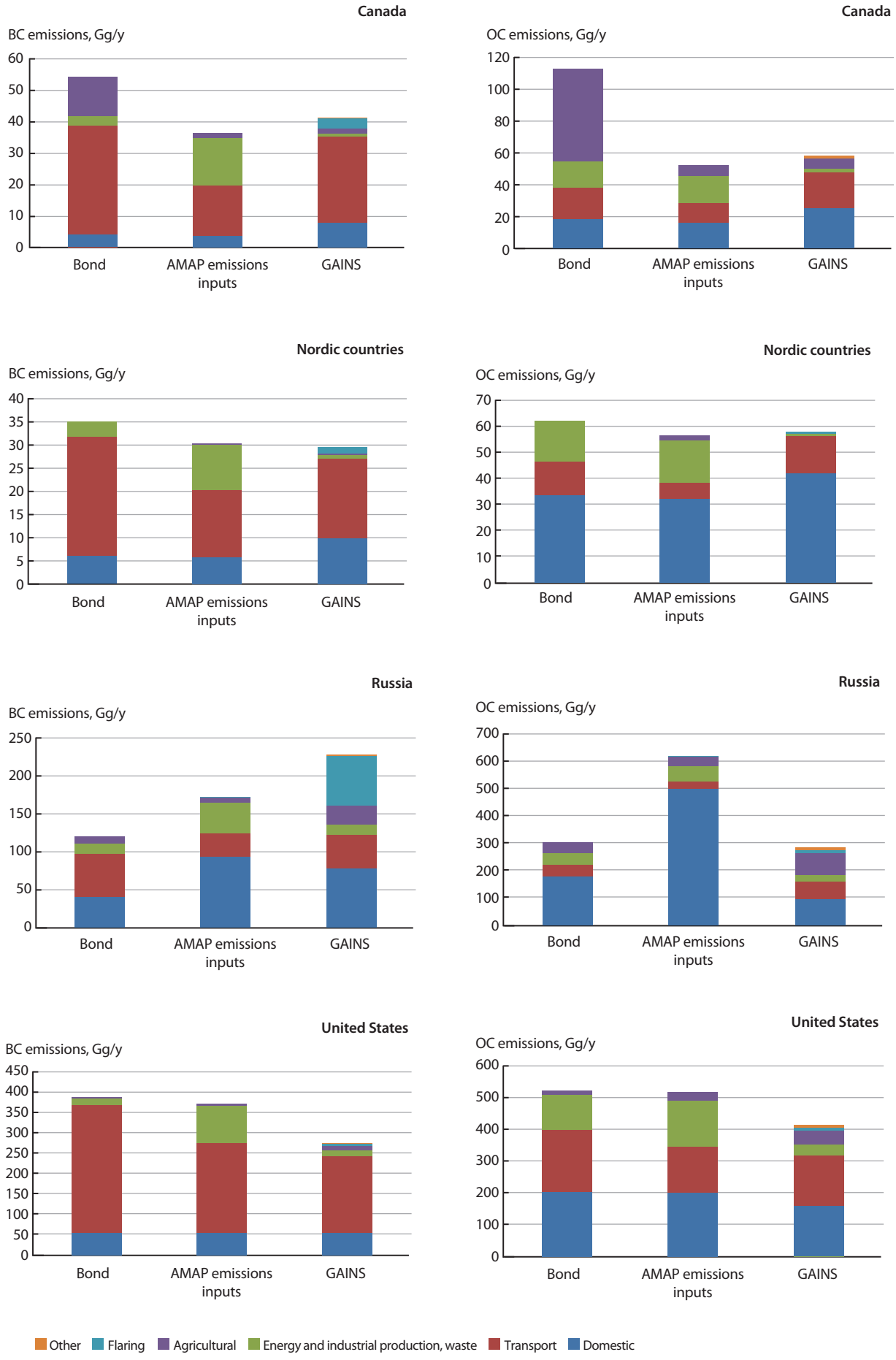

Figure 4.6. Emissions of BC (left) and OC (right) from Arctic Council nations in 2000.

of the diesel used in the industrial off-road transport and machinery. The RCP emission dataset is based on global energy statistics from the International Energy Agency, where diesel fuel consumed in machinery and tractors is allocated to non-transport sectors such as industry, consequently leading to higher emissions from the sector. The GAINS and Bond inventories, however, use national information, which often has a more detailed split of energy statistics, including finer allocation of transport sector activities (Bond et al., 2004, 2007; Amann et al., 2008a,b). In other words, part of the RCP emissions in the industry and power sector is included in the transport sector of the other two inventories. The differences in the transport sector emissions are further explained by the differences in accounting for high emitting vehicles and exhaust emission controls, for example.

Flaring is a way of discharging and disposing of gaseous and liquid hydrocarbons through combustion in offshore and onshore petroleum prospecting sites, production installations, and refineries. The GAINS model is currently the only global inventory available that includes an estimate of emissions from oil and gas flaring. It relies on country-specific gas flaring volumes from the NOAA National Geophysical Data Center and emission factors based on measurements by Johnson et al. (2011). The data sources behind the estimate are scarce and so should be considered preliminary. However, the estimate indicates the potential importance of the sector showing that the emissions of BC from flaring might contribute up to 12% of the BC emissions from the Arctic Council nations in 2000, originating primarily from Russia but with relatively significant contributions in the other regions as well.

4.1.4. Arctic shipping

The Arctic sea-ice extent, thickness and the area of multi-year ice have all decreased over the past decades (ACIA, 2005; Arctic Council, 2009). Providing these trends continue, the Arctic Ocean may become more accessible to shipping and to the Arctic's potentially vast resources, including oil, gas, minerals, and fish. In addition, interest may increase toward the shorter sea routes between Europe, Asia, and the Pacific. Distance savings of up to 25% and 50% are estimated for the Northwest Passage and Northern Sea Route, respectively, compared with the current sea routes, and they are considered to be financially viable (Corbett et al., 2010). On the other hand, apart from the uncertainties in the future of sea ice, a large number of other challenges may limit the development of future shipping operations in the Arctic area. These include governance of the sea lanes, lack of key infrastructure in the area, and harmonized Arctic vessel standards (Arctic Council, 2009). However, there is potential for increased marine activity in the Arctic area with consequent increases in emissions of BC and OC.

Following the definitions in the Second IMO GHG Study (Buhaug et al., 2009), international shipping refers to shipping between ports of different countries, as opposed to domestic shipping, which refers to shipping between ports of the same country. Both international and domestic shipping exclude military and fishing vessels. By this definition, the same ship may be engaged in international and domestic shipping operations. Arctic shipping refers to shipping activities taking place within the Arctic boundaries. Individual assessments may differ in their definition of the Arctic and do not necessarily refer to international shipping activities only.

Corbett et al. (2010) published an Arctic shipping inventory that includes BC and OC emissions from transit (international shipping) and fishing vessels. This inventory was used as input for the model simulations performed for this assessment. Annual emissions from shipping within the Arctic in 2004 were 1.2 Gg BC and 3.8 Gg OC. About two-thirds of emissions came from transit vessels, mostly container and general cargo ships, and the rest from fishing vessels. Most of the vessel activities were concentrated along the Norwegian coast and into the Barents Sea off northwest Russia, around Iceland, near the Faroe Islands and southwest Greenland as well as in the Bering Sea (Arctic Council, 2009). Activities peak in the summer and autumn months (July to November) and are about 30% higher than in winter and spring (Corbett et al., 2010).

The BC and OC emissions from Arctic shipping activities (north of 60° N) in 2000 represent 1–2% of international shipping emissions. For comparison, the corresponding share of international shipping emissions north of 40° N is 33%. Arctic shipping emissions comprise about 4% (BC) and 1% (OC) of the total anthropogenic emissions north of 60° N excluding flaring. Currently, Arctic shipping does not contribute a significant amount to the region's emissions compared to those from Arctic Council nations, but the emissions occur further north and so have a stronger regional impact (Quinn et al., 2008). Any future decline in emissions from other sectors and pollutants may increase the relative importance of within-Arctic shipping emissions.

Corbett et al. (2010) gave two future activity scenarios for Arctic shipping (Figure 4.7). The business-as-usual and high-growth scenarios (including both 'no controls' and 'maximum feasible reduction') introduce growth in activity for one or

a few vessel types and were designed to be used for impact assessment relevant for policy decision-making regarding the Arctic region. In both scenarios, BC and OC emissions are projected to increase by 2020–2050 with an increase in shipping activity. In the high-growth scenario, BC emissions from Arctic shipping could increase from about 1 Gg/y to 5 Gg/y by 2050. OC emissions would almost double from 2.7 Gg/y to 5.2 Gg/y. These increases are a concern, because the order of magnitude in 2050 is similar to emissions projected, for example, for Norway in 2020 and the emissions occur closer to areas permanently covered by ice and snow. Possible future shipping fuel quality regulations through the MARPOL Annex VI legislation on sulfur content do not necessarily reduce emissions of BC (Lack et al., 2009).

Shipping fuel quality regulations through MARPOL Annex VI legislation on sulfur content are expected to reduce the total particle emissions from shipping via reductions in sulfate and OC (Lack et al., 2009; Corbett et al., 2010). At the same time, however, there is a concern that BC emissions might increase without any BC-specific supplementary controls (Lack et al., 2009; Corbett et al., 2010). To implement some of these supplementary BC measures, lower sulfur fuels and changes in lubricating oil properties are required (Corbett et al., 2010). In order to assess the net radiative forcing the impact of reducing SO_2 emissions must be considered as well, since they contribute to climate cooling.

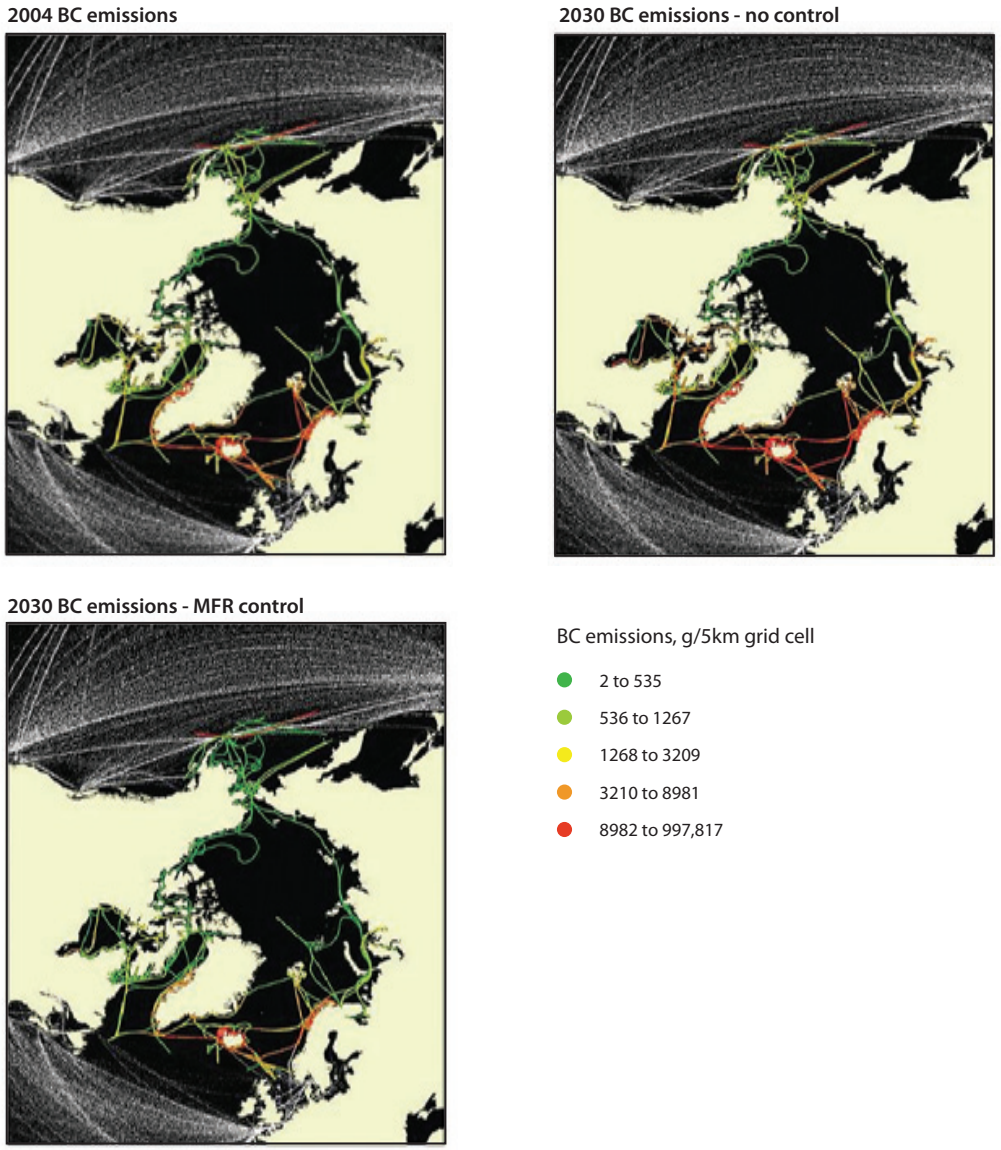

Figure 4.7. Illustration of BC emissions from Arctic shipping in 2004; and 2030 projections without emission control and with Maximum Feasible Reduction control. Source: Corbett et al. (2010).

4.1.5. Emissions in the AMAP area

Emission estimates for BC and OC for all territories within the AMAP area are presented here. The 'AMAP area' is outlined in Figure 4.8 and includes the terrestrial and marine areas north of the Arctic Circle (66°32′ N), north of 62° N in Asia, and north of 60° N in North America, modified to include the marine areas north of the Aleutian chain, Hudson Bay, and parts of the North Atlantic Ocean including the Labrador Sea. Domestic shipping emissions are included here, while international shipping was discussed in Section 4.1.4.

Emissions included in this section are all preliminary, 'work in progress' estimates. Inventories are presented from the US state of Alaska (Marcus Sarofim, Environmental Protection Agency Climate Division, pers. comm.); from the Canadian provinces of Yukon, Northwest Territories, and Nunavut (ACTFSLCF, 2011); Danish emissions from Greenland and the Faroe Islands (Winther and Nielsen, 2011; ACTFSLCF 2011), together with an estimate of emissions from Svalbard (Vestreng et al., 2009). Also presented are rough estimates of emissions ranges within the AMAP area of Russia, Norway (excluding Svalbard), Sweden, and Finland based on the RCP gridded dataset (Lamarque et al., 2010) and inventories available in ACTFSLCF (2011).

The Alaskan, Canadian, and Danish BC and OC inventories, have been estimated with methodologies similar to those used for other pollutants officially reported to national and international bodies.

Figure 4.8. Geographical coverage of the AMAP area. The Arctic Circle is also marked.

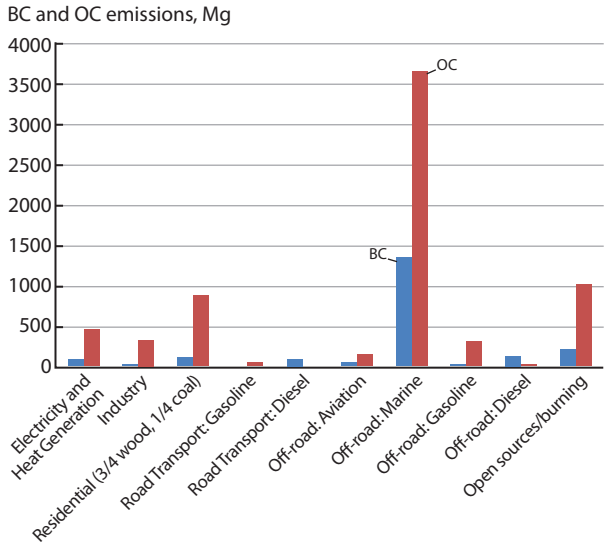

Figure 4.9. Anthropogenic emissions of BC and OC per source category in 2005 in Alaska. Source: Marcus Sarofim, Environmental Protection Agency Climate Division.

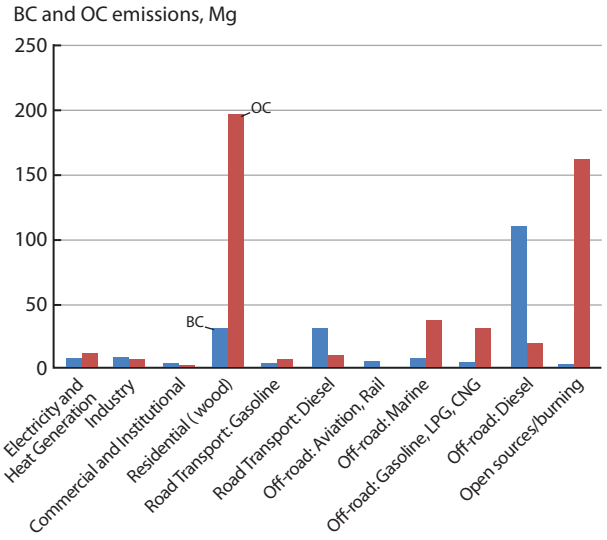

Figure 4.10. Anthropogenic emissions of BC and OC per source category in 2006 in Northern Canada (Yukon, Northwest Territories and Nunavut). Source: ACTFSLCF (2011).

Emissions for the other areas are unofficial estimates that have been derived by various methodologies.

The Alaskan preliminary emissions of anthropogenic BC and OC shown in Figure 4.9 have been estimated from the 2005 US PM2.5 inventory by the US Environmental Protection Agency. Total anthropogenic emissions are 2220 Mg BC and 7060 Mg OC. Marine vessels are the largest source of both BC (61%) and OC (52%) emissions. Open burning or prescribed burns, are the second largest source with 10% and 15% of the total BC and OC emissions, respectively. Electricity and heat generation, residential, road and off-road diesel mobile emissions each constitute about 5% of total anthropogenic BC emissions. In terms of anthropogenic OC emissions, the residential sector makes the largest contribution at 13%, electricity and heat generation (7%), and industry and off-road gasoline sources (5%) follow thereafter. The other sources included in the analysis constitute 1–2% of the total emissions. Not shown in Figure 4.9 are the large emissions from wildfires estimated at 47 000 Mg BC and 240 000 Mg OC.

Total preliminary emissions in 2006 of BC and OC from the Canadian provinces of Yukon, Northwest Territories, and Nunavut are an order of magnitude lower than the Alaskan emissions. Total anthropogenic emissions include 230 Mg BC and 490 Mg OC (Figure 4.10). For comparison, forest fires emissions of BC are estimated at 1450 Mg. The three largest anthropogenic BC sources, which make up 75% of total emissions, are off-road diesel vehicles (110 Mg), on-road diesel vehicles (32 Mg), and residential wood burning (30 Mg). The largest OC sources are residential wood burning (174 Mg), followed by anthropogenic open sources (144 Mg), domestic shipping emissions (38 Mg), and gasoline/liquid natural gas (LNG) / compressed natural gas (CNG) (20 Mg), comprising about 80% of the total OC emissions.

Emission trends of BC and OC for Greenland (60–83° N), a self-governing territory within the Kingdom of Denmark, and the Arctic archipelago of Svalbard (74–81° N) under Norwegian jurisdiction, are presented here. 85% of Greenland and 60% of Svalbard are covered by snow and ice all year around. The size and population of the two territories are very different. Greenland covers a much larger area (Greenland: 2166 086 km^2, Svalbard: 62 050 km^2) and the population is higher (Greenland: 56 452 people, Svalbard 2573 people).

Emissions of BC in Greenland constitute less than 0.5% of total emissions in the Kingdom of Denmark, while the emissions from Svalbard constitute about 1% of Norwegian emissions. Despite the low contribution to the national total emissions, releases of BC from Greenland and Svalbard may have a larger impact on the Arctic due to the high north, snow and ice covered location.

The Danish draft national inventory and projections for Greenland report total emissions of BC and OC in 2010 of 26 and 17 Mg, respectively (Winther and Nielsen, 2011). Fishery (mobile) was the largest BC and OC emission source in 2010 (60% of total). In the case of BC, fishery was followed by road transportation (13%), domestic heating (11%) and domestic shipping (8%). The next largest OC source was domestic shipping (21%). Road transportation and domestic heating represent about 5% each of

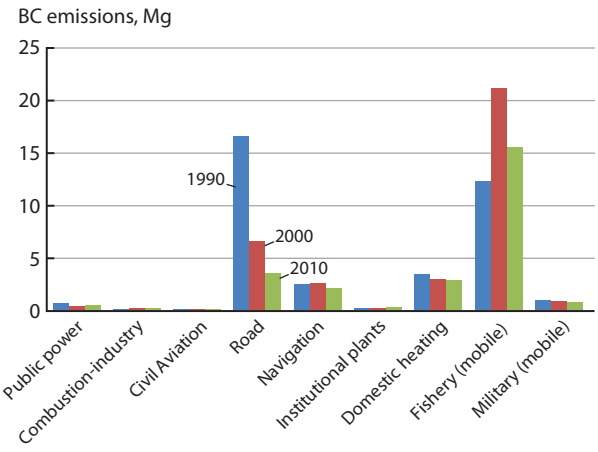

Figure 4.11. Emissions of BC in Greenland by source category in 1990, 2000 and 2010. Source: Winther and Nielsen (2011).

OC emissions (Figure 4.11). Emissions of BC and OC have decreased by about 30% between 1990 and 2010, mainly due to large reductions in road transport emissions (90%). Emissions related to fisheries have increased (26%) over the same period.

The Faroe Islands cover 1399 km^2 and have a population of 48 917. Total 2010 emissions from the Faroe Islands of BC and OC are estimated at 42 Mg and 24 Mg, respectively, which is considerably higher than the Greenland emissions, despite the lower population number. Fishing vessels are the largest source for both BC (61%) and OC (75%).

BC and OC emissions for 2007 related to activities at Svalbard were estimated at 61 and 22 Mg of BC and OC, respectively (Vestreng et al., 2009). Shipping is the largest source of emissions (90%) due to cruise traffic and transport of coal (Figure 4.12). Emissions from fishing were not included in this study due to a lack of data. Road transport is the second largest source. Emissions increased by 30% between 2000 and 2007. The higher emissions from Svalbard compared to Greenland, could be due, in part, to the difference in scope and nature of the two inventories. In the case of Svalbard, emissions from international shipping in the Svalbard zone and all marine and air traffic between Svalbard and mainland Norway are included. In addition, the source distribution in the two inventories is different and it is very likely that there were differences in the emission factors applied.

BC emissions from Iceland for 2000 range between 190 and 670 Mg. Emissions of OC range between 130 and 290 Mg (ACTFSLCF, 2011). Off-road transport dominates the BC and OC emissions in both inventories.

The Russian BC and OC emissions are highly uncertain. Emissions in the AMAP area are estimated to be between 3000 and 4000 Mg of both BC and

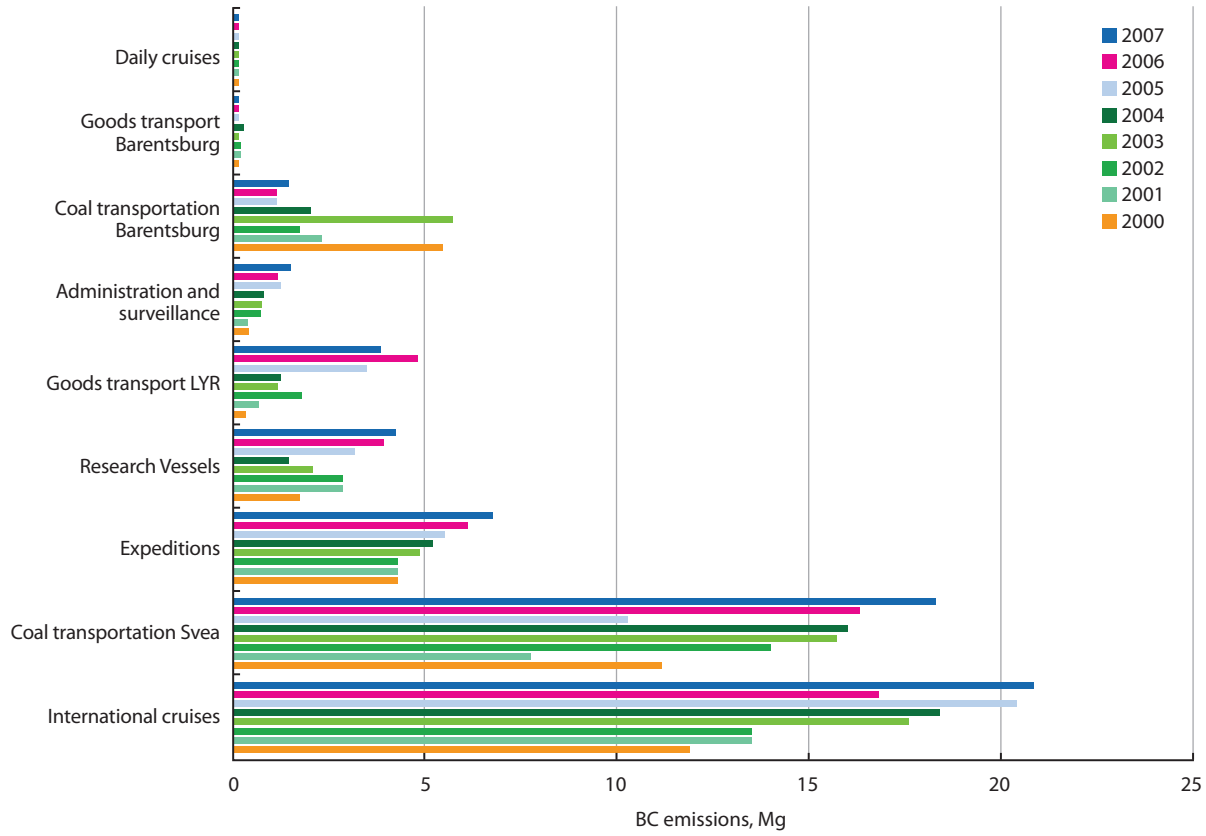

Figure 4.12. Trends in marine emissions of BC for 2000 to 2007 related to activities at Svalbard. Source: Vestreng et al. (2009).

OC based on the RCP distribution (1–2% within the AMAP area) and the total emissions in the ACTFSLCF (2011) report.

Adding all anthropogenic present-day emissions within the AMAP area yields about 3 to 7 Gg/y BC and 4 to 12 Gg/y OC (depending on the inventory). Hence, the sum of these high north emissions is comparable to individual Nordic country totals. In addition, they are several times larger than the current emission estimate for within Arctic shipping of 1.2 Gg BC and 3.8 Gg OC (see Section 4.1.4). Special attention should be given to these emissions because of their location in or close to areas covered by snow and ice the whole year around. Nevertheless, estimates of the uncertainty associated with the high north emissions are large. Efforts should be taken to refine the emission estimates from the AMAP area.

4.1.6. Forest and grassland fires (natural and semi-natural fires)

An important aspect of forest and grassland fires (and to some extent agricultural fires) is that they can effectively inject emissions higher up into the atmosphere than other ground-based emission sources. The heat and latent water release by fires can induce convection above the fires, which lifts the emitted pollutants. While the energy available from small fires may not be sufficient for the plume to penetrate the top of the boundary layer, large fires can produce deep convective columns (pyro-Cbs), which can pollute the upper troposphere (Nedelec et al., 2005) and can even penetrate the tropopause deep into the stratosphere (Fromm et al., 2000; Jost et al., 2004) where the residence time of smoke is much longer than in the troposphere. Pyro-Cb events have been documented over boreal forest fires in North America (Fromm et al., 2000; Jost et al., 2004) and Siberia (Nedelec et al., 2005). While it would be important to include these events to determine the radiative forcing of forest fire smoke (different transport patterns; longer residence times), global models currently do not consider pyro-convection and even observational data are sparse.

Today's fire inventories are typically derived by combining satellite remote sensing information with a biogeochemical model. Burnt area is either derived by applying extrapolation rules from active fire counts, or, more recently, by using burnt area remote sensing products directly (Isaev et al., 2002; Hoelzemann et al., 2004; Balzter et al., 2005; van der Werf et al., 2006; Turquety et al., 2007). Combining the burnt area information with satellite products of vegetation type and cover and a biogeochemical model of vegetation productivity allows assessment of the amount of plant material available for combustion. The various gaseous and particulate pyrogenic emissions are then derived from emission factors that convert the plant material burned to the amount of carbon released by the fire. These emission factors are constants for a given plant functional or vegetation type. The spatial and temporal resolution of inventories thus depends on the resolution of the underlying remote sensing products. Large uncertainties are involved in deriving the inventories including but not limited to, likely underestimation of area burnt in many regions, an over- or underestimation of combusted biomass, and use of emission factors that do not distinguish smoldering from free-burning fire. Only recently have attempts been made to link emission factors more dynamically to burn conditions.

The use of remotely sensed burned area and/or vegetation cover restricts fire inventories to the period these data are available. In order to assess fire regimes under changing climate and changing atmospheric conditions, dynamic vegetation models are currently being combined with empirical or process-based fire models that seek to calculate not only combusted biomass, but also to derive burnt area (Kloster et al., 2010; Lehsten et al., 2010; Pechony and Shindell, 2010; Thonicke et al., 2010). Despite substantial differences between these various approaches the models have in common that they seek to account not only for climate change effects on burn conditions, vegetation productivity and litter availability, but also separate effects of humans and lightning on ignition – and in case of humans – also on extinction (Archibald et al., 2009; Lehsten et al., 2009).

Today's global estimates of carbon emitted from wildfires range between about 2 and 4 PgC/y (van der Werf et al., 2006; Thonicke et al., 2010), with an interannual variability of 1 PgC. For the boreal region, van der Werf et al. (2006) estimated emissions to vary between about 80 and 580 TgC/y for the period 1997 to 2004, and compared these results to the 'moderate severity scenario' from Kasischke et al. (2005) that would suggest lower maximum emissions of up to about 380 TgC/y for the same period.

Wildfires in circum-boreal forest ecosystems surrounding the Arctic are a substantial contributor to BC and OC emissions. Many of the important source areas are located within the boundaries of the Arctic Council nations. For forest fires, the distinction between anthropogenic and natural emission source becomes blurred, since ignition sources can either be by humans or natural (lightning). In fact, boreal forests have co-evolved with fire as a recurring episodic event, such that ecosystems in different boreal forest regions show specific adaptations to cope with, or even rely on, fire disturbance (Johnson, 1992).

How combined effects of climate change and human interference change natural fire regimes is a non-trivial question, and an active area of research (Archibald et al., 2009; Flannigan et al., 2009b). While fire regimes are under notable human influence (e.g., human ignition as well as extinction and prevention, changes in forestry practices) (Achard et al., 2008), they are also under strong direct climate influence, for instance in the remote parts of boreal forests, or when specific weather patterns lead to uncontrollable burning (Bowman et al., 2009). Thus direct policy measures to reduce wildfire BC emissions from forest ecosystems can only be of limited influence, by targeting, for instance, the time of burning. Climate change together with enhanced productivity in a high CO_2 world leads to enhanced availability of combustible plant litter and favorable conditions for ignition and fire spread, and thus has the potential to counteract policy measures that seek to reduce anthropogenic BC emissions. Understanding present-day and future fire regimes (including intensity, severity, location and seasonality) must therefore consider the following aspects:

- Climate change may lead to hotter and drier conditions, enhancing fire risk (Amiro et al., 2009; Flannigan et al., 2009a) including the risks of extreme fire events, while in regions where climate change leads to more moist conditions fire risk, area burnt and pyrogenic emissions may decrease (Macias Fauria and Johnson, 2008). Changing burn conditions toward either a drier or moister environment (smoldering vs. open burn) are also important determinants of composition of the pyrogenic emissions including BC (Janhäll et al., 2010).
- Climate change and increasing atmospheric CO_2 concentration may yield an initially more productive vegetation and thus more biomass that serves as fuel for burning (Balshi et al., 2007; Goetz et al., 2007). However, in areas of increasing drought, effects of soil water deficit can counter those of CO_2 enhancement on productivity of vegetation, and hence litter production.
- In some areas, the combined climate and CO_2 changes can also lead to a lengthening of the growing season (already observed, see Lucht et al., 2002) and shift in vegetation composition (shrub encroachment into tundra; change in tree species composition) which also affects fire patterns (Rupp et al., 2002; Westerling et al., 2006).
- Fire can also provide a feedback on itself, since increased burning activity can reduce the overall fuel load and/or affect vegetation structural properties that affect burn patterns and emissions in turn.
- Human fire prevention and suppression strategies may also significantly affect fire regimes.

Global deforestation fires, replacing forest with pastures or crops are estimated to have contributed nearly 20% of pre-industrial to present-day radiative forcing from CO_2 (Bowman et al., 2009). In the absence of a change in the fire regime, fires that are not associated with land cover or land-use change affect the atmospheric CO_2 burden relatively little, since the carbon lost is taken up again by re-growing vegetation. However, understanding the interactions between fire, atmospheric composition and climate, demands a much broader view since burn patterns notably affect the surface energy balance both by changes in albedo, as well as by a change in sensible and latent heat fluxes in the affected regions over the course of vegetation re-growth (Randerson et al., 2006; Macias Fauria and Johnson, 2008).

The BC and OC emissions estimates for forest and grassland fires in the RCP database (Lamarque et al., 2010) for 2000 are based on Global Fire Emission Database (GFED v2, van der Werf et al., 2006, 2010). There is a large interannual variability in emissions and according to van der Werf et al. (2010) the global carbon emissions in 2000 were 17% lower than the 1997–2009 average. The differences vary by region and in boreal Russia, which accounts for over 80% of the carbon emissions in the boreal zone, the 2000 emissions were estimated to be about 10% higher than the average in 1997–2009 (van der Werf et al., 2010).

Figure 4.13 shows the global emissions from forest and grassland fires separated into the contribution from the Arctic Council nations and rest of the world. BC emissions from forest and grassland fires in the Arctic Council nations were about 60% lower than the anthropogenic emissions, but had an equal contribution in the case of OC. A high OC to BC ratio is characteristic for forest and grassland fires and thus the emissions of OC are an order of magnitude higher than BC which is important when considering the total radiative forcing associated with biomass burning. Emissions within the boundaries of the Arctic Council nations account for 9% and 17% of the global totals of BC and OC, respectively. The split between the Arctic Council nations is similar for both BC and OC. Perhaps not surprising considering its areal extent, Russia has the largest share, at about 75% of the totals of both BC and OC, followed by Canada at 15% and United States at about 10%. Emissions from the Nordic countries are estimated to be negligible.

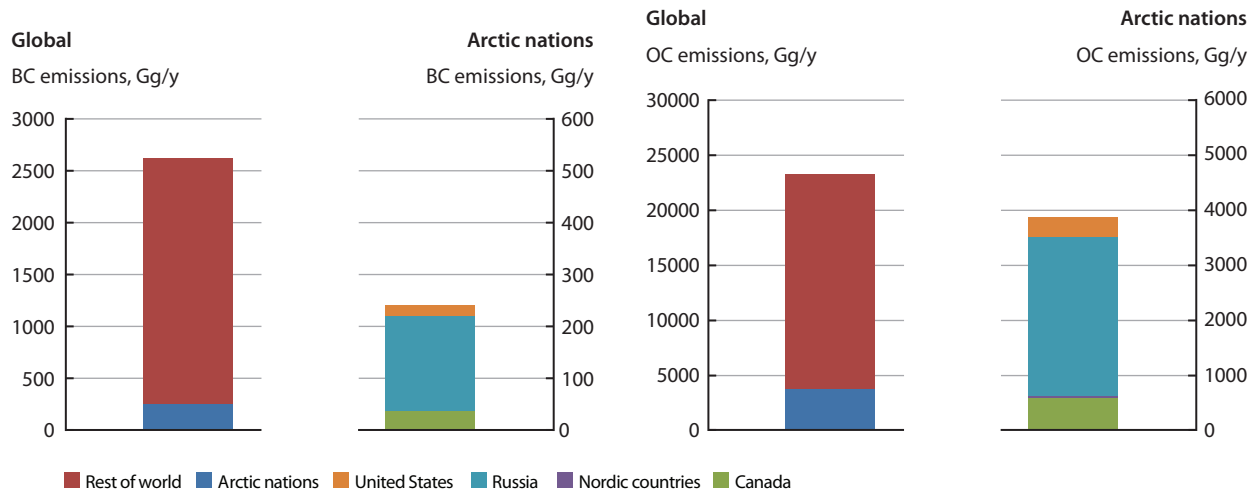

Figure 4.13. Emissions of BC (left) and OC (right) from forest and grassfires globally and in the Arctic Council nations. Emissions from the United States include those south of 40° N. Source: RCP database, van der Werf (2006).

Van der Werf et al. (2010) indicated that their recent update of the GFED database (GFEDv3) has resulted in some changes to regional estimates that have consequences for emissions. Concerning the regions of interest for their study and the year 2000, in boreal North America (Canada and Alaska) the burned area and fuel consumption estimates have increased. For Europe, the United States and Russia the estimates have decreased. As a result of these updates van den Werf et al. (2010) estimated significant increases in carbon emissions, including BC and OC.

Fire activities from forest and grassland fires are concentrated spatially and seasonally, which reflects (especially in case of fires from managed grassland) anthropogenic burn practices, as well as the co-occurrence of dry litter and ignition sources. Significant interannual variations in occurrence and scale of boreal wildfires have been identified for many geographic regions (van der Werf et al., 2010) in response to climate and weather variation. For instance Macias Fauria and Johnson (2008) have related the occurrence of boreal fires in North America with the frequency of mid-tropospheric blocking highs during the fire season, which are further related to the large-scale climatic patterns such as the Arctic Oscillation (AO, closely related to the North Atlantic Oscillation NAO) and Pacific Decadal Oscillation (PDO, related to the El Niño Southern Oscillation ENSO). The blocking highs are regions of high atmospheric pressure that block the normal westerly flow of air in mid-latitudes for several days and in spring and summer result in clear weather and high temperatures (Burton et al. 2003). Figure 4.14 presents the occurrence of BC emission fluxes in the RCP database by latitude and month for forest and grassland fires indicating that there is a significant emission flux from these sources around 60°N latitude that starts in March-April and lasts until September.

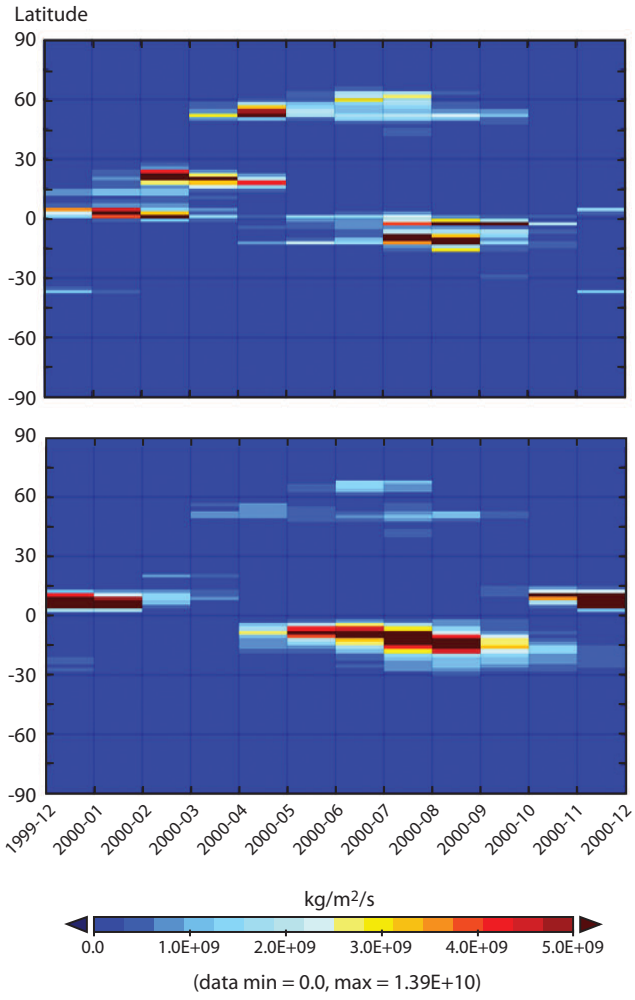

Figure 4.14. Monthly distribution of BC emission fluxes by latitude for forest fires (upper figure) and grassland fires (lower figure). Source: RCP database, van der Werf (2006).

Boreal forests are a substantial source of organic aerosol, and affect secondary organic aerosol (SOA) production from vegetation in an indirect manner. This assessment focuses on the effect of combustion related BC and OC, but a brief discussion of the vegetation SOA is given here. Biogenic volatile organic carbon (BVOC) emitted mostly from woody vegetation is the main SOA precursor. BVOC oxidation products have been shown to condense on pre-existing nano-particles and contribute to their growth and may also be involved in particle nucleation (Carslaw et al., 2010). Boreal forest is especially relevant in this context because of the type of BVOC emitted, which has a large quantity of monoterpenes and sesquiterepenes that have been shown to have a high aerosol yield (Bonn et al., 2004; Tunved et al., 2006; Haapanala et al., 2009; Rinne et al., 2009). Many of the aspects regarding changes in fire regime in response to climate change will also affect emissions of the biogenic SOA precursors, and need to be included in assessment of future biogenic vs. anthropogenic emissions and their climate effects:

- Warming will enhance emissions on leaf scale because of enhanced vapor pressure and enhanced enzymatic productivity.
- Increasing atmospheric CO_2 concentration will indirectly enhance BVOC emissions, by more production of emitting leaf area, but may also inhibit (some) BVOC production in leaves in an as yet not fully understood process (Arneth et al., 2007; Young et al., 2009).
- Changes in vegetation species composition will have large effects on BVOC emission spectra, since different tree species differ greatly in their capacity to emit BVOC, both in terms of quantity and type of BVOC (Niinemets et al., 2010).

4.1.7. BC emission inventory uncertainties

Uncertainties associated with emission inventories are one component that contributes to the overall uncertainty of estimates of radiative forcing by short-lived climate forcers. A comprehensive quantitative uncertainty estimation of emission inventories of carbonaceous aerosol was presented by Bond et al. (2004). Their analysis shows that BC emission estimates are subject to major uncertainties due to knowledge gaps in emissions parameters as well as activities in major emitting sectors.

According to Bond et al. (2004), the global emission uncertainties expressed as 95% confidence intervals were 3.1 to 10 Tg/y (-30% to +120%) for anthropogenic BC emissions and 1.6 to 9.8 Tg/y (-40% to +200%) for open biomass burning. The respective ranges for OC

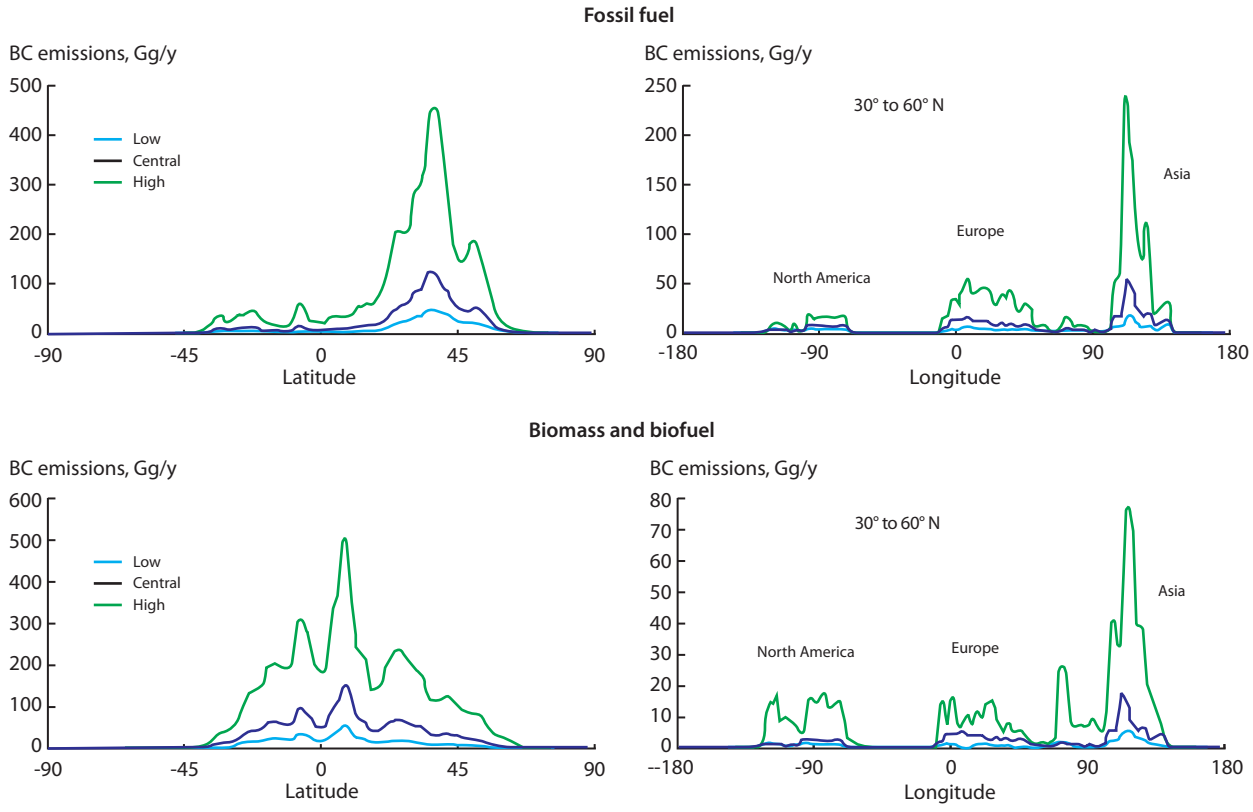

Figure 4.15. Uncertainties in BC emissions from fossil-fuel and biomass and biofuel sources by latitude (left) as well as longitudinal average emissions over 30° to 60° N (right). Source: Bond et al. (2004).

were 5.1 to 14 Tg/y (-40% to +100%) and 13 to 58 Tg/y (-50% to +130%). The top four sources of uncertainty in global emissions were identified as emissions from Chinese coke making, residential wood combustion, industrial coal combustion, and on-road diesel emissions. Bond et al. (2004) also made a qualitative regional assessment of key sectors contributing to uncertainties. Residential wood burning and diesel transport emissions (both on- and off-road diesel) have been identified as being responsible for most of the anthropogenic BC and OC emissions in the Arctic Council nations and as illustrated by Bond et al. (2004) they also are among the top sectors contributing to the emission uncertainties in the studied area.

Figure 4.15 shows uncertainties in BC emissions by latitude for fossil-fuel as well as biofuel and biomass burning sources. On the left-hand side the emissions are presented by latitude. The right-hand side figure shows the longitudinal average BC emissions within 30° and 60° N, which captures most of the emissions affecting the Arctic area. Largest uncertainty (low-high lines) is estimated for Asian emissions, and the upper confidence limit is about twice the central estimate in most regions (Bond et al., 2004).

Textor et al. (2007) studied the effect of harmonized emissions on inter-model diversity (12 models) of global aerosol burdens and observed that unifying the emission input to the models did not considerably decrease the overall model diversity. They concluded that the fate of aerosol is model dependent and to a large extent controlled by other processes than emission diversity and recommended using an ensemble of model simulations to assess the impact of emission changes. Koch et al. (2009a) drew the same conclusion when comparing model outputs with three different BC emission inventories against measurements of surface concentrations, atmospheric burdens and optical depths. The match between model outputs and measurements did not improve much with different emission inputs. However, the uncertainties in emission estimates are large and efforts to lower them are encouraged.

4.2. Future emissions scenarios

BC and OC contribute to emissions of particulate matter that are already regulated. Hence, a reduction in BC and OC emissions from several sectors is expected in the near future provided that the regulations are enforced in a timely manner, the expected reductions are achieved by the emission control measures, and that the development is not counteracted by unforeseen 'events' (e.g., abrupt changes in international economic activity). This section presents a brief summary of estimated future emission pathways; a more detailed discussion is included in the Arctic Council Task Force on Short-Lived Climate Forcers report (ACTFSLCF, 2011).

Figure 4.16 shows the sectoral distribution of BC and OC emissions in the Arctic Council nations in 2000 and 2005 as well as emission projections for 2020 and 2030 according to two GAINS scenarios:

- The 'CLE GAINS' scenario relies on the 2009 reference scenario of the International Energy Agency and includes current air pollution legislation.
- The 'Low GAINS' scenario uses the same activity scenario as CLE GAINS but assumes the implementation of a mix of ambitious technical and non-technical measures specifically targeting BC and minimizing the net-radiative forcing effect of co-emitted species. The 'low' scenario explores reductions in key sectors via measures that could be realized within the given time horizon provided strong additional incentives

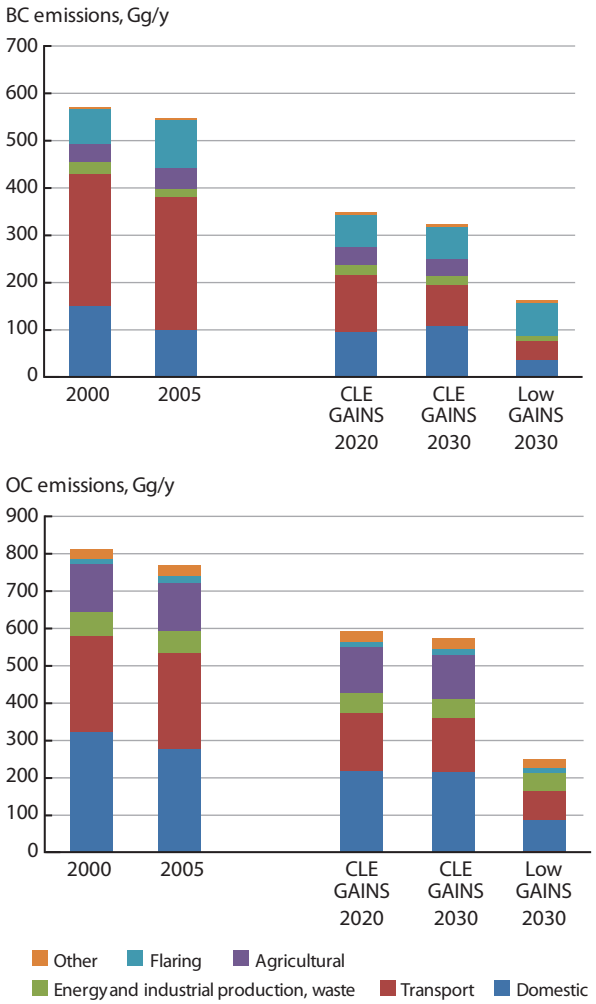

Figure 4.16. Sectoral distribution of BC and OC emissions in the Arctic Council nations in 2000 and 2005 as well as emission projections for 2020 and 2030.

are introduced, either as legislation or economic incentives accelerating certain process; this includes widespread replacement of all stoves and small-scale biomass boilers by pellet installations, use of coal briquettes instead of raw coal in the domestic sector, assuring full penetration of EURO-VI equivalent standard for road and off-road diesels, and the development of programs to eliminate high-emitters as well as open burning of agricultural waste.

BC and OC emissions are expected to decline by 37% and 23%, respectively, by 2020 due to current air pollution legislation alone (CLE GAINS). Further reductions of only a few percent are estimated for 2020 to 2030. The most effective policy measures are the tightening of emission standards in the transport sector but some OC reductions are expected in the domestic sector with the slow switch to more modern and less emitting combustion devices.

The Low GAINS scenario introduces measures to key sectors that are not affected by current legislation, for example the residential sector; or where the enforcement of existing legislation has not been effective, for example the ban on agricultural burning (Korontzi et al., 2007). It also accelerates the introduction of effective technologies in the transport sector. If these measures could be implemented by 2030, they would result in additional reductions of 51% and 56% for BC and OC, respectively, compared to the current legislation scenario.

There are also potential sectors and measures that were not included in the Low GAINS scenario. These include shifting the timing or finding alternatives for agricultural burning of crop residues so that emissions do not reach the Arctic atmosphere as effectively (Pettus, 2009). These measures would be particularly beneficial in Eastern Europe, Russia and northern Asia. Further reductions in BC in the transport sector could, for example, be achieved by introducing diesel retrofits (especially for off-road diesel machinery and stationary engines). Within- and near-Arctic sources, such as shipping and flaring in oil and gas production facilities, could also be targeted.

4.3. BC and OC emissions scenarios outside the Arctic Council nations

Figure 4.17 shows BC and OC emissions outside the Arctic Council nations in 2000 for RCP and GAINS and in 2030 with the CLE GAINS and Low GAINs scenarios. Both estimations show similar emission totals for BC but RCP is slightly lower for OC. In contrast to the emission projections for the Arctic Council nations, outside the Arctic the current legislation scenario is projected to result in BC emissions that increase by 2030 compared with 2000, and OC emissions are projected to remain at a similar level. However, introduction of the measures in the Low GAINS scenario is projected to bring significant reductions for both BC and OC, especially for emissions in the key sectors of transport and domestic combustion. On a regional level the emission changes vary. For example, emissions in the rest of Europe and the OECD countries are expected to closely follow the development presented for the Arctic Council nations. However, since a significant proportion of emissions that reach the Arctic come from outside the Arctic Council nations, the emissions presented here emphasize the need to seek international cooperation in reducing emissions of BC and OC and their impacts in the Arctic.

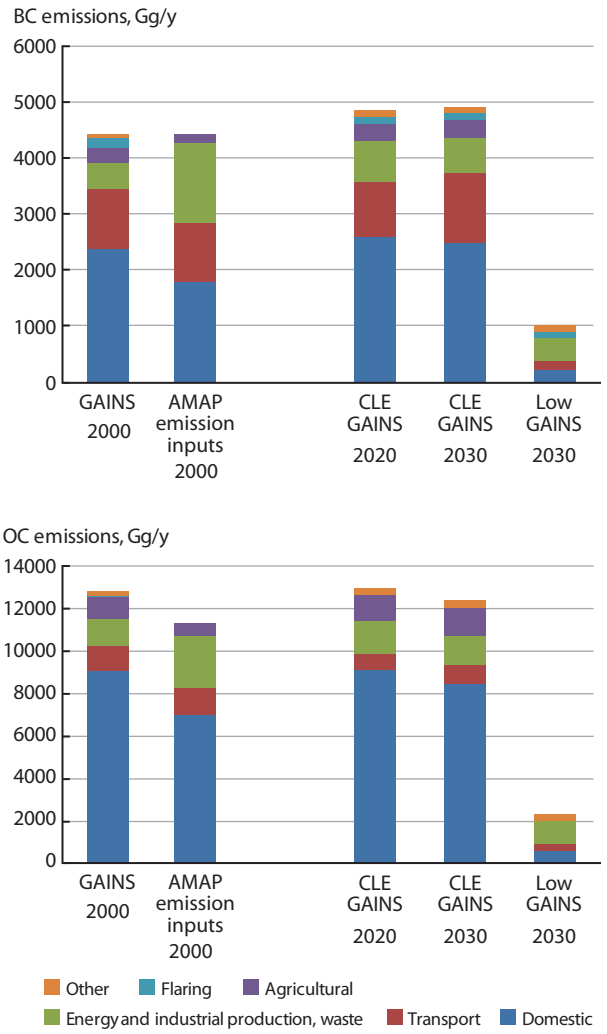

Figure 4.17. BC and OC emissions outside the Arctic Council nations.

4.4. Emissions of co-emitted species

Species co-emitted with BC, including SO_2 and OC, are also affected by the measures included in the

control scenarios. The climate impact of reducing emissions from a given source is dependent on the net-effect of all emitted species, which can be either warming or cooling. The impact of the co-emission of OC is included in this assessment. Other species including CH_4, CO, NO_X, and SO_2 have not yet been considered. However, emission inventories of these co-emitted species have been compiled for the Arctic Council nations for future work. Figure 4.18 shows the emissions of these additional species, together with BC and OC for the Arctic Council nations in 2005 and 2030.

Emissions of NO_X and CO are expected to decline in line with BC and OC by 2030 in the Arctic Council nations following current legislation, especially the implementation of further abatement technologies in the transport sector. In contrast, current legislation will lead to a slight increase in emissions of CH_4, mostly due to increased emissions from oil and gas production and distribution. Furthermore, emissions of SO_2 will decrease sharply following end-of-pipe measures and reductions in the sulfur content of fuel. Further work is needed to assess the net Arctic climate effects of the short-lived climate forcers induced by different emission abatement policies.

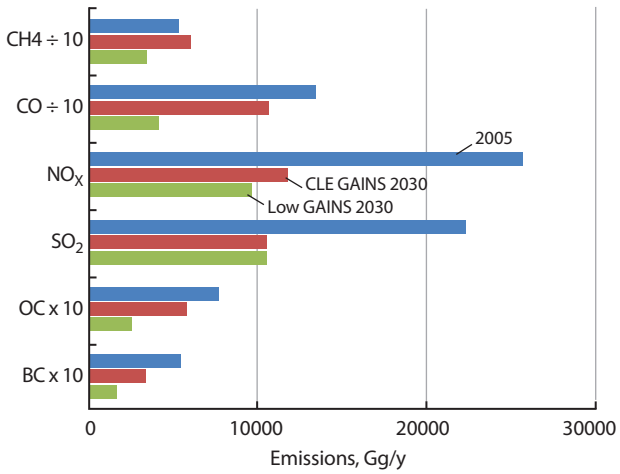

Figure 4.18. Emissions of methane (CH_4), carbon monoxide (CO), nitrogen oxides (NO_X), sulfur dioxide (SO_2) and BC and OC in the Arctic Council nations in 2005 and 2030 under the CLE GAINS and Low GAINS emissions scenarios.

Compared with current legislation, the Low GAINS scenario would bring further emission reductions in 2030 for all pollutants other than SO_2. SO_2 emissions would develop as in the current legislation case. Consequently, its cooling effect is also similar.

5. Transport of black carbon to the Arctic

5.1. Conceptual overview

In order to develop appropriate BC abatement strategies for the Arctic, the sources contributing to Arctic BC must be known quantitatively. There are currently few BC sources in the Arctic itself such that most of the Arctic BC is a result of long-range transport from source regions on the fringes of or outside the Arctic (Law and Stohl, 2007). Source attribution thus relies on correct identification of the major transport pathways and the capability of models to accurately simulate the long-range transport of BC along these pathways and the BC loss processes occurring en route.

Surfaces of constant potential temperature form shells over the Arctic, with minimum values in the Arctic boundary layer, thus building the so-called polar dome (Klonecki et al., 2003; Stohl, 2006), schematically depicted in Figure 5.1. Strong surface inversions lead to extremely high static stability of the Arctic air mass inside the dome, with associated low turbulence intensities (Strunin et al., 1997), which limits both vertical exchange between the boundary layer and the free troposphere and deposition of BC to the ground. Toward more southerly latitudes, the Arctic lower troposphere is also isolated from the rest of the atmosphere by a transport barrier, the so-called 'Arctic front' (Barrie, 1986). Because potential temperature is approximately conserved over short time scales, pollution emitted into the relatively warm air masses south of the polar dome can only be transported into the Arctic along the isentropes leading into the Arctic middle or upper troposphere above the polar dome, i.e., pathways 1 and 2 in Figure 5.1 (Carlson, 1981; Iversen, 1984; Barrie, 1986). Latent heat release by condensation of water vapor will further enhance the ascent. As a result, the lifting is typically associated with cloud formation and precipitation by which BC can be scavenged from the atmosphere and deposited at the surface with the precipitation. Stohl (2006) found that this is almost the only pathway by which BC emitted in the densely populated areas of eastern North America and southeastern Asia can reach the Arctic. Often, however, the lifting will occur over the North Atlantic or North Pacific storm tracks and the BC from these source regions will be deposited south of the Arctic (pathway 2). Only for source regions further north (Europe, Eastern Asia), will the lifting occur at the Arctic front, where BC is more likely to be deposited over snow and ice surfaces (pathway 1).

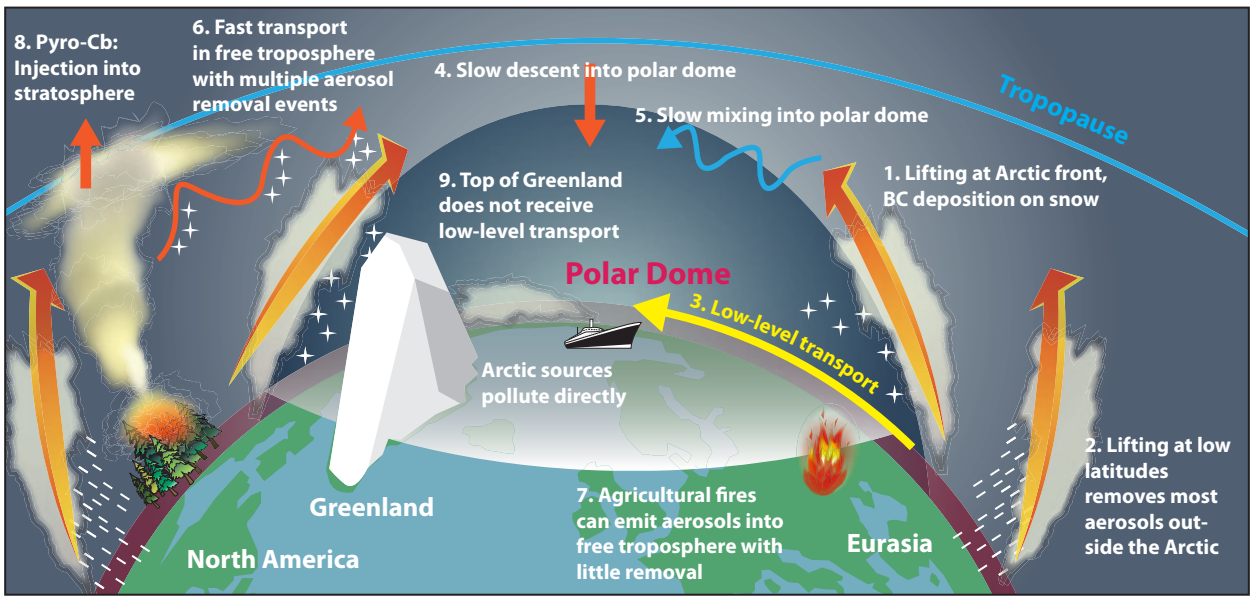

Figure 5.1. Schematic illustration of processes relevant for transport of BC into the Arctic based on the study by Stohl (2006). In reality, the polar dome is asymmetric and its extent is temporally highly variable. In addition, its southernmost extent is greatest over Eurasia. The placement of the polar dome is more typical of the winter/spring situation, whereas in summer the dome is much smaller. Also note that the dome is not homogeneous but is itself highly stratified with strong vertical gradients.

Indeed, BC concentrations in snow samples taken in different parts of Arctic Eurasia are on average a factor of three to four times higher than concentrations in snow in Arctic Canada (Doherty et al., 2010).

For BC to reach the lower troposphere in the Arctic on time scales shorter than a few weeks, its source regions must be sufficiently cold. This is generally only the case in winter and early spring over northern Eurasia where the Arctic front can be located as far south as 40° N on average in January (see figure 1 of Barrie, 1986). Strong diabatic cooling of the air at the snow-covered surfaces in Eurasia not only helps to establish the polar dome itself but also allows polluted air from northern Eurasia to penetrate the entire Arctic at low altitudes on time scales of 10 to 15 days (Stohl, 2006), depicted as pathway 3 in Figure 5.1.

BC can also penetrate the polar dome by slow descent from above (pathway 4) and by slow incorporation of extra-Arctic air via mixing into the polar dome (pathway 5). Both pathways require radiative cooling, which is a slow process (about 1 K/d) and the associated descent from the upper troposphere will take several weeks. Since the Arctic middle and upper troposphere are connected to the middle latitudes on synoptic time scales of a few days, there is no upper tropospheric Arctic air mass with unique properties. Instead, air participating in this descent will involve a mixture of relatively clean background air (pathway 6) as well as anthropogenic and biomass burning pollution plumes from various mid-latitude source regions (Warneke et al., 2009, 2010; Brock et al., 2011). All of the air involved in this process must have been lifted to the middle/upper troposphere, so some or most of the BC will have been scavenged by precipitation (e.g., along pathway 2). Nevertheless, in pollution plumes the free tropospheric BC concentrations can be higher than those near the surface (Spackman et al., 2010). Eventually, the BC that has not been scavenged can be entrained into the boundary layer in the polar dome and reach the surface by dry deposition. Loss of BC at the surface is balanced by inflow from above (Spackman et al., 2010).

At high latitudes in the Arctic, most cloud particles are ice. The settling of ice crystals can redistribute BC from higher to lower altitudes. In addition, the settling wake can lead to the downward transport of additional particles. At more southerly latitudes in the Arctic, thin liquid water clouds occur. In these cases, BC scavenging and wet deposition can be enhanced by riming whereby ice crystals collide with supercooled droplets which freeze on contact.

Biomass burning plumes follow transport pathways to the Arctic that depend on the injection height of the plume. Fire-driven convection can inject aerosols into the free troposphere (pathway 7), thus reducing the efficiency of dry and wet deposition. The result is distinct aerosol layers in the high-latitude free troposphere, which may subsequently be incorporated into the polar dome. Convection over boreal fires can be sufficiently strong to penetrate the tropopause and, thus, can inject aerosols directly into the stratosphere, where their residence time is particularly long (pathway 8).

As a result of the varied transport pathways described above, the source regions of BC found in the Arctic are different for receptor locations near the surface versus those in the middle or upper troposphere (Hirdman et al., 2010a). Figure 5.2 shows the footprint emission sensitivity (a measure of how strongly a surface source of unit strength could have influenced measurements) for four Arctic monitoring stations for transport times of up to 20 days. The station Summit on Greenland is much less sensitive to surface emissions in the Arctic than the other stations but more sensitive to emissions at low latitudes. This is a result of the high altitude of the Greenland Ice Sheet, which is far above the lower shells of the polar dome and, thus, almost isolated from low-level transport. Instead, it is more directly connected to transport from the lower latitudes (pathway 9).

The dependence of source region on altitude has three important implications. First, almost all the BC measurement data available prior to the International Polar Year were obtained near the surface (e.g., Sharma et al., 2004) but these measurements are not representative for BC in the Arctic free troposphere. Indeed, aircraft measurements obtained during POLARCAT campaigns showed that BC concentrations above the Arctic boundary layer can be higher than those in the boundary layer (Spackman et al., 2010; Brock et al., 2011). Second, BC in Arctic snow (Doherty et al., 2010) can originate from dry deposition from the lowest atmosphere as well as scavenging from lower or higher levels in the atmosphere. The sources of BC in Arctic snow will therefore be different to the sources of atmospheric BC at any given level in the atmosphere. They will reflect a mixture of sources for near-surface air (relevant for dry deposition) and sources for BC at altitudes at and below cloud-level (relevant for wet deposition). Third, historical BC records obtained from high-altitude Greenland ice cores (McConnell, 2010) cannot be taken as representative of the overall BC trends at the surface near sea level. Hirdman et al. (2010a) showed that the BC source regions for the station Summit on top of the Greenland Ice Sheet (3208 m above sea level) are located much further south than the BC source regions for Arctic monitoring sites located in the boundary layer. The latter are more influenced by low-level inflow of polluted air from high-latitude Eurasia (see Figure 5.2). If the emission trends in the respective BC source regions are different, then the trends near the Arctic surface and in the free troposphere will also be different.

The transport pathways also vary seasonally. In winter, the Arctic front is located much further south than in summer (Barrie, 1986; Heidam et al., 2004), especially over Eurasia. This allows emissions from high-latitude Eurasia to enter the Arctic via the low-level transport described above. In contrast, in summer the Arctic front approximately follows the northern coastline of Eurasia, which almost eliminates the low-altitude transport pathway. This is one reason why BC concentrations in the Arctic are much lower in summer than winter (Stohl, 2006). However, increased efficiency of wet scavenging in summer is even more important for driving the seasonal cycle of aerosols (Garrett et al., 2010).

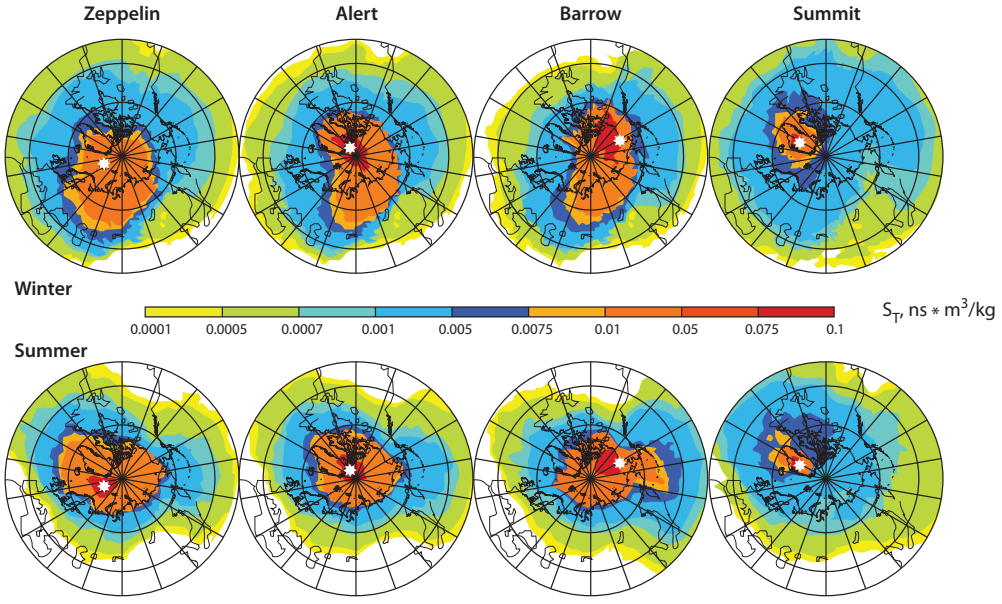

Figure 5.2. Transport climatologies of emission sensitivities for winter (top row) and summer (bottom row) for four Arctic stations (Zeppelin, Alert, Barrow, and Summit) for 2000 to 2007. Station locations are marked by a white asterisk. Source: Hirdman et al. (2010a).

Transport pathways to the Arctic vary considerably on interannual time scales. For instance, during the positive phase of the NAO, transport from all three northern hemisphere continents (Europe, North America and Asia in order of significance) into the Arctic is enhanced (Eckhardt et al., 2003; Duncan and Bey, 2004). While fluctuating efficiency of transport from the middle latitudes into the Arctic influences the interannual variability of Arctic BC concentrations (e.g., Gong et al., 2010), Hirdman et al. (2010b) found that these fluctuations are not strong enough to drive the overall BC trends in the Arctic, despite the long-term trends in the NAO.

5.2. BC source regions

Determining the source regions and/or source types of Arctic BC is difficult. Four different types of approach have generally been used: i) detailed case studies of observed BC pollution episodes; ii) statistical analysis (e.g., by factor analysis) of measurement data alone, leading to identification of major source types; iii) statistical analysis of trajectories or other output from receptor-oriented model runs, often in conjunction with BC measurement data; and iv) explicit calculation of BC source contributions with global aerosol models. As explained below, all these methods have their own problems and often the conclusions reached are contradictory.

Case studies using a combination of BC and other aerosol and trace gas measurements as well as model information often allow reliable identification of the cause of observed enhancements. For instance, Stohl et al. (2006, 2007) and Warneke et al. (2009) attributed dramatic enhancements of Arctic BC levels in summer 2004 and spring 2006 and 2008 to boreal forest fires in North America, agricultural fires in Europe and agricultural/boreal fires in Kazakhstan/Russia, respectively. Such case studies are important for identifying new processes or source categories that had been overlooked. The above studies caused a re-evaluation of Arctic BC, which was previously attributed mainly to anthropogenic sources. However, a reliable identification of the responsible BC sources is normally possible only for extreme cases where the signal is strong and attributable to a single source type/region only. How representative such events are for the overall BC levels is more difficult to quantify. A good example of how case study results can be extended was given by Warneke et al. (2010) who took the relative enhancements in biomass burning plumes over the Arctic background level measured during an aircraft campaign in April 2008 (Warneke et al., 2009) and extended the results with a multi-year transport climatology for a passive carbon monoxide tracer to estimate the average Arctic burden of various species measured by the aircraft. The results show that episodic biomass burning plumes make a small contribution to the Arctic burden for all investigated gas-phase substances, which typically have long lifetimes. However, for aerosols (especially OC and BC) the episodic biomass burning plumes in April 2008 more than doubled the (mainly anthropogenic) Arctic background burden (Figure 5.3 left). While biomass burning in spring 2008 was unusually strong, the contribution of biomass burning averaged

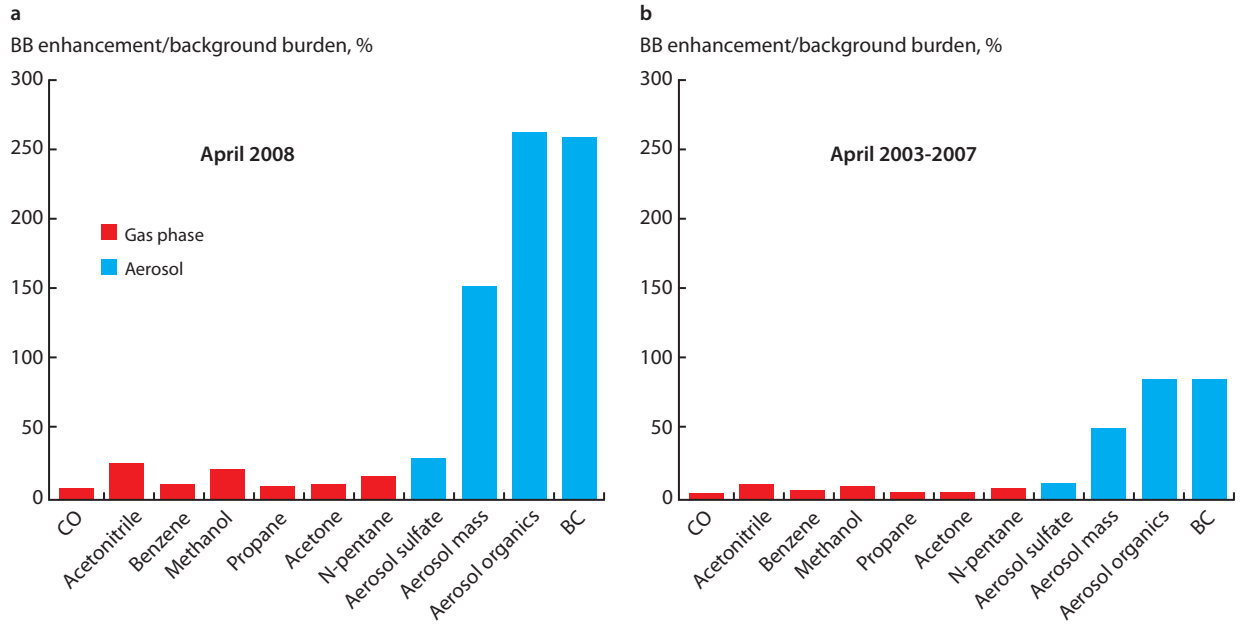

Figure 5.3. Average trace gas and aerosol enhancements due to biomass burning from emissions within the previous 20 days compared to the determined atmospheric background burden in the Arctic (north of 70° N). (a) April 2008 average, (b) April 2003–2007 average. Source: Warneke et al. (2010).

over all April months between 2003 and 2007 was still almost 100% of the contribution from background aerosol loading (Figure 5.3 right), showing the great importance of biomass burning for Arctic aerosol concentrations. Matsui et al. (2011) also showed that high-latitude anthropogenic and biomass burning sources were most important for the Arctic BC loading both in spring and summer 2008, as most of the BC from lower-latitude sources was removed by precipitation before reaching the Arctic.

Joint analysis (using, for example, chemical mass balance or factor analysis) of BC measurements with measurements of tracers for particular source types can enable the identification of contributions from different source types. For instance, von Schneidemesser et al. (2009) quantified the contributions of biomass burning, vegetative detritus and fossil fuel combustion to OC levels observed at Summit, Greenland. However, they could not attribute 96% of the observed OC and concluded that it must be of secondary origin. Hegg et al. (2009) used positive matrix factorization on data from pan-Arctic snow samples and concluded that open biomass burning (agricultural burning and boreal fires) was the dominant source of BC throughout the year.

Anthropogenic contributions from fossil fuel combustion were substantial only in winter. This is in agreement with the results of Warneke et al. (2010) but such high biomass burning fractions appear inconsistent with results from modeling studies (see below). It may be that large contributions from residential wood burning were interpreted as biomass burning as they have similar source signatures.

McConnell et al. (2007) analyzed BC concentrations in an ice core from Greenland and found a strong correlation between BC and a tracer for conifer burning in pre-industrial times, suggesting that boreal forest fires (probably mainly in North America) drove BC levels in Greenland. During industrial times, BC levels have been higher than during the pre-industrial period and the correlation with the conifer burning tracer has been much weaker, suggesting a dominant anthropogenic contribution to BC levels during the 20th century. During the last few decades of the 20th century, BC levels decreased due to reductions in anthropogenic emissions and the biomass burning source could now have become relatively more important.

A major problem when determining source contributions to Arctic BC based on measurement data alone is the aged nature of Arctic air masses, where a large number of different source types and regions can contribute to BC at the same time and the chemical signature of the mixed contribution can be different from any particular source type. The quality of certain tracers can also be degraded by chemical processes. For instance, levoglucosan, an aerosol tracer for wood burning which was for some time believed to have excellent properties as a tracer, was recently found to be degraded in the atmosphere by oxidation processes (Hoffmann et al., 2010), making detection of biomass burning plumes based on levoglucosan potentially difficult.

A large number of studies have performed a statistical analysis of trajectory or other transport model calculations combined with atmospheric BC measurement data. In principle, these methods try to identify the regions from which high measured BC concentrations are coming. For instance, Polissar et al. (1999, 2001) and Sharma et al. (2004, 2006) studied the source regions of BC measured at Barrow and Alert using trajectory statistics. Eleftheriadis et al. (2009) used a similar method for BC measured at Zeppelin station on Svalbard. Huang et al. (2010b) performed a cluster analysis of trajectories arriving at Alert. The studies all attribute the highest measured BC concentrations to Eurasian sources and none of the stations appear to 'observe' a strong influence from North America or southern Asia. For instance, Huang et al. (2010c) estimated that 67% of the BC at Alert in the Canadian high Arctic originated from the former Soviet Union, 18% from the European Union, and only 15% from North America during a 16-year period.

Hirdman et al. (2010a) combined BC concentrations derived from absorption measurements at Alert, Barrow, Summit and Zeppelin with retroplume calculations using a Lagrangian particle dispersion model. The advantage of this method is greater accuracy and a longer accounted transport time (20 days) than for the simpler trajectory calculations (typically ten days or less). For the highest 10% of the measured BC values, northern Eurasia was again identified as the main source region, especially in winter/spring (Figure 5.4). For Barrow and Alert, some influence from boreal forest fires in North America was seen. However, for summer a contribution from air masses descending from the free troposphere was identified without a clear source signature. The lack of a clear source is indicative of the main problem with this method which is even more severe for simpler trajectory calculations. While close or dominant source regions can be reliably identified, it is difficult or impossible to quantify the relative contributions from smaller or distant sources, especially if they are 'hidden' behind large sources. Yet, the unaccounted sources could potentially make a large contribution to the average measured BC. For instance, sources in Japan or China would be difficult to detect if they are masked by Russian sources. Because these are systematic methodological problems, statistical tests

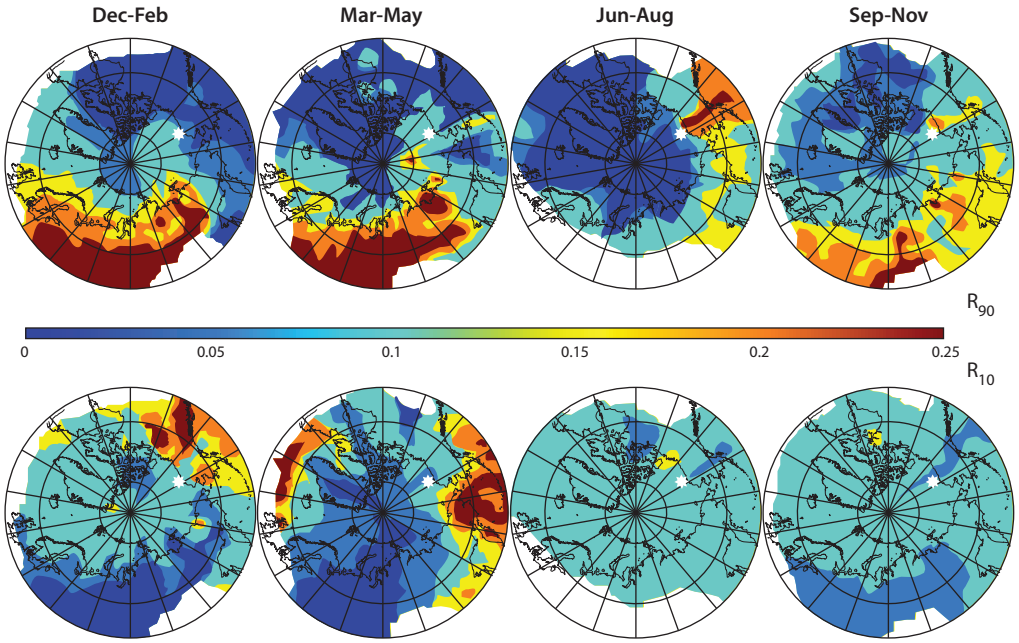

Figure 5.4. Source regions of BC for measurements at the Barrow station during 2002 to 2007, for the four seasons of the year. The results are based on a statistical analysis of BC measurements at the station combined with 20-day backward calculations with a Lagrangian particle dispersion model. The upper row shows where the highest 10% of measured BC originates from and the lower row shows where the lowest 10% of measured BC originates from. The location of Barrow is marked with a white asterisk. White areas have been excluded from the analyses because of insufficient data coverage. Source: Hirdman et al. (2010b).

do not yield proper uncertainty estimates for such contributions, leaving a possibility for contributions from low-latitude sources that cannot be identified.

Hirdman et al. (2010b) classified 3-hourly equivalent BC concentrations into different transport clusters to investigate whether changes in atmospheric transport patterns could have driven BC trends in the Arctic over the past few decades. Figure 5.5 shows the contributions of the different transport clusters to measured BC at Alert, Barrow and Zeppelin. It can be seen that only a very minor fraction of the overall downward trend of BC can be explained by changing frequencies of the different transport clusters. Rather the downward trend of BC must be driven by decreasing emissions in high-latitude regions (cluster AO) and northern Eurasia.

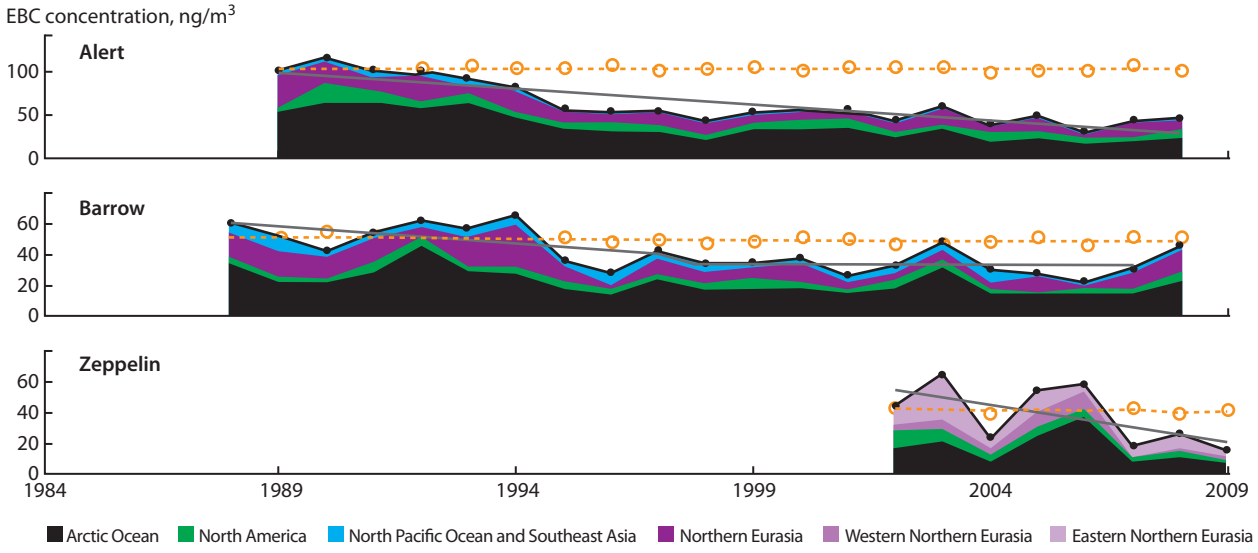

Figure 5.5. Annual mean equivalent black carbon (EBC) concentrations measured at Alert, Barrow, and Zeppelin and split into contributions from four transport clusters (Arctic Ocean, North America, North Pacific Ocean and South-East Asia, Northern Eurasia; for the Zeppelin station, Northern Eurasia is split into a western and eastern Eurasia part). The solid line shows the linear trend through the measured concentrations. The circles show the annual mean EBC concentrations when the cluster-mean concentrations are held constant over time (means over the first three years). This line is influenced only by changes in the frequencies of the four clusters. The dashed line shows the linear trend of these data. Source: Hirdman et al. (2010b).

Finally, chemistry transport models with aerosol schemes have been used to quantify the BC contributions from different source regions and/or source types. The limitation of this approach is that the accuracy of the results depends on the emission data used by the model and the skill of the model to simulate BC transport, ageing and removal processes. Models generally have difficulties simulating the seasonal cycle of BC in the Arctic and BC concentrations during the Arctic haze season are frequently underestimated, although a number of improvements have recently been achieved in some models (see below). In a multi-model study, Shindell et al. (2008) found a large diversity of model results; none of the models could successfully simulate the BC seasonal cycle measured at Barrow and Alert and all models underestimated BC concentrations in winter and early spring. Koch et al. (2009a) compared BC concentrations from several models to airborne observations during the International Polar Year and found that, despite large model diversity, all models underestimated the measured BC column loadings (by up to more than one order of magnitude for individual models). Furthermore, the shape of the simulated vertical profiles did not agree with observations, with the models underestimating BC concentrations throughout much of the troposphere but overestimating concentrations in the upper troposphere and lower stratosphere (Figure 5.6).

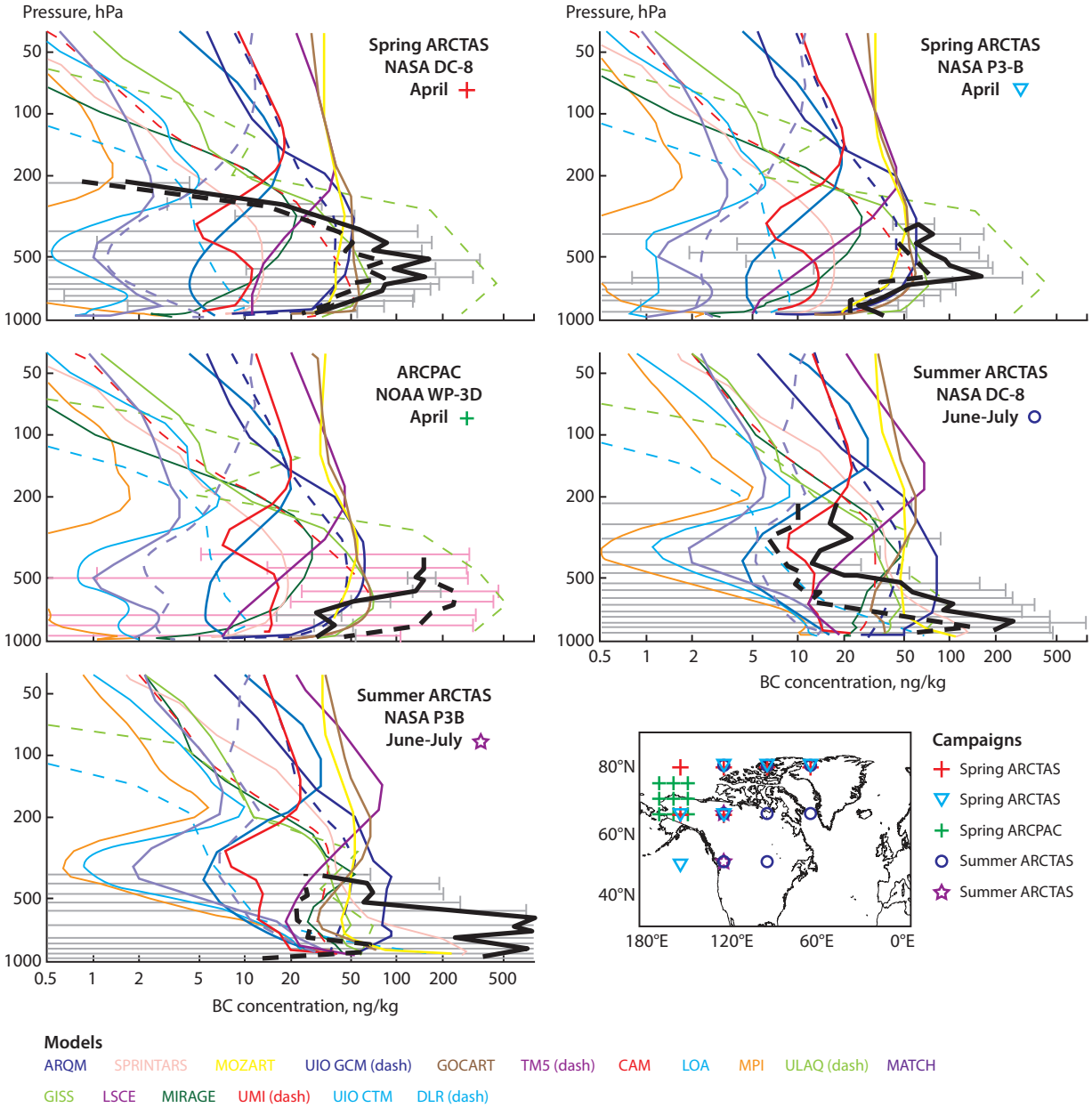

Figure 5.6. Comparison of vertical profiles of BC from a large range of models, averaged over the points in the map, with aircraft measurement data obtained within the framework of the IPY POLARCAT projects ARCPAC and ARCTAS over high-latitude North America in spring and summer 2008. Mean (solid) and median (dashed) observations are shown in black, except for (c) the ARCPAC campaign where the dashed line shows the mean of measurements from flights influenced by biomass burning. Source: Koch et al. (2009a).

Some of the discrepancy between the model output and measured values may be due to systematic measurement errors. In addition, the comparison by Koch et al. (2009a) used year 2000 emissions while the measurements were made in 2008. Nevertheless, the large underestimates by the models indicate the need for model improvement.

The limited and varying ability of models to accurately simulate observations in the Arctic may be due to a variety of reasons. Vignati et al. (2010) found that changes in a model's aerosol scheme (i.e., treatment of microphysical properties and atmospheric removal of BC) alone can change results by more than an order of magnitude in remote regions such as the Arctic. More sophisticated aerosol schemes yield results that are in better agreement with measurements. Liu et al. (2011) found that calculated Arctic BC concentrations were very sensitive to parameterizations of BC aging (conversion from hydrophobic to hydrophilic properties) and wet scavenging. Figure 5.7 shows a comparison of measured and simulated BC concentrations for three Arctic stations using Liu et al.'s (2011) original model version and the version with improved BC aging and deposition parameterizations. Winter concentrations of BC in the Arctic are increased by a factor of 100 throughout the tropospheric column and the seasonality in concentrations is more in line with observations.

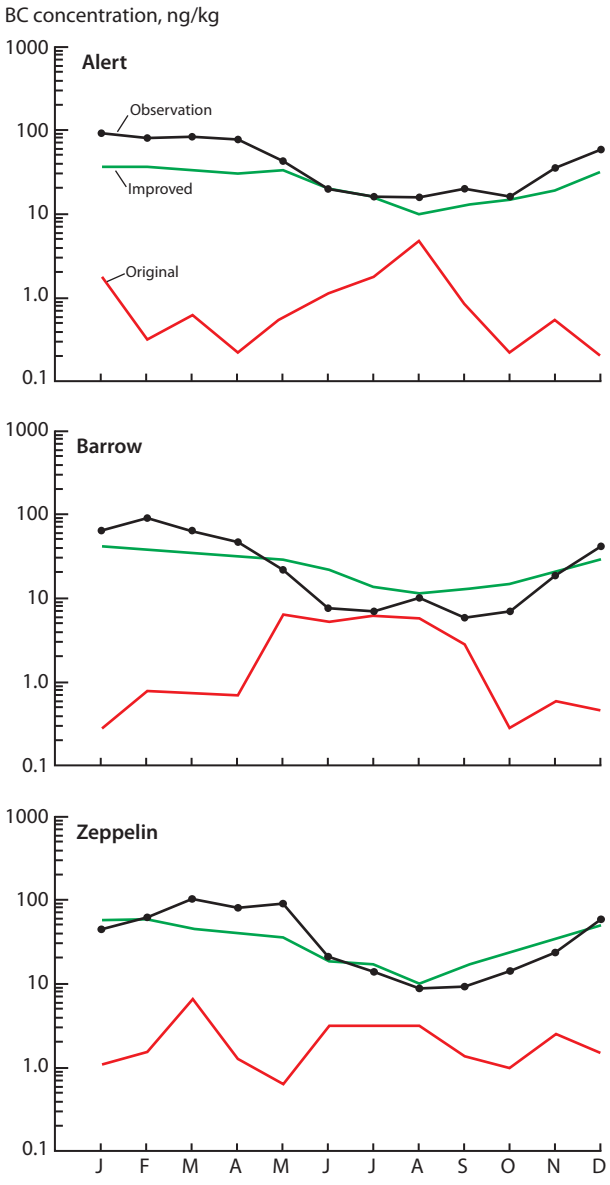

Figure 5.7. Monthly averaged concentrations of measured equivalent BC (black lines) and simulated (red line represents results from original AM3 and green line for improved AM3) BC at Alert, Barrow and Zeppelin. Measurements were made between 2000 and 2007. The simulations use observed sea ice and sea surface temperature from 1996 to 2000. Source: Liu et al. (2011).

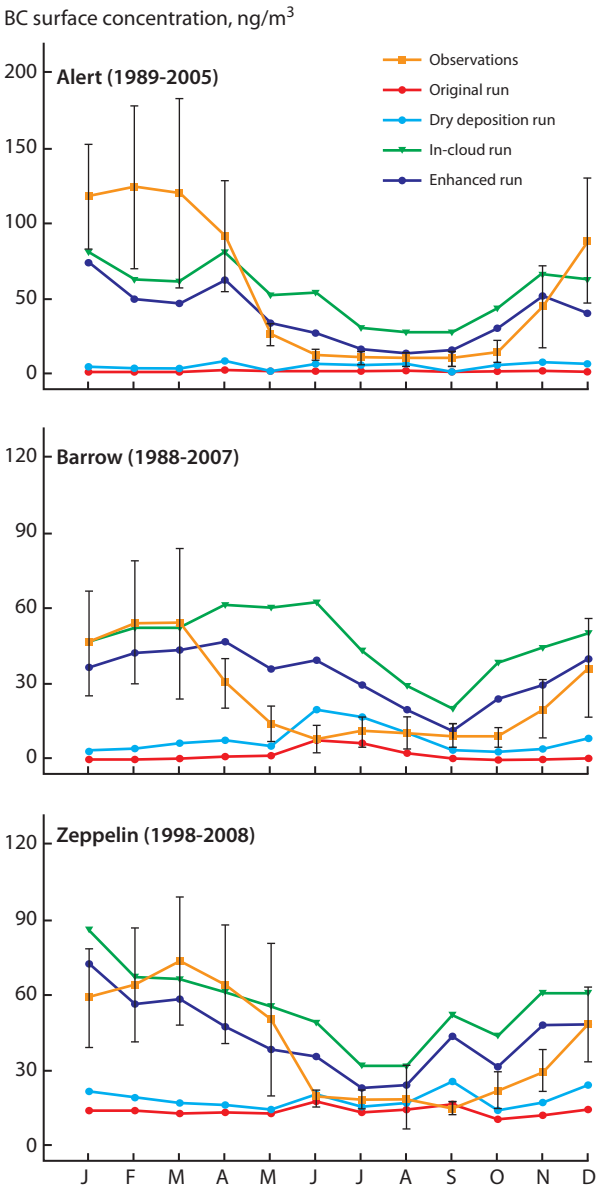

Figure 5.8. Comparison of model simulated monthly average BC surface concentration versus measured concentrations for Alert (1989-2005), Barrow (1988-2007), and Zeppelin (2001). The error bars on the observation curves represent the standard deviation of monthly values. Source: Huang et al. (2010).

Huang et al. (2010b) used different parameterizations of wet and dry deposition in a global air quality model (Global Environmental Multiscale model with Air Quality processes – GEM-AQ) to see how modeled BC concentrations compared to equivalent BC concentrations measured at Alert, Barrow, and Zeppelin. As shown in Figure 5.8, neither the original model set-up nor the configuration with removal by dry deposition is able to capture the seasonality or magnitude in the measured values. This suggests that dry deposition is not the primary removal mechanism responsible for the seasonal cycle of Arctic BC. Seasonal variations are better represented by simulations that include in-cloud and enhanced below cloud wet scavenging at all three sites. In any case, the results indicate the strong sensitivity of modeled BC concentrations to parameterizations of removal mechanisms.

Even for tracers such as carbon monoxide, which have relatively simple chemistry and have lifetimes of the order of four months, models have difficulties in the Arctic (Shindell et al., 2008). The resulting discrepancies between observations and model results is most likely to be a result of the limitations of Eulerian models to simulate the long-range transport of pollution plumes because of their inherent numerical diffusion (Rastigejev et al., 2010), a problem that affects model results in remote regions generally but that can be magnified for cross-polar transport (Sodemann et al., 2010).

Given the uncertainties discussed above, it is not surprising that global models give very different regional source contributions for Arctic BC. For instance, Koch and Hansen (2005) attributed 30% of the Arctic BC burden to anthropogenic sources in southern Asia, in contrast to most of the results based on analysis of observation data, which attribute most of the Arctic BC to biomass burning and high-latitude Eurasian anthropogenic sources (e.g., Eleftheriadis et al., 2009; Gong et al., 2010; Hirdman et al., 2010a; Matsui et al., 2011).

Output from a hemispheric-scale model is presented in Figure 5.9 for comparison with the ability of global-scale models to capture the seasonality

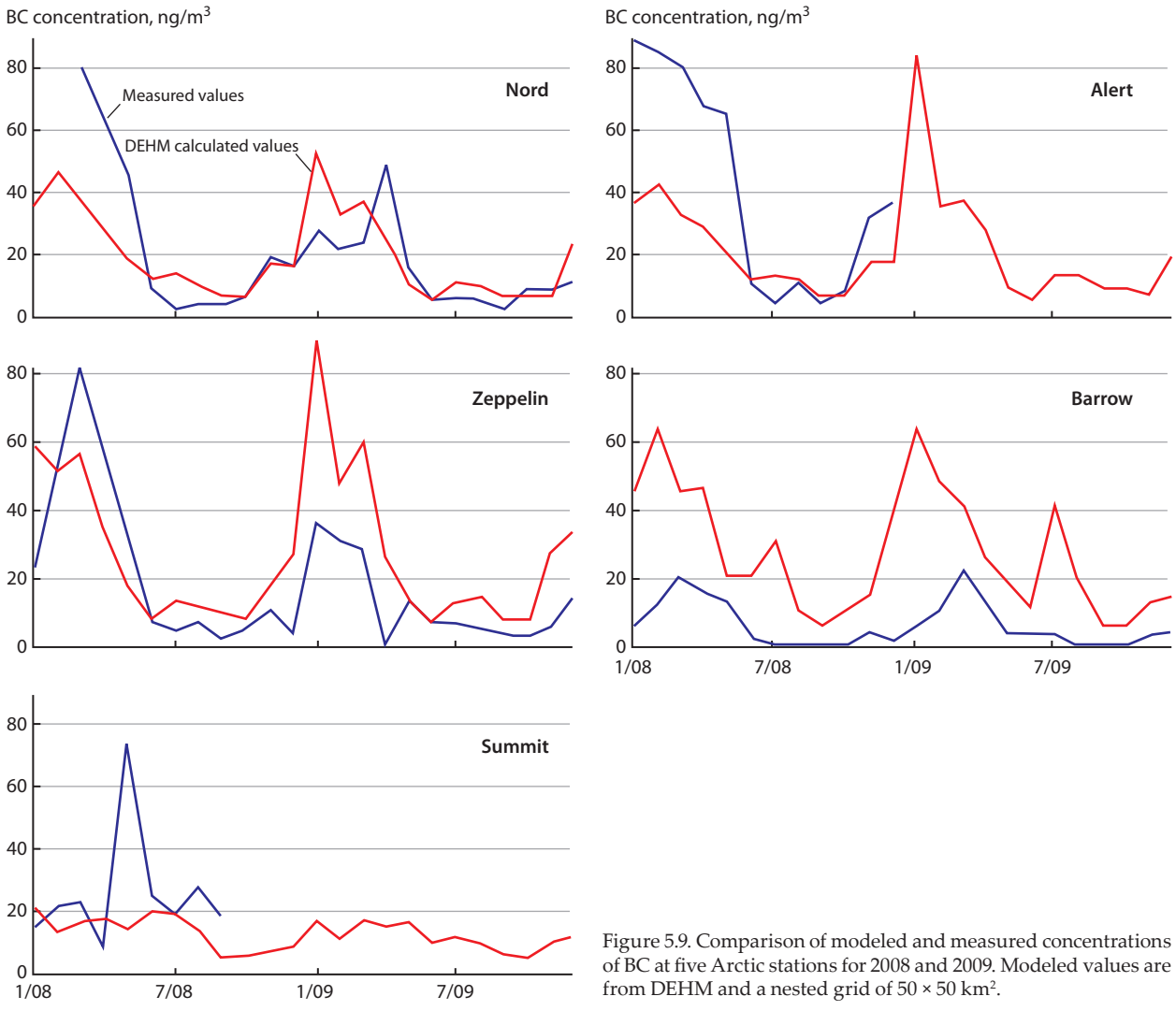

Figure 5.9. Comparison of modeled and measured concentrations of BC at five Arctic stations for 2008 and 2009. Modeled values are from DEHM and a nested grid of 50 × 50 km².

and magnitude of Arctic BC concentrations. BC concentrations simulated by the Danish Eulerian Hemispheric Model (DEHM) (Christensen, 1997) are compared to measured concentrations of equivalent BC at five Arctic stations (Station Nord, Alert, Zeppelin, Barrow, Summit). For Station Nord, Alert, and Zeppelin, the seasonal variation is reproduced qualitatively by the model. For Station Nord, Alert and Spitsbergen the model underestimates BC concentration in winter 2008 and overestimates measured values in winter 2009. At Barrow there are large discrepancies between measurements and model results with the model overestimating concentrations by up to a factor of six. With the exception of one month, model values are within a factor of two of the measurements for Summit.

Finally, monthly averaged BC concentrations simulated by the two global models used in this study (NCAR CCSM and Olso CTM2) are compared to measured values from the five Arctic stations (Figure 5.10). For this comparison, the model simulations were performed by calculating the meteorological data in a forecast mode using emission inventories from year 2000 while the measurements are from 2008 and 2009. Given the difference in emissions and meteorology between these years, the comparison is qualitative in nature. At all five stations, both models underestimate the measured equivalent BC concentrations with the degree of underestimation more severe for the NCAR CCSM simulations. The Oslo CTM2 simulations capture the seasonality in the observed BC for Nord, Zeppelin, and Alert. Both models calculate a peak in BC concentrations at Barrow in the summer rather than in spring.

In summary, observation data suggest high-latitude Eurasia to be the main source region of Arctic BC, with the highest concentrations occurring in late winter / early spring due to efficient transport from Eurasia during that period. Many models find the same source regions to be dominant but some models indicate that lower-latitude sources could also be important. Presumably, the model differences are due to different BC removal schemes and, thus, BC lifetimes in the atmosphere. Removal of BC from

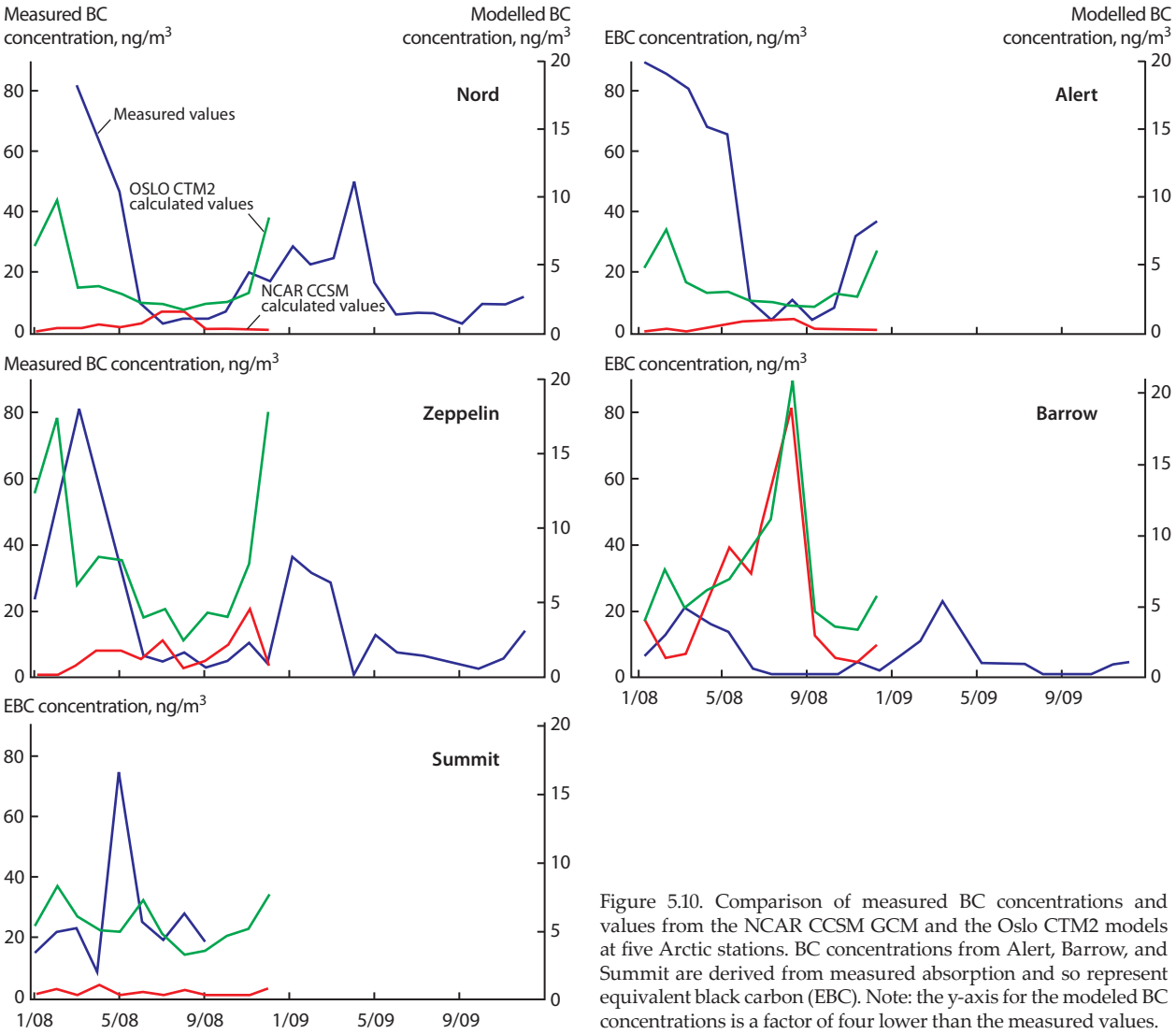

Figure 5.10. Comparison of measured BC concentrations and values from the NCAR CCSM GCM and the Oslo CTM2 models at five Arctic stations. BC concentrations from Alert, Barrow, and Summit are derived from measured absorption and so represent equivalent black carbon (EBC). Note: the y-axis for the modeled BC concentrations is a factor of four lower than the measured values.

the Arctic atmosphere can occur through a variety of processes including wet and dry deposition, settling of ice crystals, and downward transport in the settling wakes. Model treatment of these processes is, in comparison, simplistic.

Analyses of BC data also show that the decrease in BC concentrations during recent decades is due to decreasing high-latitude Eurasian emissions. Recent aircraft observation data suggest a large influence of biomass burning emissions, especially in the Arctic middle and upper troposphere. This result is partly confirmed by models. However, biomass burning emissions used in models is in need of further refinement.

6. Black carbon distribution, seasonality, and trends

Long-term records of BC concentrations in the Arctic atmosphere, based on measurements of aerosol light absorption or EC, are available from four locations: Alert, Barrow, Zeppelin and Summit. The longest of these records are from Barrow and Alert, providing data since 1988 and 1989, respectively. Zeppelin and Summit initiated the observations in the past decade. There are no monitoring networks for deposition or snow concentrations of BC and there are no monitoring programs providing regular, systematic vertical profile information for BC. Given the significant uncertainties associated with modeling BC in the Arctic system (see Section 5.2), this paucity of data represents a major limitation in developing a reliable understanding of the physical processes associated with BC transport and deposition in the Arctic.

In the following section, data available from intensive field campaigns are used to present an overview of the distribution of BC in the Arctic system, with a focus on atmospheric and snow concentrations. In Section 6.2, long-term monitoring data are used to provide a summary of the seasonality of BC in the Arctic environment.

6.1. Distribution of BC

6.1.1. Atmosphere

The magnitude of the atmospheric direct forcing by BC-containing aerosol depends on the spatial and vertical distribution of BC in the atmosphere. BC will have an increased forcing per unit mass when located in the atmosphere above reflective clouds. In a modeling experiment, Zarzycki and Bond (2010) calculated the atmospheric forcing based on the location of the BC aerosol in the atmospheric column. Globally, aerosol over low clouds accounts for 20% of the cases and 50% of the forcing. In the Arctic, where low lying, highly reflective clouds dominate through the summer months the forcing by BC aerosol over low clouds is likely to be even greater.

Limited intensive airborne field campaigns in the Arctic make it difficult to develop a measurement-based characterization of the spatial and vertical distribution of atmospheric BC in the Arctic. In addition, aircraft based research campaigns have focused on biomass burning or industrial pollution so that available data are skewed toward polluted conditions. That said, what is known about the distribution of BC in the Arctic atmosphere from measurements is discussed below.

Liu et al. (2011) used measurements from the POLARCAT ARCTAS campaign to assess the factors controlling transport of BC to the Arctic. Several profiles of BC were developed using CO < 150 ppbv as a cutoff value for biomass burning polluted values (Figure 6.1). Mean values of BC from 0 to 12 km in altitude were found to vary between 5 and 100 ng/kg and reach as high as 1000 ng/kg. There is some indication of enhancement in the lower troposphere during July, but due to the experimental design, this can not be stated conclusively. Presumably, however, an enhancement would result from increased biomass burning activities during the spring and summer periods.

Vertical profiles of BC also were measured during the POLARCAT springtime ARCPAC campaign. Flights over Alaska and the adjacent Arctic Ocean encountered aged polluted Arctic air masses and biomass burning plumes from southern Russia and southeast Siberia (Spackman et al., 2010; Warneke et al., 2010). Average concentrations of BC peaked at 150 ng/kg at 5.5 km in the aged air masses and at 250 ng/kg at 4.5 km in the biomass burning air masses (Figure 6.2) (Spackman et al., 2010). Concentrations in the biomass burning plumes were up to a factor of five greater than those in the aged air masses. For both air mass types, concentrations of BC increased with height in contrast to what is typically observed in the mid-latitudes (Schwarz et al., 2006; Koch et al., 2009a).

BC vertical profiles along with CO concentrations from the ARCPAC flights were used to evaluate deposition of BC to the surface. Near the surface, flights over open leads in the sea ice revealed

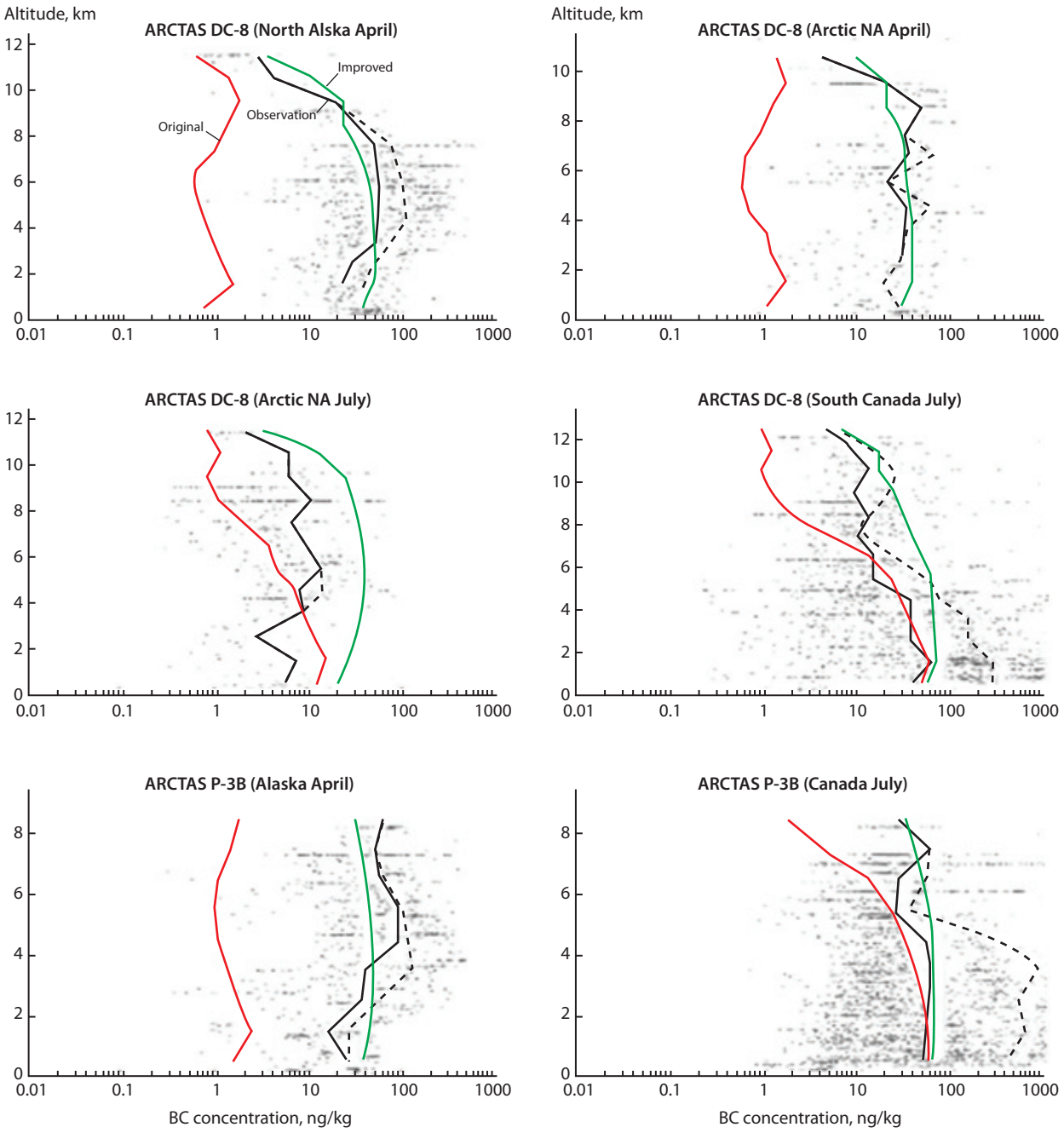

Figure 6.1. Vertical profiles of BC from selected flight tracks during the POLARCAT-ARCTAS campaigns. Black dots represent 1 min average of observed values; the solid and dashed black lines represent mean values over 1 km altitude bins for background (CO < 150 ppbv) and BC concentrations, respectively; the red line is the model profile with the original model configuration; the green line indicates results from improved simulation. Source: Liu et al. (2011).

a positive vertical gradient in BC mass with no similar gradient observed for CO. From these data, Spackman et al. (2010) concluded that open leads in the sea ice increase vertical mixing and entrainment of BC-containing aerosol from the free troposphere which may enhance deposition of BC to the surface.

The ARCTAS and ARCPAC campaigns confirmed observations made during the AGASP experiments in the 1980s. Airborne measurements during AGASP in March and April 1983 revealed episodes of long-range transport of pollution from the mid-latitudes (Schnell, 1984; Parungo, 1990). CO profiles showed enhanced concentrations at lower elevations and 'patchy' haze layers with elevated concentrations at higher altitudes (Parungo, 1990). Hansen and Rosen (1984) reported distinct layers aloft of equivalent BC (Figure 6.3).

Irregular, intensive field campaigns, although limited in their ability to provide a comprehensive picture of pan-Arctic BC profiles, indicate that the Arctic atmosphere is highly structured with respect to aerosols and BC. This vertical stratification has

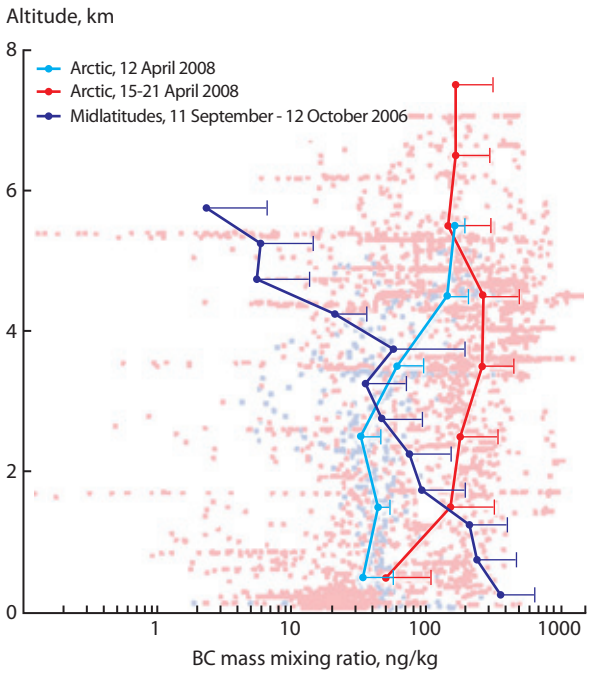

Figure 6.2. Vertical profiles of BC mass mixing ratio during ARCPAC. The data in blue are from a flight in an aged Arctic air mass and the data in red are from four flights in biomass burning plumes. The small dots and line markers denote 30 sec averages and 1 km mean values. The horizontal bars indicate one standard deviation on both sides of the mean but are only shown for the positive side. Source: Spackman et al. (2010).

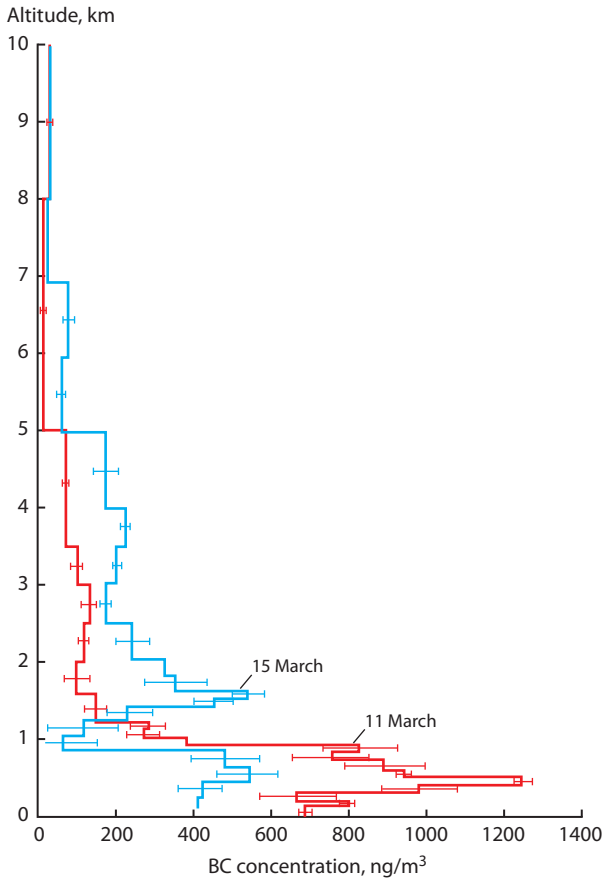

Figure 6.3. Two vertical profiles of BC measured over Barrow during the AGASP flights. Source: Hansen and Rosen (1984).

long been recognized with the first 'banded-haze' structures reported by Navy reconnaissance pilots in the 1950s (Mitchell, 1957). For this reason, surface based measurements must be recognized to only provide a view of concentrations and trends of BC in the lower atmosphere. Routine measurements of the vertical distribution of BC in the atmosphere are required for a complete picture of the distribution of BC in the Arctic and associated climate impacts.

6.1.2. Snow

There is no long-term monitoring program devoted to measuring BC concentrations in snow. Two comprehensive pan-Arctic studies have been conducted (Clarke and Noone, 1985; Doherty et al., 2010) which provide a 'snapshot' of BC concentrations in snow for given times and locations. These data sets comprise individual observations rather than a time series so do not reflect the natural variability that exists due to changes in emission, transport, and deposition. Additional observations have been reported for smaller research campaigns, which are discussed below.

Clarke and Noone (1985) reported concentrations of BC in snow for samples collected in Alaska, the Canadian Arctic, Greenland, Svalbard, and the European Arctic. BC concentrations were derived from measurements of spectral light absorption of filtered snow samples and standards prepared from Carbon Black (Monarch 71, Cabot Corp.). The BC concentration averaged over all samples collected was 25 ng/g with a standard deviation of 18 ng/g. These concentrations correspond to a 2% decrease in albedo of the snowpack and a maximum in BC-snow/ice forcing in June of 5 to 8 W/m^2.

In a follow-on survey to that of Clarke and Noone (1985), Doherty et al. (2010) presented the results of a multi-year campaign that provided widely distributed measurements of BC in Arctic snowpacks. This study, consisting of 1200 samples as opposed to ~60 from Clarke and Noone (1985), provides a more comprehensive picture of spatial and temporal variability of BC deposition in Arctic snow. These measurements indicate that eastern Russia is the most polluted region, with concentrations a factor of two higher than those of the Canadian sub-Arctic, and even higher than those from near Tromsø, Norway, one of the Arctic's largest cities (Table 6.1). Greenland has the lowest concentrations, which are thought to be the most representative of background atmospheric concentrations). Compared to Clarke and Noone (1985), there is an indication of a decrease in concentrations for Canada, Alaska, and Svalbard. It is difficult to assess this decrease quantitatively

(Doherty et al., 2010), however, given the small sample number of Clarke and Noone (1985) and the different analysis methods used between the two studies. However, the expectation is that there should be less BC in the surface snow now, than earlier (matching the atmospheric trends), and there is no evidence contrary to this presumption (Doherty el al., 2010).

In addition to the surveys of Clarke and Noone (1985) and Doherty et al. (2010), snow samples were collected in the Central Arctic, the Amundsen Gulf on the Canadian coast, and the Northern Dvina Delta on the northern coast of Russia (Shevchenko et al., 2010). Concentrations of BC in snow varied from 6 to 52 ng/g (17 ng/g on average) which is in line with those reported by Doherty et al. (2010).

6.2. Seasonality in atmospheric BC concentrations

Measurements of particle number concentration, aerosol light scattering and absorption, and aerosol optical depth made during the AGASP experiments in the 1980s revealed the occurrence of springtime episodes of long-range transport of pollution from the mid-latitudes to Barrow (Schnell, 1984; Parungo, 1990). A continuous record of particle number concentration and light scattering measurements at Barrow between 1976 and 1993 showed the strong seasonality of these transport events with highest values in the spring and winter and lowest values in the summer and autumn (Bodhaine, 1989; Bodhaine and Dutton, 1993). The Barrow long-term data were some of the first to provide evidence for the seasonality in transport pathways to the Arctic as well as the seasonality in wet scavenging as described in Section 5.

Similarly, measurements in the Russian Arctic from research vessels and land sites using an aethelometer reveal information about the seasonality of equivalent BC concentrations at the surface. These measurements, which began in the early 1990s, are summarized in Table 6.2.

In general, the lowest equivalent BC concentrations were recorded in remote background areas (at Wrangel Island, Severnaya Zemlya Archipelago, in the Kara Sea and near Franz Josef Land). For comparison, BC concentrations measured at Zeppelin station, Svalbard from June to September are less than 0.01 μg/m^3 (Eleftheriadis et al., 2009). Average BC concentrations in the marine boundary layer over the White Sea in August in different years varied from 0.12 to 0.55 μg/m^3 depending on meteorological conditions. The lowest BC concentrations were registered in the central part of the White Sea and the highest were in vicinity of the large industrial centre Arkhangelsk (up to 1 μg/m^3) (Pol'kin et al., 2004, 2008).

There is a stable trend of decreasing mass concentration of BC from the end of winter to summer. For example, BC concentrations at Wrangel Island decrease from the start of April to late May; the average BC concentration in Tiksi (Lena River delta) decreased from 0.31 μg/m^3 in February 1995 to 0.064 μg/m^3 in August 1995 (Fukasawa et al., 1997).

The winter/spring pollution resulting from long-range transport has become known as Arctic Haze. Through observations of aerosol optical properties or chemical components, primarily sulfate, Arctic Haze has been detected at several Arctic monitoring sites including Barrow, Alert, Station Nord, Zeppelin, Karasjok (69.5° N) and Svanvik (69.45° N) in northern Norway, Oulanka (66.3° N) in northern Finland, and Janiskoski (69° N) in western Russia (Quinn et al., 2007). However, there are very few long-term measurements of BC or a proxy of BC in the Arctic. The longest published records are for Alert and Barrow; hence they are the focus of the following discussion.

Sharma et al. (2006) published a 15-year record (1989 to 2003) of equivalent BC concentrations from

Table 6.1. Spatial aggregates of BC measurements (2005-2009). Source: Doherty et al. (2010).

		C_{BC}^{equiv} ng/g	C_{BC}^{max} ng/g	C_{BC}^{est} ng/g
Snow samples				
Arctic Ocean, spring	median	12±5	9±3	7±3
Arctic Ocean, summer	median	14±15	10±10	8±8
Canadian& Alaskan Arctic	median	14±7	10±4	8±3
Canadian sub-Arctic	median	20±12	15±9	14±9
Greenland, spring	median	7±3	5±2	4±2
Greenland, summer	median	3±3	2±2	1±1
western Russia	average	34	30	27
eastern Russia	median	48±90	39±59	34±46
Svalbard	median	18±12	14±10	13±9
Tromsø, Norway	median	29±16	24±14	21±12
Sea ice samples				
Arctic Ocean, summer	median	15±20	9±11	7±7

C_{BC}^{equiv} is the amount of BC that would need to be present to account for the wavelength-integrated total light absorption from 300 to 750 nm.

C_{BC}^{max} is the mass of BC per mass of snow if all aerosol light absorption at 650–700 nm is due to BC.

C_{BC}^{est} is the estimated true mass of BC per mass of snow derived by separating the spectrally resolved total light absorption into BC and non-BC fractions.

Table 6.2. Equivalent black carbon concentrations in the atmosphere over the Russian Arctic seas and adjacent land.

Place	Time	BC, μg/m^3	Source
Wrangel Island	April 1989	0.049 ± 0.025	Radionov[a], unpubl. data
Wrangel Island	May 1989	0.025 ± 0.010	Radionov[a], unpubl. data
Tiksi	February 1995	0.31	Fukasawa et al., 1997
Tiksi	May 1995	0.081	Fukasawa et al., 1997
Tiksi	July 1995	0.064	Fukasawa et al., 1997
Severnaya Zemlya	March – May 1990	0.014 – 0.514	Polissar, 1993
N Barents Sea near Franz Josef Land	September 1998	0.07	Kopeikin et al., 2010
White Sea	August 2003	0.55 ± 0.6	Pol'kin et al., 2004
White Sea	August 2006	0.12 ± 0.13	Kozlov et al., 2009
White Sea	August 2007	0.31 ± 0.23	Pol'kin et al., 2008, 2011
Kara Sea	September 2011	0.09 ± 0.21	Pol'kin et al., 2011

[a] Arctic and Antarctic Research Institute (AARI), St. Petersburg, Russia.

Alert and Barrow using filter-based absorption measurements. As for light scattering at Barrow, equivalent BC concentrations were high during the winter/spring season and low during summer at both sites (Figure 6.4). Concentrations during both seasons were shown to vary by one to two orders of magnitude from year to year indicating variability in the strength of sources and transport. The increase in equivalent BC takes place in mid-October at both sites but the rate of increase is faster at Alert. The decrease begins two to three weeks earlier at Barrow (end of March) than at Alert (mid-April). Using a calculated back trajectory analysis, Sharma et al. (2006) showed that both sites are affected by transport from Russia and North America with Alert also affected by Europe and Barrow by the Pacific region. The highest winter/spring concentrations observed at both sites corresponded to transport from Russia but concentrations were lower at Barrow due to a longer transport time from the source region and more opportunity for depositional losses.

While Arctic Haze peaks in winter and early spring, biomass burning is at a maximum in spring and summer. Once snowmelt has occurred in agricultural regions in southern Russian, fires are set to remove plant residue (Soja et al., 2004). Additional burning occurs late in summer after the harvest. Boreal forest fires begin in April and can continue through late summer depending on local conditions. With efficient transport north, fire plumes laden with OC and BC may reach the Arctic and undergo wet and dry deposition during the spring melt resulting in BC-snow albedo forcing and local surface warming (Flanner et al., 2009).

Warneke et al. (2010) reported that episodic biomass burning plumes transported to the Arctic in spring 2008 led to a 260% increase in the

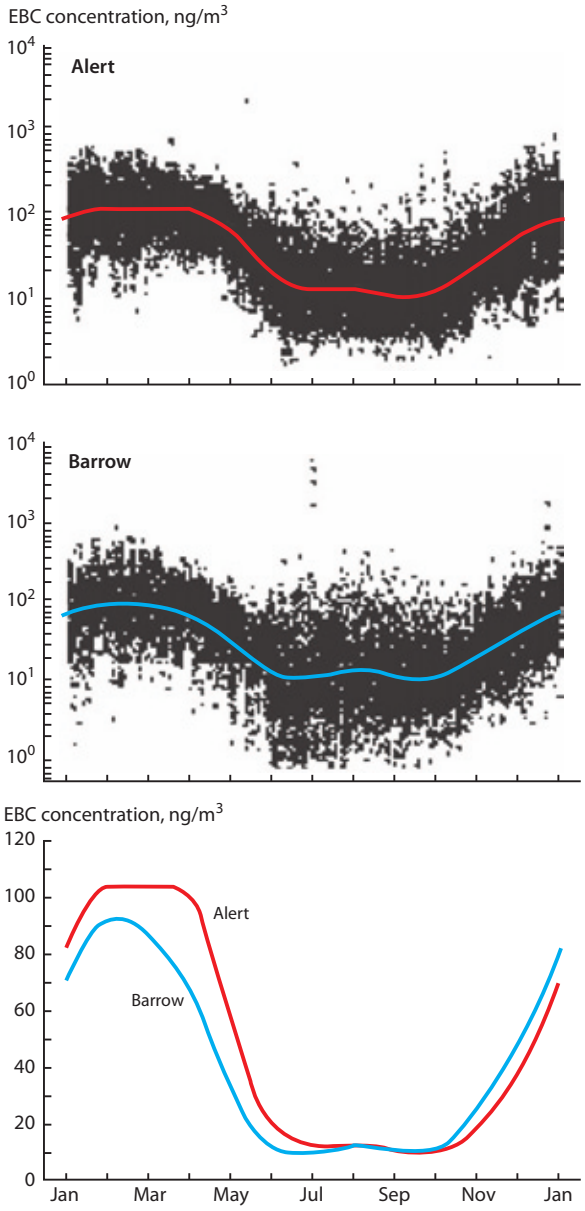

Figure 6.4. Seasonal variability in equivalent BC concentrations at Alert and Barrow. Source: Sharma et al. (2006).

atmospheric burden of OC and BC above the Arctic Haze background. The Arctic Haze background is defined here as anthropogenic emissions from northern Eurasia. April averages from 2003 to 2007 show that the influence of biomass burning was smaller but still increased OC and BC concentrations 80% above the Arctic Haze background. With the likelihood of increased fire activity under a warming climate (e.g., Flannigan et al., 2001), the seasonality of both traditional industrial Arctic Haze and biomass burning must be considered when assessing climate impacts of pollutants transported to the Arctic.

6.3. Trends

6.3.1. Historical trends

The gridded emissions presented by Lamarque et al. (2010) indicate the historical trend in anthropogenic, global BC emissions between 1850 and 2000. Figure 6.5 reveals the generally increasing trend with a peak around 1920 and a rapid rise around 1970. The zonal distribution of emissions between 1750 and 2000 is shown in Figure 6.6. The 1920 peak is due to high emissions in the northern mid-latitudes while the rapid increase between 1970 and 2000 is due to increased emissions at lower latitudes.

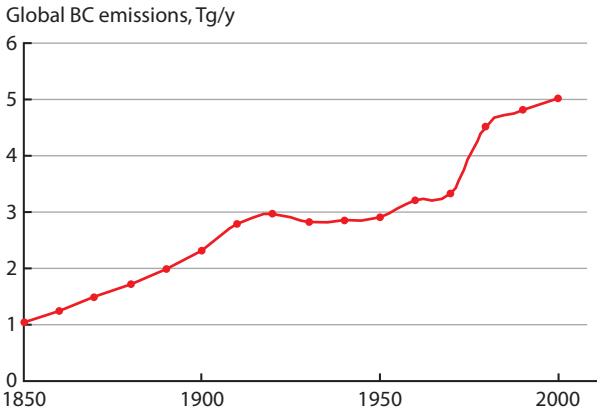

Figure 6.5. Global amount of emission of BC from anthropogenic sources. Source: Lamarque et al. (2010).

6.3.2. Measured trends

Any rigorous analysis of trends in Arctic BC concentrations is based on surface measurements. Aircraft data are too infrequent. As a result, trend analyses yield a picture of the behavior of BC at the altitude of the monitoring site but not at higher altitudes that may be subject to different sources and emissions. The first reported trend analysis for Arctic Haze did not focus on BC or aerosol light absorption but did reveal information about changes in the emissions of pollutants that reach the Arctic. Bodhaine and Dutton (1993) examined the Barrow aerosol light scattering and optical depth data records from 1977 to 1993 for the months of March and April when Arctic Haze is at a maximum. Both aerosol light scattering and optical depth peaked in 1982 followed by a factor of two decrease between 1982 and 1993. Bodhaine and Dutton hypothesized that the decrease was due to reductions in emissions from the former Soviet Union due to economic factors and from Europe due to stricter pollution controls. Other factors including changes in transport could have played a role (Jaffe et al., 1995).

Quinn et al. (2007) examined the March trends in aerosol light absorption at Barrow and found a 61%

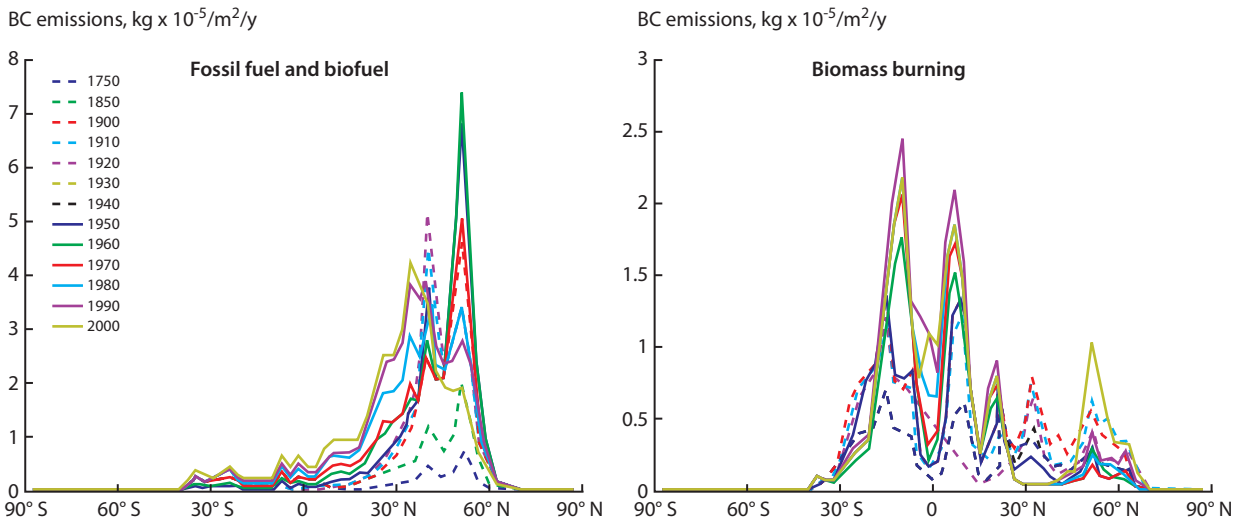

Figure 6.6. Zonal annual mean BC emissions from (a) fossil fuel and biofuel and (b) biomass burning. Source: Skeie et al. (2011).

decrease for the March monthly average between 1988 and 2006. Sharma et al. (2006) performed a similar analysis for Alert and Barrow for the years 1989 to 2003. They reported a decrease in wintertime (January to April) equivalent BC concentrations of 49% for Alert and 33% for Barrow. The differences between the two analyses for Barrow are most likely to be due to the inclusion of different months. The Sharma et al. (2006) analysis indicates a slight increase in equivalent BC at both sites starting in 2000/01 with the increase being greater at Barrow than Alert. Further analysis is required to assess the significance of this trend in the decade to come.

A measurement-based trend analysis of Arctic Haze aerosol based on 30 years of data (1976 to 2008) at Barrow focused on tracer species able to reveal information about the sources of pollutants to the Arctic during the Arctic Haze season (Quinn et al., 2009). Tracers for combustion of heavy residual oil (non-crustal vanadium), fossil fuel combustion (SO_4^{2-}), and anthropogenic mining and ferro-alloy manufacturing (non-crustal manganese) were included in the analysis. It was found that emissions from the source regions to the Arctic had decreased but that the source regions themselves had remained the same over this 30-year period. Further analysis is required to assess if these results also apply to BC.

Ice core data reveal the history of BC concentrations in deposited snow, and indirectly in the atmosphere over the past several hundred years. McConnell et al. (2007) reported BC concentrations from two Greenland ice cores spanning the period 1800 to 2000. Prior to 1850, BC was strongly correlated with vanillic acid, a tracer of biomass burning, indicating a forest fire source early in the data record. From the beginning of the record until ~1850, the correlation coefficient of BC to vanillic acid for annual concentrations is 0.87 ($p < 0.0001$). After 1850, the correlation between BC and vanillic acid decreases in winter but remains strong during summer. The reduced correlation in winter is attributed to an increase in an anthropogenic source of BC. Maximum BC concentrations were found during the period from 1906 to 1910. Concentrations of BC in the ice core range from a pre-industrial minimum of 1.7 ng/g to a maximum in 1908 of 20 ng/g. In the past decade, concentrations ranged between 1 and 10 ng/g, in agreement with most published records of snow observations (McConnell et al., 2007).

Most evidence provided from snow measurements and surface-based atmospheric measurements of BC indicate that less BC exists in the Arctic today than during prior periods. However, a complete picture of BC concentrations in the atmosphere and seasonal and temporal variability remains elusive. While Clarke and Noone (1985) reported that a significant component of the BC atmospheric burden is accounted for in the snow, more recent studies indicate that a significant component of BC is transported through or across the Arctic without being deposited or washed out (Sodemann et al., 2010; Warneke et al., 2010). The recent estimates of radiative forcing (RF) of BC when situated over highly reflective low lying clouds highlight the importance of this portion of the atmosphere, for which there are no long-term observations or proxies.

7. Mechanisms of Arctic climate forcing by black carbon

Black carbon influences the Arctic climate through several different mechanisms, as illustrated in Figure 1.2. First, atmospheric BC directly warms the Arctic atmosphere by absorbing solar radiation that would otherwise have been reflected to space or absorbed by the surface. Second, BC deposited to snow and ice surfaces reduces albedo and enhances solar absorption at the surface, initiating snow and ice melt earlier in the season. Third, cloud distributions, lifetime, and microphysical properties are influenced by aerosols through indirect and semi-direct effects, which alter both the shortwave (solar) and longwave (terrestrial) energy budgets. Fourth, Arctic climate is altered by BC radiative forcing exerted outside the Arctic, via changes in energy transport carried by the atmosphere and oceans, which can similarly amplify or reduce the local impacts of Arctic radiative forcing. These processes are summarized here in the context of the Arctic climate.

7.1. Atmospheric forcing

Direct atmospheric forcing by BC is greatest during summer, when insolation is substantial, and becomes negligible during polar winter. The daily-mean radiative efficiency (units of W/g) of BC in the Arctic summer atmosphere is greater than in most other environments on Earth because of long sunlight exposure and the pervasiveness of reflective clouds, snow, and sea ice, which facilitate strong forcing by absorptive matter (e.g., Cess, 1983).

The following discussions refer to top-of-atmosphere (TOA) and surface radiative forcings. These quantities refer to the instantaneous changes in TOA or surface net radiative energy flux that would occur if the forcing agent (e.g., BC) were suddenly removed. The forcings are often averaged over at least one year to represent annual-mean values. Although surface forcings have a more immediate impact on surface temperatures, TOA values are generally better predictors of global surface temperature response after the surface-atmosphere system has reached equilibrium. For example, all atmospheric aerosols exert negative shortwave surface forcing by reducing the amount of sunlight incident on the surface, but atmospheric heating produced by BC (which has a positive TOA forcing) typically warms the surface after the surface-atmosphere system has fully equilibrated, indicating that the TOA value is more

Figure 7.1. MODIS Terra image at 1935 UTC on 5 July 2004, showing transport of smoke from boreal forest fires (red dots) burning in Alaska and Canada into the Arctic, illustrating the different forcings exerted by the smoke over dark versus bright surfaces. For more information on this case, see Stohl et al. (2006).

representative. When neither 'TOA' nor 'surface' is indicated, a top-of-atmosphere effect is implied.

Aerosol radiative forcing is, in general, strongly influenced by the albedo of the underlying surface, as illustrated in Figure 7.1. All mixtures of BC and OC (including pure OC) exert positive TOA radiative forcing over reflective snow (Flanner et al., 2009), even though OC exerts a negative forcing globally (e.g., Forster et al., 2007). Highly scattering sulfate, with a visible-band single-scatter albedo of the order of 1 to 10^{-7}, exerts a weakly negative forcing over snow. In summer, however, Arctic surfaces are rarely covered uniformly with fresh snow, as leads open up in sea ice and melt ponds form on the surface. These changes in surface albedo contribute to a decrease in atmospheric aerosol forcing. Similarly, it is reasonable to expect that aerosol forcing will become less positive or more negative as cryospheric cover and surface albedo are reduced under a warming climate, thus leading to a weak negative feedback on climate change (Flanner et al., 2009). Just as important as surface albedo, however, is cloud cover. Similar to their effect over snow, aerosols can exert a strong, positive radiative forcing when lofted over reflective clouds and exposed to sunlight. Aerosols beneath thick clouds and shielded from sunlight, however, exert only a weak forcing. Thus, the altitude of aerosol layers and their transport pathways into the Arctic, combined with cloudiness, have an important bearing on direct radiative forcing.

Although there are numerous published estimates of global radiative forcing by BC (e.g., Ramanathan and Carmichael, 2008, and references therein), few isolate the Arctic regional component (although some describe Arctic temperature changes). Koch and Hansen (2005), applying the GISS ModelE GCM, found an annual-mean Arctic (defined here as 60 to 90° N) TOA forcing from global emissions of fossil and biofuel BC of 0.53 and 0.005 W/m^2 from co-emitted OC. Contributions from biomass burning BC and OC were 0.11 and -0.02 W/m^2, respectively. Forcing by biomass burning OC is negative because of greater emissions during summer, when Arctic-mean forcing is negative because of less sea ice, snow, and cloud cover. Flanner et al. (2009), applying the NCAR CAM 3.1 model (Collins et al., 2006), found (from their run 'PD1') a present-day Arctic forcing from all sources of BC and OC of 0.55 W/m^2, similar to Koch and Hansen (2005). It is important to note that there is strong interannual variability in Arctic forcing associated with biomass burning (e.g., Van der Werf et al., 2006), especially in the boreal forest zone. Flanner et al. (2007) showed that Arctic BC+OC forcing varied from 0.49 in 2001 to 0.74 W/m^2 in 1998, due only to differences in biomass burning. Using a version of CAM 3.5 driven with meteorological fields (as opposed to model atmospheric dynamics), Bond et al. (2011) estimated Arctic BC+OC forcing of 0.40 W/m^2. These studies all applied similar inventories of fossil and biofuel emissions, based on Bond et al. (2004).

Simulations discussed in the Section 7.2 show smaller Arctic BC TOA forcings (from all sources) of 0.12 and 0.14 W/m^2 produced, respectively, with the new NCAR CAM 4.0 and Oslo-CTMx models. The cause of lower BC forcing in CAM 4.0 is attributed primarily to lower Arctic BC burdens, as opposed, for example, to a large increase in BC content above clouds. Figure 7.2 shows the annual cycle of Arctic BC burden as simulated with CAM 3.1 (Flanner et al., 2009), CAM 3.5 with offline meteorology (Bond et al., 2011), and CAM 4.0 with model-simulated dynamics (this report). The new CAM 4.0 simulations apply emissions from Lamarque et al. (2010), which are very similar to the emissions used by Flanner et al. (2009) and Bond et al. (2011). Hence, differences in transport and deposition, rather than differences in emissions, appear to be the dominant cause of the reduced burden and forcing seen in CAM 4.0. However, the CAM 4.0 results discussed in Section 7.2 were derived from very short (1-year) simulations, whereas Bond et al. (2011) and Flanner et al. (2009) reported multi-year averages. Hence, it is also possible that initial conditions used for the single year of CAM 4.0 simulations produced an anomalously low Arctic burden, relative to the climate mean state. Additional modeling studies are needed to isolate the roles of model physics, emissions, forcing meteorology, interannual variability and initial conditions in producing these inter-model differences.

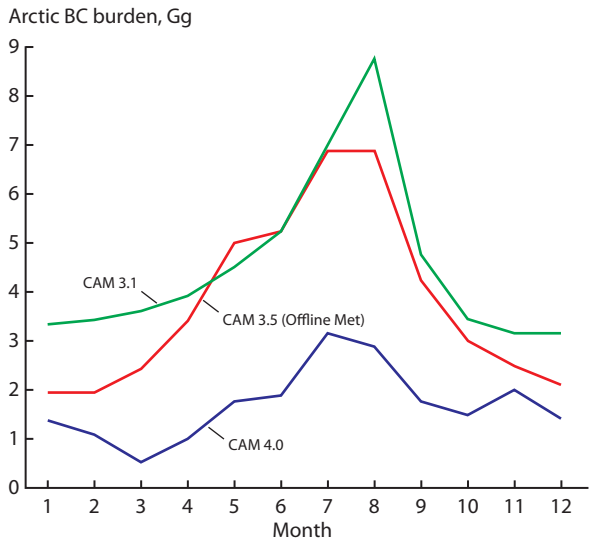

Figure 7.2. Comparison of Arctic BC burden from CAM 4.0 simulations used in this report with previously calculated burdens from CAM 3.1 and CAM 3.5 with offline meteorology.

7.2. Indirect and semi-direct atmospheric forcing

By decreasing cloud droplet size, aerosols can increase cloud optical thickness (the first indirect effect) and cloud lifetime (the second indirect effect) (e.g., Twomey, 1977). Both of these changes exert a TOA cooling effect by causing more solar energy to be reflected to space. Aerosol-induced increases in cloud droplet concentrations also, however, increase cloud emissivity (Garrett and Zhao, 2006; Lubin and Vogelmann, 2006), especially when acting on thin clouds which are prevalent in the Arctic. Increased emissivity leads to increased net surface longwave flux and warming during all seasons. In the Arctic, the net influence of these aerosol indirect effects is likely to be cooling during summer and warming during winter, when the solar cloud cooling effects become negligible (e.g., Quinn et al., 2008).

Aerosols also alter cloud forcing via semi-direct effects. Through atmospheric heating, BC (especially in the upper troposphere) can stabilize the atmosphere and increase low-level cloud formation, which is one reason why atmospheric BC forcing efficacy is found, in some studies, to be less than that of CO_2 (e.g., Hansen et al., 2005). In other circumstances, BC-induced heating can inhibit cloud formation (e.g., through decreased convection associated with increased stability) or increase the evaporation rate of clouds (e.g., through solar heating by interstitial BC), leading to enhanced warming when sunlight is present (e.g., Ackerman et al., 2000; Cook and Highwood, 2004; Jacobson, 2010). Decreased precipitation caused by BC-induced cloud burn-off has the additional effect of increasing BC atmospheric residence time (through decreased wet deposition), which amplifies BC forcing (Jacobson, 2002).

Owing to the challenges associated with modeling these microphysical processes on large scales, the level of scientific understanding of BC forcing via indirect and semi-direct processes, especially within the Arctic, is quite low. Indirect effects associated with ice- and mixed-phase clouds, in particular, are uncertain (Lohmann and Feichter, 2005), and isolation of the BC contribution to indirect cloud forcing is challenging because the incremental influence of BC depends strongly on pre-existing aerosol concentrations and the BC mixing state with other species (especially sulfate). Koch et al. (2009b) reported Arctic-wide TOA cloud indirect forcing (net shortwave + longwave) for all aerosol emission changes between 1890 and 1995 of +0.15 and +0.68 W/m^2, where the two numbers represent cloud changes without and with (respectively) simultaneous greenhouse gas changes. The large difference between these numbers supports the argument that thermodynamic processes (e.g., cloud phase changes associated with a warming environment) have a larger impact on polar cloud forcing than microphysical effects (Jones et al., 2007). Most of the positive indirect forcing reported by Koch et al. (2009b) was attributed to decreased cloud liquid water path, especially during summer, which decreased the cloud shortwave cooling effect. Alterskjær et al. (2010) applied the CAM-Oslo global aerosol/climate model to calculate surface radiative forcing of aerosol indirect effects caused by changes in all aerosols between the pre-industrial and present periods. They estimated a positive longwave surface forcing of 0.55 (0.10 to 0.85) W/m^2, averaged from 71 to 90° N, and a negative shortwave surface forcing of -0.85 (-1.29 to -0.52) W/m^2, where the ranges indicate minimum and maximum values obtained from eleven sensitivity experiments. During winter, the longwave warming effect dominates, while the shortwave cooling effect dominates in summer. In the annual-mean, they suggest the net anthropogenic indirect surface forcing falls between -0.98 and +0.12 W/m^2, with a central estimate of -0.30 W/m^2.

Globally, the indirect and semi-direct effects of aerosols are negative and lead to cooling. Yet, both the sign and magnitude of aerosol indirect forcing in the Arctic are uncertain. Current studies indicate that the net aerosol indirect and semi-direct effects are less negative in the Arctic than in the global-mean, and may even be positive (Koch et al., 2009b; Alterskjær et al., 2010; Jacobson, 2010).

7.3. Snow and ice forcing

Part-per-billion concentrations of BC deposited to snow and sea ice can reduce surface albedo for two main reasons. First, the absorptivity (mass absorption cross-section) of BC is about five orders of magnitude greater than ice in the visible part of the spectrum. Second, multiple scattering in surface snow greatly increases the path-length of photons and the probability that they encounter non-ice particles (Warren and Wiscombe, 1980; Wiscombe and Warren, 1980). Moreover, small changes in snow albedo can exert a large influence on climate by altering the timing of snow melt and triggering snow/ice-albedo feedback (Hansen and Nazarenko, 2004; Jacobson, 2004; Flanner et al., 2007). Hence, snow darkening drives an equilibrium temperature response, per unit of radiative forcing, several times greater than CO_2 (Hansen and Nazarenko, 2004; Flanner et al., 2007; Koch et al., 2009b). The primary reason for this high efficacy is that all of the energy associated with the forcing is deposited

directly into the cryosphere – a component of the Earth System responsible for powerful positive feedback (e.g., Budyko, 1969; Robock, 1983; Flanner et al., 2011), whereas energy associated with other forcing mechanisms is distributed throughout other components. A second reason may relate to snow metamorphism feedback, where accelerated snow aging leads to both darker snow (in the near-infrared spectrum) and greater visible albedo perturbation from absorbing impurities (Flanner and Zender, 2006; Flanner et al., 2007).

Current model estimates of global present-day BC/snow forcing span 0.03 to 0.11 W/m^2 (Jacobson, 2004; Hansen et al., 2005; Flanner et al., 2007, 2009; Koch et al., 2009b; Rypdal et al., 2009; Shindell and Faluvegi, 2009), smaller than the earliest estimate of 0.16 W/m^2 (Hansen and Nazarenko, 2004), which was derived by assuming spatially-homogeneous albedo reductions. A central estimate of 0.04 W/m^2 was achieved (Bond et al., in prep.) by correcting model biases relative to a field survey that included more than 1000 Arctic snow samples (Doherty et al., 2010).

The snow/ice forcing by BC is much greater within the Arctic than in the global mean. Arctic-mean snow forcing in the present-day control simulation ('PD1') discussed by Flanner et al. (2009) was 0.27 W/m^2, with contributions of 0.19 and 0.08 W/m^2 from, respectively, land-based snow and sea ice. Land and sea-ice contributions are nearly equal, however, when averaging over 66 to 90° N instead of 60 to 90° N. In this simulation, Arctic land-based snowpack and sea ice absorbed an additional 0.52 and 0.24 W/m^2 because of BC. There is some interannual variability in snow forcing associated with biomass burning emissions, although significantly less than with atmospheric BC forcing (Flanner et al., 2007). This appears to be due to the seasonality of emissions and Arctic snow/ice cover. Much of the variability in boreal forest fire activity occurs in summer, when there is less snow and ice over which to exert forcing. The importance, however, of variability in agricultural emissions and early-season boreal forest fire activity (e.g., Korontzi et al., 2006; Stohl et al., 2006) needs to be explored in greater detail, as Flanner et al. (2007) only considered two years (1998 and 2001) that differed strongly only in terms of annual-mean emissions. Furthermore, although Arctic-mean snow forcing is much greater than global-mean, roughly 60% of the global snow/ice forcing occurs outside the Arctic.

7.4. Dynamical influence on response to forcing

Finally, radiative forcing exerted by BC outside the Arctic may have a significant influence on Arctic climate via dynamical changes. Similarly, dynamical energy transport may strongly reduce or amplify the impact of Arctic forcing on Arctic climate. Annually, the Arctic radiates much more energy to space than it absorbs from the sun, implying that there is a large net flux of energy transported into the Arctic via the oceans and atmosphere. Most of this meridional energy transport from mid-latitudes to the Arctic is believed to occur via the atmosphere (e.g., Trenberth and Caron, 2001). Because meridional energy transport comprises a significant share (~100 W/m^2) of the Arctic surface energy budget (e.g., Serreze et al., 2007b), small changes in dynamics can translate into large energy forcings on Arctic climate.

Shindell (2007), applying the NASA GISS coupled atmosphere–ocean model, found that aerosol direct, aerosol indirect, and O_3 forcing exerted within the Arctic resulted in a winter temperature response of the opposite sign as the forcing. Spring and summer Arctic climate changes were relatively insensitive to local direct atmospheric aerosol forcing, but autumn climate responded quite sensitively (and with the same sign as the forcing) to both local aerosol and O_3 forcing. Arctic climate response was correlated with both northern hemisphere extratropical (20 to 90° N) and global direct aerosol forcing, and the response was greatest in winter and smallest in summer. Similar results were found by Shindell and Faluvegi (2009), who reported Arctic annual-mean cooling in response to positive Arctic forcing by atmospheric BC, but strong Arctic warming in response to positive forcing by extratropical (28° to 60° N) BC and other short-lived climate forcing agents. Unlike BC, Arctic forcing by SO_4 caused an Arctic temperature response of the same sign as the forcing. Similar studies need to be repeated with other climate models to improve understanding of the importance for Arctic climate of BC forcing exerted in different regions and during different seasons.

7.5. Summary

In summary, processes determining the net Arctic energy budget and climate are complex, introducing uncertainty in understanding the influence of short-lived climate forcing agents on Arctic climate. Some features are, however, clear. Direct radiative forcings within the Arctic by atmospheric and snow/ice-deposited BC are both positive. Co-emitted OC also exerts a direct positive forcing when lofted over snow, ice, and clouds, and the net BC+OC direct forcing within the Arctic (from all sources) is also positive. The two largest sources of uncertainty in translating these forcings into Arctic climate change originate

from i) cloud indirect and semi-direct response to Arctic BC and OC, and ii) dynamical changes in meridional energy transport. Current modeling studies suggest that cloud changes are insufficient to offset the positive direct forcing by Arctic BC+OC, and may even enhance it. Studies conducted with one model (Shindell, 2007; Shindell and Faluvegi, 2009) do suggest that changes in energy transport into the Arctic can be of similar and opposite sign as the local forcing. Including basic treatment of cloud indirect effects and BC/snow darkening, Shindell and Faluvegi (2009) did, however, find that global BC emissions contributed to Arctic warming during the 20th century. Jacobson (2010), applying a model that includes numerous cloud, aerosol, and gas microphysical processes, snow albedo changes from BC, and dynamical energy transport, reported that eliminating all fossil BC+OC and biofuel BC+OC+gas emissions would reduce Arctic warming after 15 years by 1.7 °C. Eliminating only fossil BC+OC emissions would reduce Arctic warming by 1.2 °C over the same time frame.

Finally, the influence of BC and other short-lived forcing agents must also be considered in combination with greenhouse forcing. The Arctic has warmed substantially during the past 20 years, while observations indicate that BC concentrations are likely to have declined. However, as more surface area within the Arctic (integrated over space and time) approaches temperatures where melt can occur, incremental changes in the local energy budget caused by short-lived forcing agents may cause non-linear changes in snow/ice melt, surface albedo, and local climate change.

8. Linking sources to Arctic radiative forcing

8.1. Introduction to modeling studies conducted for this report

Previously reported studies have, for the most part, focused on the transport of BC to the Arctic from broadly defined regions (e.g., North America, Europe, East Asia, South Asia), subsequent deposition, and the resulting radiative forcing (Koch and Hansen, 2005; Flanner et al., 2007; Koch et al., 2007, 2009b; Shindell et al., 2008). The modeling studies conducted for this report focus on the transport of specific sources within and outside the Arctic Council nations to determine their relative contributions to the burden of BC in the Arctic atmosphere and underlying snow and ice. From this information, the radiative forcing by BC and co-emitted OC has been determined for the sources and geographical regions considered. As shown in Figure 1.3, the ultimate goal when determining the impact of BC and co-emitted species on Arctic climate is to establish quantitatively a link between emissions from BC sources, transport to the Arctic, burden in the Arctic atmosphere and underlying snow and ice, sign and magnitude of each radiative forcing mechanism, and the resulting climate response. Linking emissions to climate response, however, requires extensive simulations with fully coupled global climate models. Moreover, climate responses to small radiative forcings (such as caused by emissions from small geographic regions) cannot be distinguished from natural variability without a large ensemble of simulations. The computer (and manpower) required for such an exercise is far beyond the resources available for this assessment. However, very useful information can be drawn from the simple model experiments described below toward identifying effective mitigation strategies.

A series of specific model experiments were conducted to answer the following questions:

1. How much do the individual Arctic Council nations and source sectors contribute to the atmospheric burden of BC in the Arctic and what is the corresponding radiative forcing?
2. How much of the BC burden in Arctic snow and ice and its corresponding radiative forcing is due to each of the individual Arctic Council nations and source sectors?
3. How do these contributions by the Arctic Council nations compare to those of the Rest of the World (ROW) as a whole and by latitude band? ROW refers to all countries that are not Arctic Council nations.
4. What is the estimated radiative forcing due to the projected increases in global and within-Arctic shipping between now and 2050?

How these regional radiative forcings cause an Arctic climate response is addressed in Section 8.4.6 and is based on very limited results published in the literature.

As discussed in the previous sections, BC-containing aerosols can affect the radiative balance of the Earth through a number of mechanisms including aerosol indirect effects that result in a change in cloud properties or cloud distribution. The level of scientific understanding of these processes

is generally very low and quantitatively assessing the magnitude of the resulting forcing requires extensive model experiments. Hence, aerosol-cloud interactions and aerosol indirect effects are not included in the dedicated model experiments described here. This analysis is limited to the direct effect (absorption and scattering of solar radiation by BC-containing aerosols in the atmosphere) and the reduction of surface albedo through BC deposition on snow or the BC snow/ice effect. For both forcing mechanisms, the absolute magnitude of forcing and the forcing per unit emission are averaged annually and over the Arctic. The magnitude of the absolute forcing reflects the size of the emissions from a given source and region and how efficiently those emissions are transported to the Arctic. The forcing normalized by emission indicates the impact of a unit mass from a particular source on Arctic forcing.

8.2. Emissions used

Sources and emissions of BC and co-emitted OC are described in detail in Section 4. The emissions used in this model study were obtained from the compilation by Lamarque et al. (2010), which for BC were based on inventories from Bond et al. (2007) and Junker and Liousse (2008). Within-Arctic shipping emissions were based on the no controls, high growth scenario of Corbett et al. (2010) for 2005, 2030, and 2050 added to the IPCC RCP scenario for 2000.

The BC and OC emissions were split according to region and source sectors for the main Arctic nations or group of countries including the USA, Canada, Russia, and Nordic countries where the Nordic countries include Denmark (including Greenland), Finland, Iceland, Norway and Sweden (Table 8.1) and for the ROW countries. In addition to these country and region specific emissions, a second set of emission data for specific latitude bands was developed. Forcing from global and within-Arctic (north of 60° N) shipping emissions is also quantified.

There is considerable seasonal variation in some of the source sectors listed in Table 8.1. For example, the domestic source is larger in winter than in summer as it includes wood burning for heating. Unfortunately, specific data on the seasonality of the emissions were only available for open biomass burning (grass and forest) at the time of the model simulations. As a result, annually averaged emissions were used for the remaining sources. The lack of seasonality in the domestic sector might lead to an underestimation of the BC-snow/ice effect since too much is emitted during the snow-free seasons, while atmospheric direct RF could be overestimated because of excessive burdens during the sunlit season. For agricultural burning there are spring, summer and autumn emissions, and it is difficult to assess the impact of the lack of seasonality without applying seasonally-resolved emission inventories.

Table 8.1. Regional and sectoral emissions of BC (Gg/y) used in the model experiments.

	Transport		Energy + Industry + Waste		Domestic		Agricultural burning		Grass + Forest burning	
	BC	OC	BC	OC	BC	OC	BC	OC	BC	OC
USA	218	146	93	140	56	200	6.1	29	23	330
Canada	16	12	15	17	3.6	17	1.5	7.2	36	602
Nordic countries	15	6.4	9.7	16	5.8	32	0.3	1.5	0.3	5.4
Russia	32	32	40	51	93	497	7.4	35	179	2910
ROW	1060	1250	1430	2440	1790	7010	130	624	2340	19000

	Total BC	Total OC
60° – 90° N	57	750
50° – 60° N	640	3900
40° – 50° N	810	2100
90° S – 40° N	6260	29100
Global shipping 2005	13.2	142
Global shipping 2030	13.3	142
Global shipping 2050	13.6	145

	BC	OC
Arctic shipping 2005	1.65	2.58
Arctic shipping 2030	2.04	2.21
Arctic shipping 2030	2.63	2.87

ROW: Rest of the World, i.e., countries that are not Arctic Council nations; Nordic countries: Norway, Sweden, Finland, Denmark and Iceland.

8.3. Model description

Two global models participated in the dedicated model experiments described above including the NCAR CCSM4 (Gent et al., in press) as operated at the University of Michigan and the OsloCTM2 operated at CICERO/University of Oslo (Table 8.2).

The CCSM and previous versions of CAM have been used previously in a coupled mode as a climate model to study the climate impacts of BC on snow (Flanner et al., 2007, 2009). For this study, however, the model was set up as an offline CTM (passive aerosols advected with model winds) to efficiently calculate potential climate impacts in terms of radiative forcing. This simpler setup was required due to the objective of the study to quantify the contribution from a large number of combinations of regions and sources (31 altogether).

Parameterizations of the key processes affecting BC vary between the two models. In addition, there are differences in the meteorological conditions. The CCSM is a free-running climate model initialized with Y2000 climate, while the CTM2 uses 'real' meteorological data for 2006 obtained from the European Centre for Medium-Range Weather Forecasts (ECMWF). A key parameter affecting the range of BC transport from different sources is the aging time (see Sections 2 and 5). In CCSM, all BC and OC is emitted in hydrophobic form and becomes hydrophilic with an e-folding time of 1.2 days.

The treatment of BC aerosols in snow is described by Flanner et al. (2007) (and references therein) for the CCSM model and by Rypdal et al. (2009) for the OsloCTM2 model. Both CCSM and OsloCTM2 calculate the BC budget in snow from BC scavenging by precipitation and dry deposition parameters defined by each model. During melting or sublimation, the BC tends to accumulate in the upper layer of the snow. In the OsloCTM2, all BC is retained in the upper layer, while in the CCSM a certain fraction is assumed to be flushed out by the melt water. Heat generated from absorbed radiation by BC in the snow can also lead to growth in snow grain size. Larger grain sizes mean that the radiation can penetrate deeper into the snowpack and the BC becomes more efficient at absorbing radiation, resulting in a positive feedback.

8.4. Model results

8.4.1. Contribution to change in BC burden

In the model results, as throughout the rest of the document, the Arctic is defined as the region extending from 60° to 90° N. Each model was used to calculate the change in the atmospheric burden of BC in the Arctic due to emissions from the different source sectors and regions.

Figure 8.1 shows the change in the Arctic annual tropospheric BC burden (total mass of BC in the lower atmosphere) due to emissions from the different sources and regions considered. In general, there is reasonable agreement between the two models in the calculated changes in BC burdens with respect to the ranking of sources. Emissions from the ROW contribute most to the Arctic BC burden for all source sectors considered except for grass plus forest fires which is dominated by emissions from Russia. For most cases, BC burdens derived from the NCAR CCSM are lower than those derived from the Oslo CTM2. This difference could be due, in part, to the treatment of transport pathways and atmospheric lifetimes by each model. The average global lifetime of BC emitted from all sources from the Arctic Council

Table 8.2. Description and configuration for the two models employed in the AMAP analysis.

	CCSM University of Michigan	Oslo CTM2 University of Oslo
Base model	NCAR Community Climate System Model 4.0	Global offline chemistry tracer model (Skeie et al., 2011). RF calculations: Radiative transfer model (Myhre et al., 2007)
Resolution	1.9° × 2.5° Slab ocean	T42 (2.8° × 2.8°), 40 vertical layers below 30 km
Configuration	Active atmosphere, land, sea ice, and slab ocean model (active ocean/ice needed for sea-ice aerosol forcing). Initial conditions: Y2000 climate	Input of met data: 2006 meteorological fields from ECMWF
Aerosol scheme	Bulk aerosol model (Rasch et al., 2001)	Bulk scheme with aging times depending on season and latitude (Section 3.4)
Snow treatment	Snow aerosol effect: SNICAR (Snow, Ice, and Aerosol Radiative model) (Flanner et al., 2007, 2009). Sea-ice aerosol effect: Briegleb and Light (2007)	BC in snow. Simple column budget module (Rypdal et al., 2009)
Model run length	Model length: 14 month run (2 month spin-up + one full year)	Offline, 2006

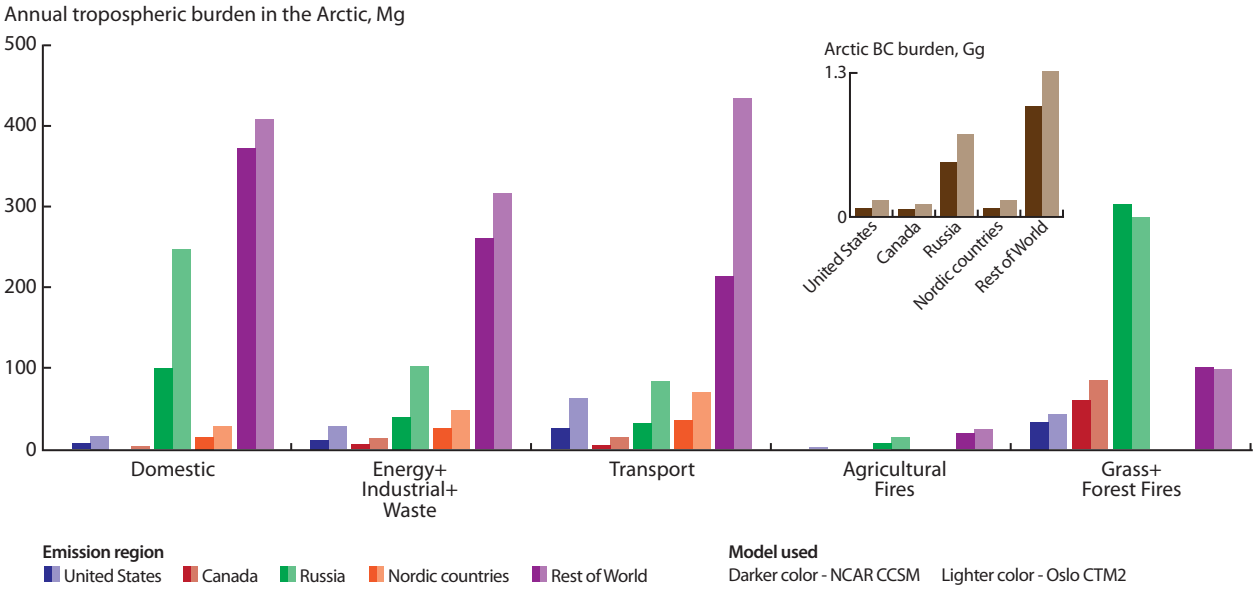

Figure 8.1. Change in the annual tropospheric burden of BC in the Arctic due to the source sectors and regions shown. Calculated change in the burden is shown for the two models used. Arctic burden of BC summed over all source sectors for each region is shown in the inset.

nations is 3.8 days in the CCSM model and 4.7 days in the OsloCTM2 model. With a longer lifetime, more BC reaches the Arctic before removal from the atmosphere. The burden of BC derived from Russian grass plus forest fires is larger as calculated by CCSM than OsloCTM2. This difference may be due to more transport at higher altitudes in CCSM.

The BC burdens in snow were not sampled explicitly in these simulations, only the radiative forcings due to albedo changes were reported. However, both models have reported BC burdens in snow from previous simulations (see Figure 8.2). Both models show a sharp gradient in the BC snow burdens from the source regions at mid-latitudes where the concentrations reach 500 to 1000 ng/g on average over the snowy season (CCSM) or spring (March – May, OsloCTM2). In the Arctic, typical concentrations are 5 to 50 ng/g with higher values in the eastern Arctic and lowest values on the Greenland Ice Sheet. Median BC concentrations measured in Arctic snow samples collected between 2005 and 2009 ranged from 3 to 34 ng/g, with the highest concentrations measured in northeastern Siberia, and the lowest values measured in Greenland (Doherty et al., 2010). The higher atmospheric burdens in the OsloCTM2 model do not translate into higher concentrations of BC in the snow due to assumptions about aging from a hydrophilic to a hydrophobic aerosol. In the OsloCTM2 model, a larger fraction of BC is in a hydrophobic state resulting in a longer lifetime and less susceptibility to wet scavenging compared to the CCSM model.

8.4.2. Contribution to RF in the Arctic

Radiative forcing (RF), annually and globally averaged, has become the standard metric to compare potential climate impacts of different mechanisms on a global scale (e.g., IPCC, 2007). In keeping with this metric, RF annually averaged over the Arctic (60° to 90° N) is presented in this section for the different source sectors and regions considered here.

Atmospheric direct RF averaged annually and over 60° to 90° N due to BC and BC plus co-emitted OC is shown in Figure 8.3 for the different source sectors within the Arctic Council nations and the ROW. The ranking of RF due to the different regions and sources is similar for the two models. For both models, the atmospheric direct RF is largest for ROW emissions in all source categories except for grass plus forest fires which is dominated by Russia. This reflects the large magnitude of ROW emissions relative to those of the Arctic Council nations.

As for the calculated BC burdens, the direct RF due to BC calculated by CCSM is lower than that calculated by CTM2. However, model differences in RF due to grass and forest fires are not as great as the differences in calculated BC burdens for this source sector. CCSM generally gives a higher RF per unit of BC burden change, indicating that more BC is transported to higher altitudes and ends up above cloud, a situation which enhances RF by a dark aerosol. Including the co-emitted OC (Figure 8.3, lower panel) does not change the RF or ranking significantly for most source sectors. An exception is the domestic source in Canada for which the high OC

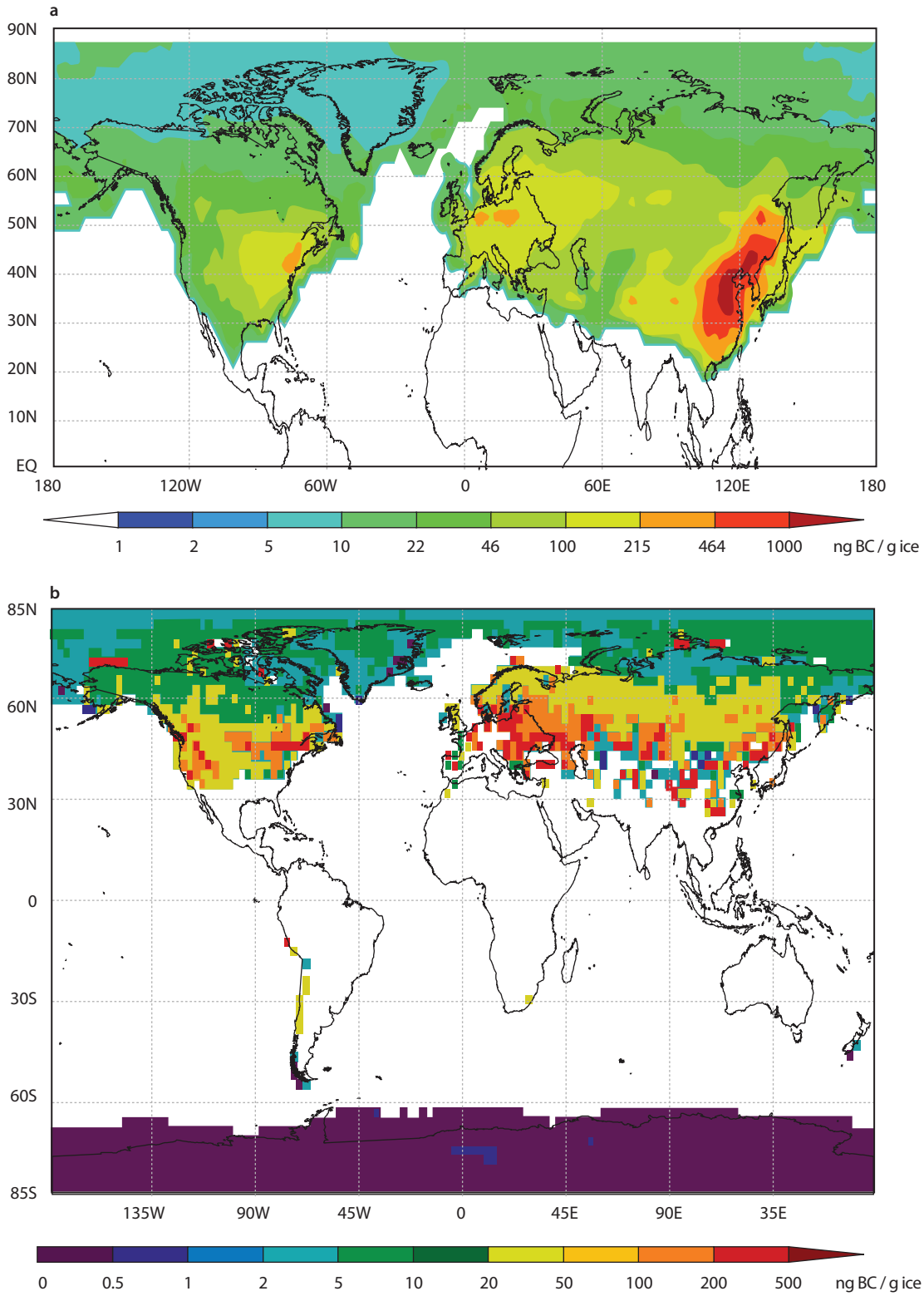

Figure 8.2. Simulated concentrations of BC in snow in the two models from previous simulations (a) BC in snow in 1998 from fossil fuel, biofuel and biomass burning sources of BC estimated using CCSM, Flanner et al. (2007) and (b) BC in snow in 2000 during the period March to May, estimated using OsloCTM2 (Skeie et al., 2011).

content leads to a net negative direct RF. In addition, CCSM calculated RF decreases for grass and forest fires from all regions due to the high OC content. This result may appear to contradict that of Flanner et al. (2009) who showed that OC has a positive forcing over pure snow surfaces. However, here the Arctic forcings are averaged from 60° to 90° N and, during the summer and autumn months, much of this area is not covered by snow or ice. In addition, model grid cells are large and generally have partial surface exposure of open water, bare ice, and vegetation which also decreases the column forcing caused by

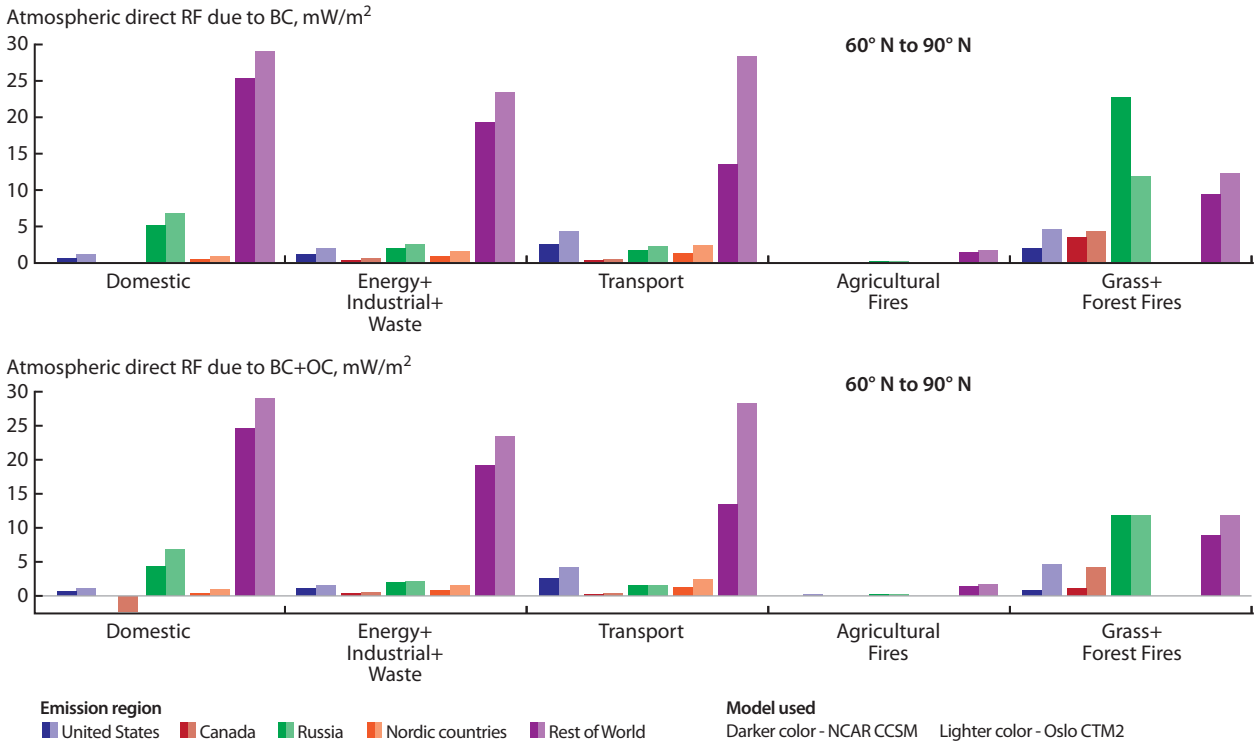

Figure 8.3. Annually averaged atmospheric direct RF due to BC (upper) and BC + OC (lower) aerosols in the atmosphere north of 60° N from the NCAR CCSM and Oslo CTM2 models.

atmospheric OC.

BC deposited on snow and ice reduces the albedo of the surface and leads to a positive radiative forcing with a particularly high efficacy (see Section 7.3). The radiative forcing north of 60° N due to this mechanism as calculated by the CCSM and CTM2 models is shown in Figure 8.4. The BC-snow/ice RF is of the same magnitude as the atmospheric RF. Again, the larger sources from ROW countries and the open biomass burning sources from Russia dominate.

For many of the cases in Figure 8.4, BC-snow/ice RF calculated by CCSM is greater than that calculated by CTM2. This difference may be due to the change in grain size accounted for by CCSM and the resulting enhancement in absorption.

A comparison of the absolute radiative forcing

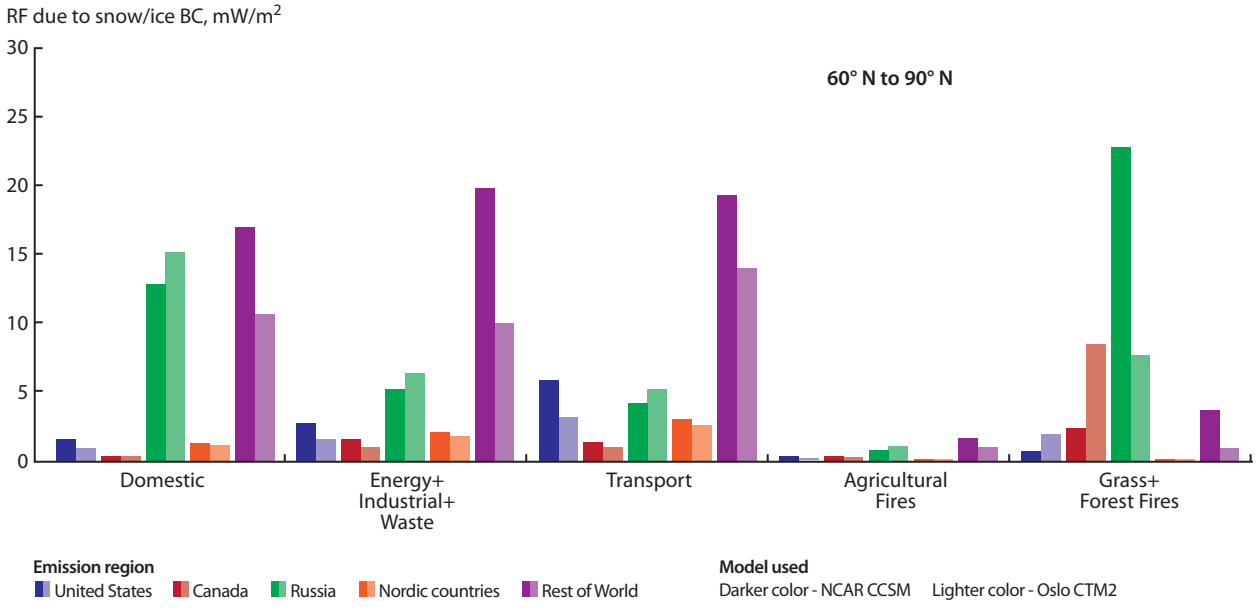

Figure 8.4. Annually averaged RF due to surface albedo reduction of BC aerosols deposited on snow and sea ice north of 60° N in the CCSM and CTM2 models.

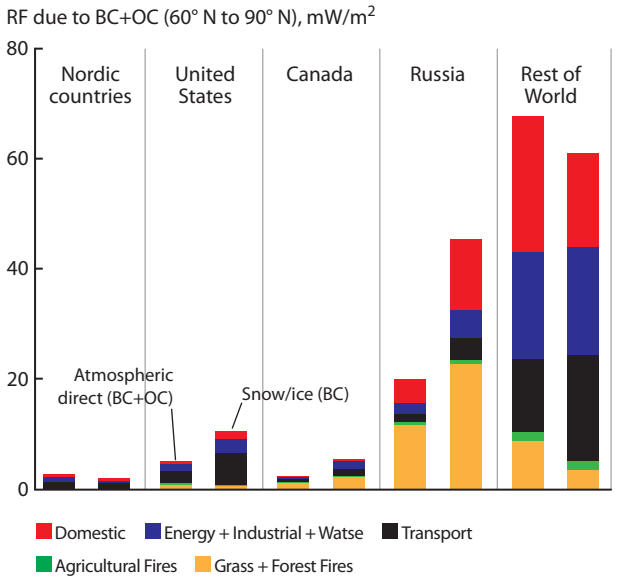

Figure 8.5. Absolute radiative forcing due to BC and co-emitted OC by source sector and region within the Arctic Council nations compared to ROW. Results are from the NCAR CCSM model.

due to emissions from the Nordic countries, the USA, Canada, Russia, and the ROW is shown in Figure 8.5. Absolute RF within the Arctic is greatest for emissions from Russia and the ROW.

8.4.3. RF per unit emission

In order to assess the potential for cost effective mitigation it is of interest to compare various sources in terms of RF per unit of emission. RF for some sources may be relatively small in absolute numbers but may yield a significant RF per kilogram emitted. The model calculations show that emissions from high latitude regions (e.g., from the Nordic countries and the open biomass burning sources from Russia and Canada) have consistently higher RF per unit emitted BC than emissions in lower latitude regions (Figure 8.6). Emissions from the USA and ROW in general have the lowest normalized RFs. Including co-emitted OC does not change the normalized Arctic RFs significantly.

Figure 8.7 shows the normalized BC-snow/ice

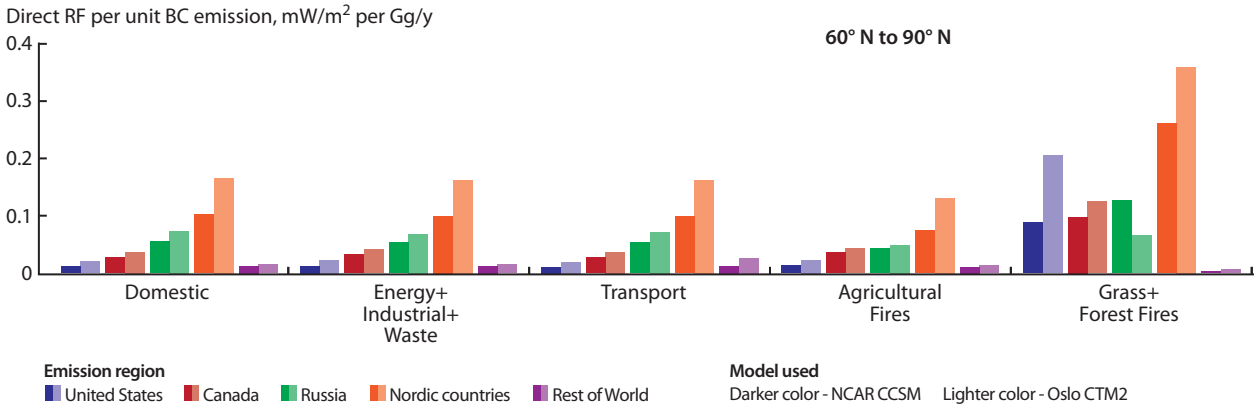

Figure 8.6. Normalized direct RF by BC north of 60° N for the CCSM and CTM2 models.

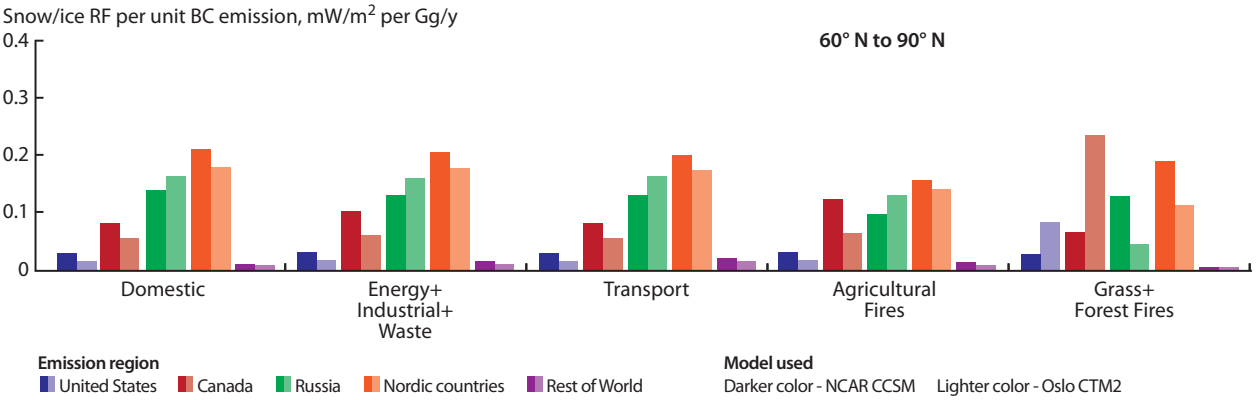

Figure 8.7. BC snow/ice RF north of 60° N for the CCSM and CTM2 models. The RF is normalized to the BC emissions.

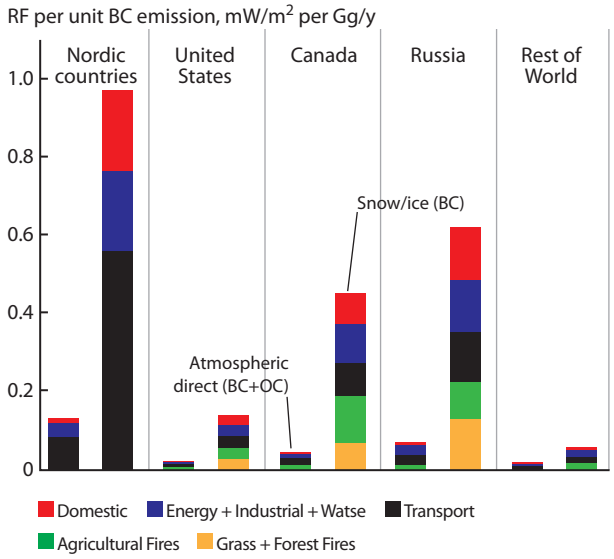

Figure 8.8. Normalized RF due to BC and OC in the atmosphere and BC deposited onto snow and ice. Results are from the NCAR CCSM model.

RF. Again, high latitude sources yield the greatest normalized forcings due to their proximity to the Arctic.

Figure 8.8 summarizes the normalized radiative forcing due to BC+OC in the atmosphere and BC deposited onto snow and ice.

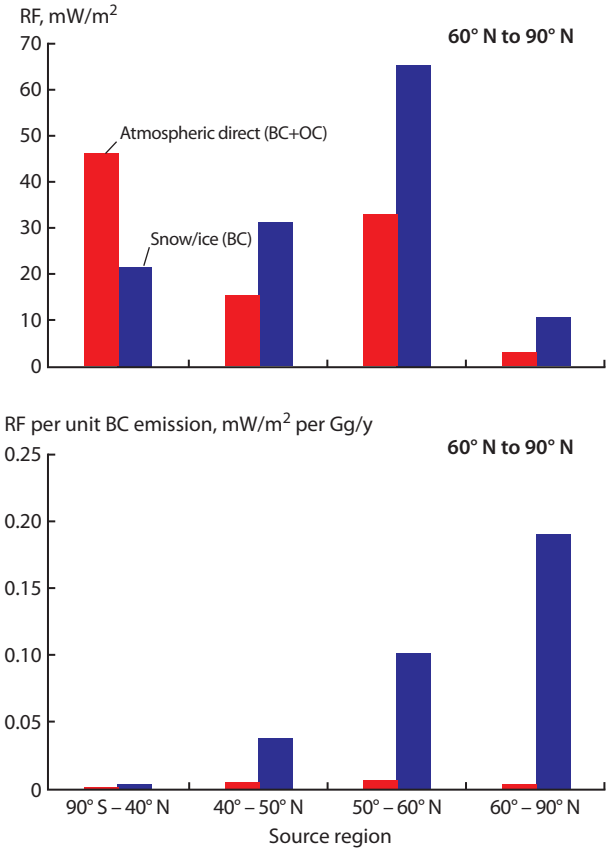

Figure 8.9. Absolute (upper) and normalized per unit emission (lower) atmospheric direct RF due to BC + OC and BC-snow/ice RF as a function of latitude band. The NCAR CCSM model was used for these calculations.

8.4.4. RF by latitude of emissions

It has been suggested that emissions north of 40° N have a large impact on the Arctic particularly in winter and spring when the polar dome extends to the mid-latitudes over Europe and Asia (see Section 5). To test this assumption and to compare the potential impact of sources on Arctic climate as a function of latitude between 40° and 90° N, a set of experiments was performed with emissions gridded by latitude band. The latitude bands included in the analysis were 90° S to 40° N, 40° to 50° N, 50° to 60° N, and 60° to 90° N.

Figure 8.9 shows both absolute and normalized RF as a function of latitude band for both the atmospheric direct effect and the BC-snow/ice effect. In absolute terms (Figure 8.9, top panel) emissions in the most southerly latitude band (90° S to 40° N) result in the largest direct RF due to the magnitude of the emissions of BC in the northern hemisphere tropics and mid-latitudes. Atmospheric direct RF is also relatively large for the 40° to 60° N latitude band because of the magnitude of emissions and likelihood of transport to the Arctic. Emissions within the Arctic (60° to 90° N) result in a smaller absolute direct RF because of their lower magnitude compared to emissions in more southerly latitude bands. Absolute BC-snow/ice RF increases with latitude between 40° and 60° N. This result confirms that emissions from lower latitudes are less effectively deposited in the Arctic since they reach the Arctic at higher altitudes (see also Section 5). Normalized BC-snow/ice RF increases dramatically with increasing latitude band (Figure 8.9, lower panel) confirming the efficiency with which sources close to the Arctic are transported to and deposited within the Arctic. This result also indicates that per unit emission, sources within the Arctic yield the largest RF.

8.4.5. RF due to projected increases in global and Arctic shipping

The within-Arctic shipping inventory of Corbett et al. (2010) was used to assess the increase in RF due to the increase in shipping emissions expected to occur as sea-ice extent declines over the next several decades. Although the model calculations are based on a shipping inventory, the results can be applied to any increasing point source within the Arctic.

The atmospheric direct RF and BC-snow/ice

RF resulting from global shipping emissions are significantly larger than those due to Arctic shipping emissions because of the difference in magnitude of emissions (Figure 8.10, top panel). As expected, the increase in emissions within the Arctic results in an increase in RF. Normalizing the forcing per unit emission once again indicates the significance of sources near to and within the Arctic (Figure 8.10, bottom panel). This result can be generalized to any BC source within the Arctic that is expected to increase over the next several decades.

Normalized net forcing (atmospheric direct forcing due to BC and BC snow/ice forcing) due to emissions from Arctic Council nations, the latitude bands described above, and global and within-Arctic shipping are compared in Figure 8.11. The comparison emphasizes the significance of close-to-Arctic and within Arctic sources relative to more distant sources on a forcing per unit emission basis.

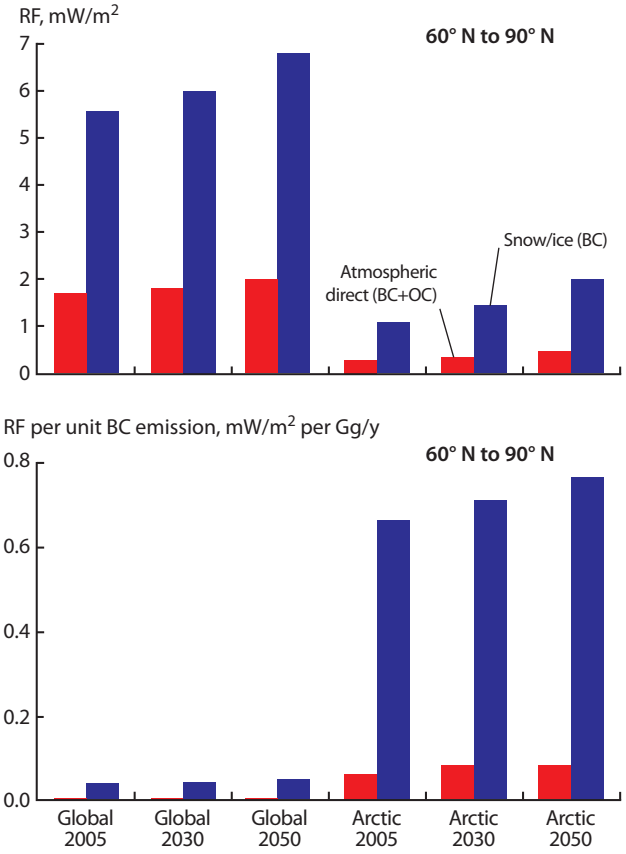

Figure 8.10. Absolute (upper) and normalized (lower) RF due to projected increases in global and Arctic shipping. The NCAR CCSM model was used for the calculations.

8.4.6. Relation between RF and temperature change

The concept of radiative forcing was developed primarily for long-lived greenhouse gases to evaluate how different perturbations in the Earth's radiation balance would affect global mean temperatures. Several studies have shown that there is no simple relation between RF and temperature response in a given region (e.g., Boer and Yu, 2003) especially for absorbing aerosols in the Arctic (Shindell and Faluvegi, 2009). A second aspect of the relation between RF and temperature is whether equal RF from different forcing agents (e.g., CO_2 versus BC) would cause equal temperature change, i.e. have equal efficacies (cf. Section 7.2). In the global mean, the efficacy of the atmospheric direct effect for BC has a range of 0.74 to 1.3 (IPCC, 2007). For the BC-snow/ice effect the estimated efficacy is considerably greater than 1.0 (1.7 to 4.5, Hansen et al., 2005; Flanner et al., 2007) as BC on snow leads to earlier snowmelt and thus a strong reduction in the surface albedo. Because this forcing triggers a strong local feedback the efficacy becomes significantly enhanced.

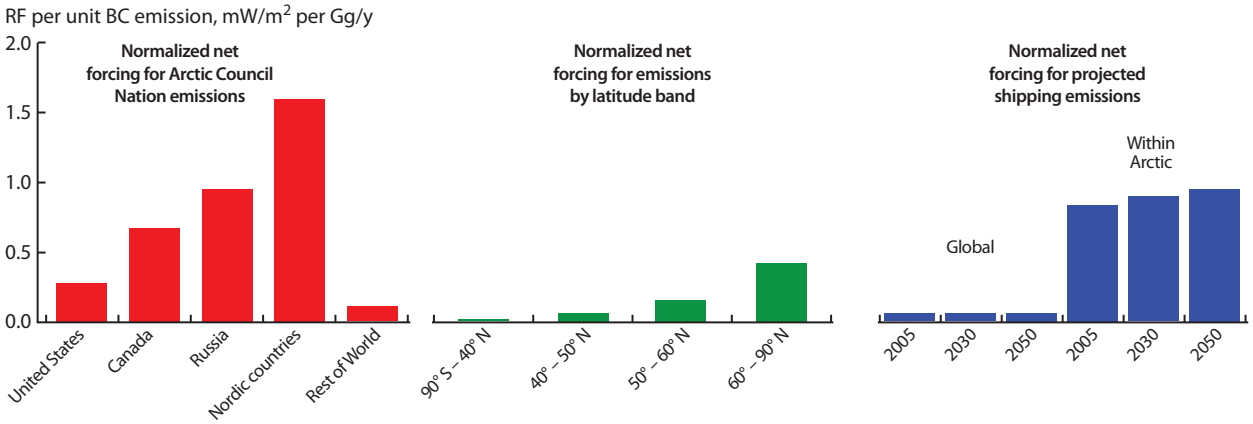

Figure 8.11. Summary of normalized net forcing (includes atmospheric direct forcing by BC and BC-snow/ice forcing) due to emissions from Arctic Council nations and ROW, the latitude bands considered, and global and within-Arctic shipping.

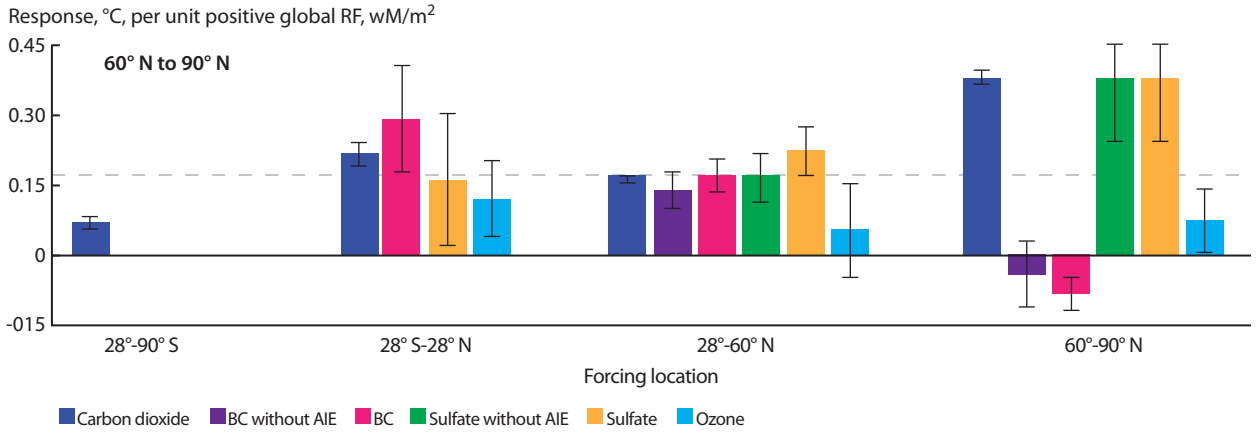

Figure 8.12. Arctic (60° to 90° N) surface air temperature sensitivity to different forcing mechanisms and locations, as calculated by the GISS global climate model. Colors indicate the type of forcing applied and the band in which the forcing was applied is given on the x-axis. The sensitivity (y-axis) is normalized to the global mean RF such that it is the surface air temperature change per unit positive global RF. Global mean response to tropical forcing is shown by the dashed line for comparison. AIE (Aerosol Indirect Effect). Source: Shindell and Faluvegi (2009).

Figure 8.12 shows the first simulation with a global climate model of the response in the surface temperature in the Arctic (60° to 90° N) to radiative forcings applied in different latitude bands. The RF is derived by perturbing the background BC vertical profiles in the model. (A significant fraction of the BC in the Arctic region is located in the upper troposphere and originates from mid-latitude sources.) According to the GISS model, the positive RF of BC in the Arctic atmosphere leads to a negative or near zero response in the Arctic surface temperature (i.e., negative or zero regional climate efficacy). If the RF from BC is located at mid-latitudes (28° to 60° N) the response in the Arctic is equal to the CO_2 response. Preliminary results with the Norwegian NorESM model seem to confirm these results (Maria Sand, Department of Geoscience, University of Oslo, pers. comm.). Preliminary results conducted with CCSM, however, show that the Arctic warms in response to isolated, positive Arctic forcing from atmospheric and snow-deposited BC. These differences in regional efficacy might be due to inclusion of the snow deposition effect in CCSM, but more experiments are needed to confirm this result.

There are probably several physical processes interacting to explain the response to RF from BC at high latitudes. First, in the Arctic, the flux of sensible heat is from the atmosphere to the surface (the opposite of what happens in mid-latitude and tropical regions). In the atmosphere, the heat is transported to the Arctic from mid-latitudes primarily by transient eddies (i.e. traveling extra-tropical cyclones). When absorbing aerosols become more abundant at higher altitudes, the stratification of an already stable Arctic troposphere becomes more stable and less heat is transported to the surface. Also, heating of air above the surface by absorbing aerosols tends to decrease the horizontal temperature gradient between the Arctic and the mid-latitudes potentially leading to less intense extra-tropical cyclones and thus less heat transport to the Arctic (Shindell and Faluvegi, 2009).

It can be concluded that there is considerable uncertainty in how Arctic climate responds to forcings exerted at different latitudes, altitudes, and times of the year (see Section 7.4, Shindell and Faluvegi, 2009). Within-Arctic BC emissions may exert a stronger Arctic surface warming, per unit local forcing, than extra-Arctic emissions reaching the Arctic because local emissions will tend to absorb solar energy lower in the atmosphere, and are also more likely to deposit to snow and ice surfaces where they directly heat the surface. More research, however, is needed on this topic.

9. Summary findings on impacts of black carbon on Arctic climate and relevance to mitigation actions

The model calculations performed for this assessment have allowed for the determination of the sources of BC that yield a positive radiative forcing in the Arctic. However, a full climate model, which was beyond the scope of this study, is required to determine the resulting temperature response. In addition, radiative forcing by CH_4 and O_3, which is positive in the Arctic, has not been assessed in this report. Thus, the conclusions below that focus on BC radiative forcing represent a partial perspective on the influence of short-lived climate forcers on Arctic climate.

Comparisons of modeled BC concentrations with BC measurements in the Arctic reveal that almost all models still have considerable problems capturing the Arctic BC concentrations both at the surface and aloft, despite recent model improvements. Comparisons of the BC surface concentrations simulated by the two models used in this assessment with data from five Arctic monitoring stations show that the two models used here are no exception. Therefore, radiative forcing calculations based on these models are highly uncertain. The summary findings below are guided by the model results but are also based on the available literature and the subjective expert judgment of relevant processes by the authors of this report.

- Reductions in the emissions of CO_2 are the backbone of any meaningful effort to mitigate climate change. The limited focus of this assessment on BC is not meant to distract from primary efforts on CO_2 reductions or mislead mitigation action toward a sole focus on BC.
- BC deposited to Arctic snow and ice results in a positive radiative forcing.
- BC deposited to Arctic snow and ice exerts a greater warming than the within-Arctic direct atmospheric radiative forcing by BC.
- Climate models indicate that *global direct atmospheric forcing* due to BC leads to Arctic warming. Direct atmospheric forcing by BC that has been transported into the Arctic at high altitudes may have a relatively small impact on Arctic surface temperatures since warming at high altitudes reduces atmospheric energy transport into the Arctic. The positive forcing due to within-Arctic BC sources, is more likely to cause surface warming because of solar heating near the surface and the greater likelihood of BC deposition to snow and ice surfaces.
- Arctic climate is strongly coupled to the northern hemisphere climate and is thus sensitive also to extra-Arctic radiative forcings.
- The global forcing due to BC results in a poleward transfer of heat energy, indicating that global strategies to manage emissions must remain a priority to ameliorate Arctic climate change.
- OC species that are co-emitted with BC and that reach the Arctic are unlikely to compensate for the positive radiative forcing due to BC and, over snow and ice covered surfaces, may themselves exert a positive forcing within the Arctic.
- Highly scattering sulfate aerosol exerts a weakly negative forcing over snow. As fresh snow melts over the summer and the surface albedo decreases, sulfate aerosol forcing becomes more negative.
- Carbonaceous aerosol (both BC and OC) emitted near or within the Arctic will have the greatest impact on Arctic climate. Emissions in close proximity to or within the Arctic are more likely to cause surface warming and to be deposited to snow and ice surfaces than emissions further south.
- The BC snow/ice *radiative forcing per unit of BC emitted* increases with latitude and is larger for the Arctic Council nations than for the Rest of the World. As a result, the Nordic countries are associated with the largest *forcing per unit of BC emission* due to emissions occurring at the highest latitudes.
- Within-Arctic BC sources (e.g., shipping, flaring) have a large impact on low-altitude BC concentrations and BC deposition in the Arctic and, thus, are likely to have a large forcing *per unit emission*.
- Forest, grassland and agricultural fires are the source types in Canada and Russia that dominate BC+OC radiative forcing in the Arctic. Fossil fuel combustion (e.g., diesel engines) is the dominant source in the USA, Nordic countries and ROW. Forest, grassland and agricultural fires from Arctic Council nations dominate the within-Arctic forcing *per unit of emission*.

- Domestic (e.g., wood stove) sources within the Nordic countries and Russia have a substantial influence on within-Arctic forcing. Their relative importance is likely to increase following implementation of regulative measures on transport emissions.
- Both the sign and magnitude of aerosol indirect forcing in the Arctic are uncertain. Globally averaged, the indirect and semi-direct effects are negative. For the Arctic, however, current studies indicate that the net aerosol indirect and semi-direct effects lead to smaller negative forcing than on the global average, or may even cause positive forcing.
- As snow and ice disappear from the Arctic, it is possible there will be a regime change shifting the relative influence of atmospheric forcing and snow/ice forcing such that, overall, forcing due to BC and co-emitted OC becomes more negative, less warming.
- Currently, there is no single appropriate environmental indicator to assess the Arctic climate response to changes in BC and OC emissions that are transported to Arctic regions. Hence, an integrated evaluation using observations, reported emissions, and models is required.

10. Information and science needs

The past few years have seen a concentrated effort within the scientific community to measure BC (or a proxy of BC) and OC in the Arctic and to quantitatively estimate the impacts of BC and OC on climate globally and regionally, including the Arctic. One of the major achievements has been the development of emissions information specific to the Arctic region. However, there remain specific actions and analyses which, if undertaken to improve the quantitative estimates of the effects of short-lived climate forcers on Arctic climate, could provide further guidance for the development of both Arctic nation and global mitigation strategies.

10.1. Recommendations for improved characterization of spatial and vertical distribution of BC and OC in the Arctic environment and deposition processes

- Improve the accuracy of measurements of BC and OC and further understanding of the effects of the measurement method on the retrieved concentration values.
- Continue efforts to resolve and/or standardize monitoring methods and protocols for BC and OC to ensure data comparability among national programs, field campaigns, and emission studies.
- Improve tracer based characterization of biomass burning and fossil fuel combustion sources to Arctic BC and OC at the surface and aloft to improve source identification of Arctic BC.
- Add long-term surface monitoring sites in regions that are currently under represented and/or anticipated to experience increased emissions to establish baselines and assess future impacts.
- Implement measurements of BC and/or aerosol light absorption at long-term surface monitoring sites that currently have no such measurements (Tiksi, Valdardai, Amderma, and the White Sea in Russia; Behchoko in Canada; Denali (IMPROVE), Poker Flats, and Homer in Alaska; Summit in Greenland) for spatial characterization of Arctic BC.
- Implement measurements of OC, ^{14}C (for differentiation of biomass and fossil fuel combustion sources), and additional tracer species at all long-term monitoring sites for source identification of measured BC.
- Undertake systematic, vertically resolved (surface to aloft) observations of BC and OC for vertical characterization of Arctic BC.
- Implement routine measurements of BC and tracer species in snow in close proximity to long-term atmospheric monitoring sites to characterize BC deposition processes and sources of deposited BC.
- Undertake process studies for characterizing aerosol removal during atmospheric transport and dry and wet deposition or for development of seasonally and spatially resolved deposition rates.
- Perform detailed case studies and statistical analyses of pan-Arctic BC, OC, and tracer data to determine dominant source types and regions

using methods independent of complex chemistry transport and climate models.

- Make intensive field campaign and long-term monitoring data sets publically available.
- Initiate a data recovery project to put all relevant observations available into a single accessible format.

10.2. Recommendations for emissions information

- Continue development of SLCF emission inventories for Arctic Council nations, and the Arctic region, for current year and for anticipated Arctic development scenarios using consistent methods.
- Continue development of national, regional, and global inventories of BC and co-emitted species as follows:
  - compare and harmonize different emission data sets;
  - improve the temporal resolution of key source sections. Monthly resolution is a minimum requirement to capture seasonality in emissions from domestic heating, agricultural fires, and forest and grassland fires; and
  - improve and validate the spatial allocation of emissions in the northern latitudes.
- Legislation, new technologies and future trends in, for example, energy use are important drivers of emissions of BC and co-emitted short-lived climate forcers. The effect of these drivers should be reflected in the emission inventories and future emission projections and changes in them should be monitored and incorporated.
- Improved understanding of several near-Arctic sources is needed. These include emission factors and activity data for shipping, diesel generators, agricultural and forest fires, and onshore and off shore oil and gas exploration. For the latter, emissions from flaring, compressor stations, and pipeline transport are often unknown.
- Satellite and monitoring data should be utilized to validate and refine spatial and temporal distribution of emissions in the inventories.

10.3. Recommendations for model development, evaluation and application

- Apply existing chemical transport models and climate models to evaluate the impact of within-Arctic and global SLCF and LLCF (long-lived climate forcer) emissions on Arctic climate with the objective of clarifying:
  - relative contributions of extra-Arctic and Arctic forcing and the resulting climate response;
  - relative contributions of atmospheric direct forcing and snow/ice forcing for current and future climate;.
  - relative importance of SLCF forcing and LLCF forcing over the next 100 years; and
  - source region and source type resolved Arctic forcing.
- Evaluate model output with appropriate observational data sets including surface, aircraft, and satellite-based observations.
- Incorporate state of the art aerosol – cloud processes, carbon cycle chemistry, and cloud processes into chemical transport models and climate models to provide an integrated assessment of BC and co-emitted species, CH_4, and O_3 forcing on Arctic climate and climate response.
- Test the sensitivity of model results to model resolution and reduce possible numerical problems at and around the North Pole.
- Perform sensitivity calculations with revised wet deposition schemes to further evaluate the influence of this process on model results (including radiative forcing and identification of source regions). Test alternative schemes and compare with observational data to improve deposition schemes in general and to select the best available scheme.

References

Abel, S.J., J.M. Haywood, E.J. Highwood, J. Li and P.R. Buseck, 2003. Evolutions of biomass burning aerosol properties from an agricultural fire in southern Africa. Geophysical Research Letters, 30:1783.

Achard, F., H.D. Eva, D. Mollicone and R. Beuchle, 2008. The effect of climate anomalies and human ignition factor on wildfires in Russian boreal forests. Philosophical Transactions of the Royal Society B, 363:2329-2337.

ACIA, 2004. Impacts of a Warming Arctic. Arctic Climate Impact Assessment. 139 pp. Cambridge University Press.

ACIA, 2005. Arctic Climate Impact Assessment. 1042 pp. Cambridge University Press.

Ackerman, A.S., O.B. Toon, D.E. Stevens, A.J. Heymsfield, V. Ramanathan and E.J. Welton, 2000. Reduction of tropical cloudiness by soot. Science, 288: 1042-1047.

ACTFSLCF, 2011. An Assessment of Emissions and Mitigation Options for Black Carbon for the Arctic Council countries. Arctic Council Task Force on Short-Lived Climate Forcers. Technical report, 2011.

Alterskjær, K., J E. Kristjánsson and C. Hoose, 2010. Do anthropogenic aerosols enhance or suppress the surface cloud forcing in the Arctic? Journal of Geophysical Research, 115: D22204.

Amann, M., I. Bertok, J. Cofala, C. Heyes, Z. Klimont, P. Rafaj, W. Schöpp and F. Wagner, 2008a. Baseline emission projections for the revision of the Gothenburg protocol up to 2020. Background paper for the 42nd Session of the Working Group on Strategies and Review of the Convention on Long-range Transboundary Air Pollution, Geneva, September 8-10, 2008.

Amann, M., I. Bertok, J. Cofala, C. Heyes, Z. Klimont, P. Rafaj, W. Schöpp and F. Wagner, 2008b. National Emission Ceilings for 2020 based on the 2008 Climate and Energy Package. NEC Scenario Analysis Report No. 6.

AMAP, 2011. Snow, Water, Ice and Permafrost in the Arctic (SWIPA) 2011. Arctic Monitoring and Assessment Programme (AMAP), Oslo, Norway.

Amiro, B.D., A. Cantin, M.D. Flannigan,and W.J. de Groot, 2009. Future emissions from Canadian boreal forest fires. Canadian Journal of Forest Research, 39:383-395.

Archibald, S., D.P. Roy, B.W. van Wilgen and R.J. Scholes, 2009. What limits fire? An examination of drivers of burnt area in Southern Africa. Global Change Biology, 15:613-630.

Arctic Council, 2009. Arctic Marine Shipping Assessment 2009 Report (AMSA). Arctic Council, April 2009, 2nd edition.

Arneth, A., P.A. Miller, M. Scholze, T. Hickler, G. Schurgers, B. Smith and C.I. Prentice, 2007. CO_2 inhibition of global terrestrial isoprene emissions: Potential implications for atmospheric chemistry. Geophysical Research Letters, 34:L18813.

Arnott, W.P., H. Moosmuller and C.F. Rogers, 1997. Photoacoustic spectrometer for measuring light absorption by aerosol: Instrument description. Atmospheric Environment, 33:2845-2852.

Balshi, M.S., A. McGuire, A. David and 15 others, 2007. The role of historical fire disturbance in the carbon dynamics of the panboreal region: A process-based analysis. Journal of Geophysical Research, 112:G02029.

Balzter, H.; F.F. Gerard, C.T. George and 8 others, 2005. Impact of the Arctic Oscillation pattern on interannual forest fire variability in Central Siberia. Geophysical Research Letters, 32:L14709.

Barrie, L.A., 1986. Arctic air pollution – An overview of current knowledge. Atmospheric Environment, 20:643- 663.

Bergstrom, R.W., 1973. Extinction and absorption coefficients of the atmospheric aerosol as a function of particle size. Contributions to Atmospheric Physics, 46:223-234.

Birch, M.E. and R.A. Cary, 1996. Elemental carbon-based method for monitoring occupational exposures to particulate diesel exhaust. Aerosol Science and Technology, 25:221-241.

Björk, R.G. and U. Molau, 2007. Ecology of alpine snowbeds and the impact of global change. Arctic, Antarctic and Alpine Research, 39:34-43.

Bodhaine, B.A., 1989. Barrow surface aerosol: 1976 – 1986. Atmospheric Environment, 23:2357-2369.

Bodhaine, B.A. and E.G. Dutton, 1993. A long-term decrease in Arctic Haze at Barrow, Alaska. Geophysical Research Letters, 20: 947-950.

Boer, G.J. and B. Yu, 2003. Climate sensitivity and response. Climate Dynamics, 20:415-429.

Bond, T.C. and R.W. Bergstrom, 2006. Light absorption by carbonaceous particles: An investigative review. Aerosol Science and Technology, 40:27-67.

Bond, T.C., T.L. Anderson and D. Campbell, 1999. Calibration and intercomparison of filter-based measurements of visible light absorption by aerosols. Aerosol Science and Technology, 30:582-600.

Bond, T.C., D.G. Streets, K.F. Yarber, S.M. Nelson, J.-H. Woo and Z. Klimont, 2004. A technology-based global inventory of black and organic carbon emissions from combustion. Journal of Geophysical Research, 109:D14203.

Bond, T.C., G. Habib and R.W. Bergstrom, 2006. Limitations in the enhancement of visible light absorption due to mixing state. Journal of Geophysical Research, 111:D20211.

Bond, T.C., E. Bhardwaj, R. Dong, R. Jogani, S. Jung, C. Roden, D.G. Streets and N.M. Trautmann, 2007. Historical emissions of black and organic carbon aerosol from energy-related combustion, 1850–2000. Global Biogeochemical Cycles, 21:GB2018.

Bond, T.C., C. Zarzycki, M.G. Flanner and D.M. Koch, 2011. Quantifying immediate radiative forcing by black carbon and organic matter with the specific forcing pulse. Atmospheric Chemistry and Physics, 11:1505-1525.

Bonn, B.; R. von Kuhlmann and M.G. Lawrence, 2004. High contribution of biogenic hydroperoxides to secondary organic aerosol formation. Geophysical Research Letters, 31:L10108.

Bowman, D.M.J.S., J.K. Balch, P. Artaxo and 19 others, 2009. Fire in the Earth system. Science, 324:481-484.

Briegleb, B.P. and B. Light, 2007. A delta-eddington multiple scattering parameterization for solar radiation in the sea ice component of the Community Climate System Model, Tech. Rep. NCAR/TN–472+STR, National Center for Atmospheric Research.

Brock, C.A., J. Cozic, R. Bahreini and 39 others, 2011. Characteristics, sources, and transport of aerosols measured in spring 2008 during the Aerosol, Radiation, and Cloud Processes Affecting Arctic Climate (ARCPAC) project. Atmospheric Chemistry and Physics, 11:2423-2453.

Budyko, M.I., 1969. The effects of solar radiation on the climate of the earth. Tellus, 21:611-619.

Buhaug, Ø., J.J. Corbett, Ø. Endresen and 14 others, 2009. Second IMO GHG Study 2009. International Maritime Organization (IMO). London, April 2009.

Burton, P.J., C. Messier, D.W. Smith and W.L. Adamowicz (Eds.), 2003. Towards Sustainable Management of the Boreal Forest. NRC Research Press. 1039 pp.

Carlson, T.N., 1981. Speculations on the movement of polluted air to the Arctic. Atmospheric Environment, 15:1473-1477.

Carslaw, K.S., O. Boucher, D.V. Spracklen, G.W. Mann, J.G.L. Rae, S. Woodward and M. Kulmala, 2010. A review of natural aerosol interactions and feedbacks within the Earth system. Atmospheric Chemistry and Physics, 10:1701-1737.

Cess, R.D., 1983. Arctic aerosols: Model estimates of interactive influences upon the surface-atmosphere clear-sky radiation budget. Atmospheric Environment, 17:2555-2564.

Chapin, F.S., M. Sturm, M. C. Serreze and 18 others, 2005. Role of land-surface changes in Arctic summer warming. Science, 310:657-660.

Chow, J.C., J.G. Watson, L.C. Pritchett, W.R. Pierson, C.A. Frazier and R.G. Purcell, 1993. The DRI thermal/optical reflectance carbon analysis system: Description, evaluation, and applications in U.S. air quality studies. Atmospheric Environment, 27A:1185-1201.

Chow, J.C., J.G. Watson, L.-W.A. Chen, W.P. Arnott and H. Moosmüller, 2004. Equivalence of elemental carbon by thermal/optical reflectance and transmittance with different temperature protocols. Environmental Science and Technology, 38:4414-4422.

Christensen, J.H., 1997. The Danish Eulerian hemispheric model - A three-dimensional air pollution model used for the Arctic. Atmospheric Environment, 31:4169-4191.

Chuang, C.C., J.E. Penner, J.M. Prospero, K.E. Grant, G.H. Rau and K. Kawamoto, 2002. Cloud susceptibility and the first aerosol indirect forcing: Sensitivity to black carbon and aerosol concentrations. Journal of Geophysical Research, 107:4564.

Clarke, A.D. and K.J. Noone, 1985. Soot in the Arctic snowpack: a cause for perturbations in radiative transfer. Atmospheric Environment, 19:2045-2053.

Clarke, A.D., Y. Shinozuka, V.N. Kapustin, S. Howell, B. Huebert, S. Doherty, T. Anderson, D. Covert, J. Anderson, X. Hua, K.G. Moore II, C. McNaughton, G. Carmichael, and R. Weber. 2004. Size distributions and mixtures of dust and black carbon aerosol in Asian outflow: Physiochemistry and optical properties. Journal of Geophysical Research, 109: D15S09.

Cofala, J., M. Amann, Z. Klimont, K. Kupiainen and L. Höglund-Isaksson, 2007. Scenarios of global anthropogenic emissions of air pollutants and methane until 2030. Atmospheric Environment, 41:8486-8499.

Collins, W.D., C. Bitz, M.L. Blackmon and 12 others, 2006. The community climate system model version 3 (CCSM3). Journal of Climate, 19:2122-2161.

Cook, J. and E.J. Highwood, 2004. Climate response to tropospheric absorbing aerosols in an intermediate general-circulation model. Quarterly Journal of the Royal Meteorological Society, 130:175-191.

Corbett, J.J., D.A. Lack, J.J. Winebrake, S. Harder, J.A. Silberman and M. Gold, 2010. Arctic shipping emissions inventories and future scenarios. Atmospheric Chemistry and Physics, 10:9689-9704.

Doherty, S.J., S.G. Warren, T.C. Grenfell, A.D. Clarke and R.E. Brandt, 2010. Light-absorbing impurities in arctic snow. Atmospheric Chemistry and Physics, 10:11647-11680.

Duncan, B.N. and I. Bey, 2004. A modeling study of the export pathways of pollution from Europe: Seasonal and interannual variations (1987–1997). Journal of Geophysical Research, 109:D08301.

Eckhardt, S., A. Stohl, S. Beirle, N. Spichtinger, P. James, C. Forster, C. Junker, T. Wagner, U. Platt and S.G. Jennings, 2003. The North Atlantic Oscillation controls air pollution transport to the Arctic. Atmospheric Chemistry and Physics, 3:1769-1778.

Eleftheriadis, K., S. Vratolis and S. Nyeki, 2009. Aerosol black carbon in the European Arctic: Measurements at Zeppelin station, Ny-Ålesund, Svalbard from 1998–2007. Geophysical Research Letters, 36:L02809.

Elvidge, C.D., K. Buagh, B. Tuttle, D. Ziskin, T. Ghosh, M. Zhizhin and D. Pack, 2009. Improving Satellite Data Estimation of Gas Flaring Volumes. Year Two Final Report to the GGFR. Earth Observation Group, NOAA National Geophysical Data Center. 64 pp.

Flanner, M.G. and C.S. Zender, 2006. Linking snowpack microphysics and albedo evolution. Journal of Geophysical Research, 111:D12208.

Flanner, M.G., C.S. Zender, J.T. Randerson and P.J. Rasch, 2007. Present day climate forcing and response from black carbon in snow. Journal of Geophysical Research, 112:D11202.

Flanner, M.G., C.S. Zender, P.G. Hess, N.M. Mahowald, T.H. Painter, V. Ramanathan and P.J. Rasch, 2009. Springtime warming and reduced snow cover from carbonaceous particles. Atmospheric Chemistry and Physics, 9:2481-2497.

Flanner, M.G., K.M. Shell, M. Barlage, D.K. Perovich and M.A. Tschudi, 2011. Radiative forcing and albedo feedback from the Northern Hemisphere cryosphere between 1979 and 2008. Nature Geoscience, 4:151-155.

Flannigan, M.D., I. Cambell, B.M. Wotton, C. Carcaillet, P. Richard and Y. Bergeron, 2001. Future fire in Canada's boreal forest: Paleoecology results and general circulation model – Regional climate model simulations. Canadian Journal of Forest Research, 31:854-864.

Flannigan, M.D., M.A. Krawchuk, W.J. de Groot, B.M. Wotton and L.M. Gowman, 2009a. Implications of changing climate for global wildland fire. International Journal of Wildland Fire, 18:483-507.

Flannigan, M., B. Stocks, M. Turetsky and M. Wotton, 2009b. Impacts of climate change on fire activity and fire management in the circumboreal forest. Global Change Biology, 15:549-560.

Forster, P., V. Ramaswamy, P.Artaxo and 12 others, 2007. Changes in atmospheric constituents and in radiative forcing. In: Climate Change 2007: The Physical Science Basis. Contribution of Working Group I to the Fourth Assessment Report of the Intergovernmental Panel on Climate Change. Cambridge University Press.

Fromm, M., J. Alfred, K. Hoppel, J. Hornstein, R. Bevilacqua, E. Shettle, R. Servranckx, Z. Li and B. Stocks, 2000. Observations of boreal forest fire smoke in the stratosphere by POAM III, SAGE II, and lidar in 1998. Geophysical Research Letters, 27:1407-1410.

Fukasawa, T., S. Ohta, N. Murao, S. Yamagata and V.N. Makarov, 1997. Aerosol observations in the Siberian Arctic. Proc. NIPR Symp. Polar Meteorol. Glaciol, 11:150-160.

Fuller, K.A., W.C. Malm and S.M. Kreidenweis, 1999. Effects of mixing on extinction by carbonaceous particles. Journal of Geophysical Research, 104:15941-15954.

Garrett, T.J. and C. Zhao, 2006. Increased Arctic cloud longwave emissivity associated with pollution from mid-latitudes. Nature, 440:787-789.

Garrett, T.J., C. Zhao, X. Dong, G.G. Mace and P.V. Hobbs, 2004. Effects of varying aerosol regimes on low-level Arctic stratus. Geophysical Research Letters, 31:L17105.

Garrett, T.J., C. Zhao and P.C. Novelli, 2010. Assessing the relative contributions of transport efficiency and scavenging to seasonal variability in Arctic aerosol. Tellus, 62B:190-196.

Gent, P.R., G. Danabasoglu, L.J. Donner and 19 others, 2011. The Community Climate System Model Version 4. Journal of Climate, 24:4973-4991.

Ghose, M. and S. Majee, 2007. Characteristics of hazardous airborne dust around an Indian surface coal mining area. Environmental Monitoring and Assessment, 130:17-25.

Goetz, S.J., M.C. Mack, K.R. Gurney, J.T. Randerson and R.A. Houghton, 2007. Ecosystem responses to recent climate change and fire disturbance at northern high latitudes: observations and model results contrasting northern Eurasia and North America. Environmental Research Letters, 2:045031.

Gong, S.L., T.L. Zhao, S. Sharma, D. Toom-Sauntry, D. Lavoué, X.B. Zhang, W.R. Leaitch and L.A. Barrie, 2010. Identification of trends and interannual variability of sulfate and black carbon in the Canadian High Arctic: 1981–2007. Journal of Geophysical Research, 115:D07305.

Haapanala, S., A. Ekberg, H. Hakola, V. Tarvainen, J. Rinne, H. Hellen and A. Arneth, 2009. Mountain birch - Potentially large source of sesquiterpenes into high latitude atmosphere. Biogeosciences, 6:2709-2718.

Hadley, O.L., C.E. Corrigan, T.W. Kirchstetter, S.S. Cliff, and V. Ramanathan, 2010. Measured black carbon deposition on the Sierra Nevada snow pack and implication for snow pack retreat. Atmospheric Chemistry and Physics, 10:7507-7513.

Hall, A. and X. Qu, 2006. Using the current seasonal cycle to constrain snow albedo feedback in future climate change. Geophysical Research Letters, 33:L03502.

Hansen, J. and L. Nazarenko, 2004. Soot climate forcing via snow and ice albedos. Proceedings of the National Academy of Sciences, 101:423-428.

Hansen, A.D.A. and H. Rosen, 1984. Vertical distributions of particulate carbon, sulfur, and bromine in the Arctic haze and comparison with ground-level measurements at Barrow, Alaska. Geophysical Research Letters, 11:381-384.

Hansen, A.D.A., H. Rosen and T. Novakov, 1982. Real time measurement of the absorption coefficient of aerosol particles. Applied Optics, 21:3060-3062.

Hansen, J., M. Sato, R. Reudy and 42 others, 2005. Efficacy of climate forcings. Journal of Geophysical Research, 110:D18104.

Hegg, D.A., S.G. Warren, T.C. Grenfell, S.J. Doherty, T.V. Larson and A.D. Clarke, 2009. Source attribution of black carbon in Arctic snow. Environmental Science and Technology, 43:4016-4021.

Heidam, N.Z., J. Christensen, P. Wåhlin and H. Skov, 2004. Arctic atmospheric contaminants in NE Greenland: levels, variations, origins, transport, transformations and trends 1990-2001. Science of the Total Environment, 331:528.

Hirdman, D., H. Sodemann, S. Eckhardt, J.F. Burkhart, A. Jefferson, T. Mefford, P.K. Quinn, S. Sharma, J. Ström and A. Stohl, 2010a. Source identification of short-lived air pollutants in the Arctic using statistical analysis of measurement data and particle dispersion model output. Atmospheric Chemistry and Physics, 10:669-693.

Hirdman, D., J.F. Burkhart, H. Sodemann, S. Eckhardt, A. Jefferson, P.K. Quinn, S. Sharma, J. Ström and A. Stohl, 2010b. Long-term trends of black carbon and sulphate aerosol in the Arctic: changes in atmospheric transport and source region emissions. Atmospheric Chemistry and Physics, 10:9351-9368.

Hoelzemann, J.J., M. Schultz, G.P. Brasseur, C. Granier and M. Simon, 2004. Global wildland fire emission model (GWEM): Evaluating the use of global area burnt satellite data. Journal of Geophysical Research, 109:D14S04.

Hoffmann, D., A. Tilgner, Y. Iinuma, and H. Herrmann, 2010. Atmospheric stability of levoglucosan: A detailed laboratory and modeling study. Environmental Science and Technology, 44:694-699.

Huang, L., S.L. Gong, S. Sharma, D. Lavoué and C.Q. Jia, 2010a. A trajectory analysis of atmospheric transport of black carbon aerosols to Canadian high Arctic in winter and spring (1990–2005). Atmospheric Chemistry and Physics, 10:5065-5073.

Huang, L., S.L. Gong, C.Q. Jia and D. Lavoué, 2010b. Relative contributions of anthropogenic emissions to black carbon aerosol in the Arctic. Journal of Geophysical Research, 115:1-11.

Huang, L., S.L. Gong, C.Q. Jia and D. Layouvé, 2010c. Importance of deposition processes in simulating the seasonality of the Arctic black carbon aerosol. Journal of Geophysical Research, 115:D17207.

Huntzicker, J.J., R.L. Johnson, J.J. Shah and R.A. Cary, 1982. Analysis of organic and elemental carbon in ambient aerosol by a thermal-optical method. In: Wolff G.T. and R.L. Klimisch (Ed). Particulate Carbon: Atmospheric Life Cycle, pp. 79-88. Plenum Press.

IPCC, 2001. Climate Change 2001: Synthesis Report. A Contribution of Working Groups I, II, and III to the Third Assessment Report of the Intergovernmental Panel on Climate Change. Watson, R.T. and the Core Writing Team (Eds.). Cambridge University Press, 398 pp.

IPCC, 2007. Climate Change 2007: Synthesis Report. Contribution of Working Groups I, II and III to the Fourth Assessment Report of the Intergovernmental Panel on Climate Change. Core Writing Team, Pachauri, R.K and Reisinger, A. (Eds.). 104 pp.

Isaev, A.S., G.N. Korovin, S.A. Bartalev, D.V. Ershov, A. Janetos, E.S. Kasischke, H.H. Shugart, N.H.F. French, B.E. Orlick and T.L. Murphy, 2002. Using remote sensing to assess Russian forest fire carbon emissions. Climatic Change, 55:235-249.

Iversen, T., 1984. On the atmospheric transport of pollution to the Arctic. Geophysical Research Letters, 11:457-460.

Jacobson, M.Z., 2002. Control of fossil-fuel particulate black carbon plus organic matter, possibly the most effective method of slowing global warming. Journal of Geophysical Research, 107:3527-3542.

Jacobson, M.Z., 2004. Climate response of fossil fuel and biofuel soot, accounting for soot's feedback to snow and sea ice albedo and emissivity. Journal of Geophysical Research, 109:D21201.

Jacobson, M.Z., 2010. Short-term effects of controlling fossil-fuel soot, biofuel soot and gases, and methane on climate, arctic ice, and air pollution health. Journal of Geophysical Research, 115:D14209.

Jaffe, D., T. Iversen and G. Shaw, 1995. Comment on "A long term decrease in Arctic haze at Barrow, Alaska" by B.A. Bodhaine and E.G. Dutton. Geophysical Research Letters, 22:739-740.

Janhäll, S., M.O. Andreae and U. Pöschl, 2010. Biomass burning aerosol emissions from vegetation fires: particle number and mass emission factors and size distributions. Atmospheric Chemistry and Physics, 10:1427-1439.

Johnson, E.A., 1992. Fire and Vegetation Dynamics: Studies from the North American Boreal Forest. Cambridge University Press, 129 pp.

Johnson, M.R., R.W. Devillers and K.A. Thomson, 2011. Quantitative field measurement of soot emission from a large gas flare using Sky-LOSA. Environmental Science and Technology, 45:345-350.

Jones, A., J.M. Haywood and O. Boucher, 2007. Aerosol forcing, climate response and climate sensitivity in the Hadley Centre climate model. Journal of Geophysical Research, 112:D20211.

Jost, H.J., K. Drdla, A. Stohl and 17 others, 2004. In-situ observations of mid-latitude forest fire plumes deep in the stratosphere. Geophysical Research Letters, 31:L11101.

Junker, C. and C. Liousse, 2008. A global emission inventory of carbonaceous aerosol from historic records of fossil fuel and biofuel consumption for the period 1860-1997. Atmospheric Chemistry and Physics, 8:1195-1207.

Kasischke, E.S., E.J. Hyer, P.C. Novelli, L.P. Bruhwiler, N.H.F. French, A.I. Sukhinin, J.H. Hewson and B.J. Stocks, 2005. Influences of boreal fire emissions on Northern Hemisphere atmospheric carbon and carbon monoxide. Global Biogeochemical Cycles, 19:GB1012.

Klimont, Z., J. Cofala, J. Xing, W. Wei, C. Zhang, S. Wang, J. Kejun, P. Bhandari, R. Mathura, P. Purohit, P. Rafaj, A. Chambers, M. Amann and J. Hao, 2009. Projections of SO_2, NOx, and carbonaceous aerosols emissions in Asia. Tellus, 61B:602-617.

Klonecki, A., P. Hess, L. Emmons, L. Smith, J. Orlando and D. Blake, 2003. Seasonal changes in the transport of pollutants into the Arctic troposphere – Model study. Journal of Geophysical Research, 108(D4):8367.

Kloster, S., N.M. Mahowald, J.T. Randerson, P.E. Thornton, F.M. Hoffman, S. Levis, P.J. Lawrence, J.J. Feddema, K.W. Oleson and D.M. Lawrence, 2010. Fire dynamics during the 20th century simulated by the Community Land Model. Biogeosciences, 7:1877-1902.

Koch, D. and J. Hansen, 2005. Distant origins of Arctic black carbon: A Goddard Institute for Space Studies ModelE experiment. Journal of Geophysical Research, 110:D04204.

Koch, D., T.C. Bond, D. Streets, N. Unger, and G.R van der Werf, 2007. Global impacts of aerosols from particular source regions and sectors. Journal of Geophysical Research., 112:D02205.

Koch, D., M. Schulz, S. Kinne and 47 others, 2009a. Evaluation of black carbon estimations in global aerosol models. Atmospheric Chemistry and Physics, 9:9001-9026.

Koch, D., S. Menon, A.D. Genio, R. Ruedy, I. Alienov and G.A. Schmidt, 2009b. Distinguishing aerosol impacts on climate over the past century. Journal of Climate, 22:2659-2677.

Kopeikin, V.M., I.A. Repina, E.I. Grechko and B.I. Ogorodnikov, 2010. Measurements of the soot aerosol content in the near-water layer in Southern and Northern Hemispheres. Atmospheric and Oceanic Optics, 23:444-450.

Korontzi, S., J. McCarty, T. Loboda, S. Kumar and C. Justice, 2006. Global distribution of agricultural fires in cropland from 3 years of Moderate Resolution Imaging Spectroradiometer (MODIS) data. Global Biogeochemical Cycles, 20:GB2021.

Kozlov, V.S., A.B. Tikhomirov, M.V. Panchenko, V.P. Shmargunov, V.V. Pol'kin, S.M. Sakerin, A.P. Lisitsyn and V.P. Shevchenko, 2009. Optical and microphysical parameters of aerosol in the near-water atmosphere of the White Sea as assessed from the data of simultaneous shipborne and coast-based measurements in August 2006. Atmospheric and Oceanic Optics, 22:767-776.

Kupiainen, K. and Z. Klimont, 2007. Primary emissions of fine carbonaceous particles in Europe. Atmospheric Environment, 41:2156-2170.

Kuwata, M., Y. Kondo, M. Mochida, N. Takegawa and K. Kawamura, 2007. Dependence of CCN activity of less volatile particles on the amount of coating observed in Tokyo. Journal of Geophysical Research, 112:D11207.

Lack, D., E. Lovejoy, T. Baynard, A. Pettersson and A. Ravishankara, 2006. Aerosol absorption measurement using photoacoustic spectroscopy: Sensitivity, calibration, and uncertainty developments. Aerosol Science and Technology, 40:697-708.

Lack, D.A., C.D. Cappa, D.S. Covert, T. Baynard, P. Massoli, B. Sierau, T.S. Bates, P.K. Quinn, E.R. Lovejoy and A.R. Ravishankara, 2008. Bias in filter-based aerosol light absorption measurements due to organic aerosol loading: Evidence from ambient measurements. Aerosol Science and Technology, 42:1033-1041.

Lack, D.A., J.J. Corbett, T. Onasch and 13 others, 2009. Particulate emissions from commercial shipping: Chemical, physical, and optical properties. Journal of Geophysical Research, 114:D00F04.

Lamarque, J.-F., T.C. Bond, V. Eyring and 18 others, 2010. Historical (1850-2000) gridded anthropogenic and biomass burning emissions of reactive gases and aerosols: methodology and application. Atmospheric Chemistry and Physics, 10:7017-7039.

Law, K.S. and A. Stohl, 2007. Arctic air pollution: Origins and impacts. Science, 315:1537-1540.

Leaitch, W.R., U. Lohmann, L.M. Russell and 8 others, 2010. Cloud albedo increase from carbonaceous aerosol. Atmospheric Chemistry and Physics, 10:7669-7684.

Lee, D.S., G. Pitari, V. Grewe, K. Gierens, J.E. Penner, A. Petzold, M. Prather, U. Schumann, A. Bais, T. Berntsen, D. Iachetti, L.L. Lim and R. Sausen, 2009. Transport impacts on atmosphere and climate: Aviation. Atmospheric Environment, 44:4678-4734.

Lehsten, V., K. J. Tansey, H. Balzter, K. Thonicke, A. Spessa, U. Weber, B. Smith and A. Arneth, 2009. Estimating carbon emissions from African wildfires. Biogeosciences, 6:349-360.

Lehsten, V., P. Harmand, I. Palumbo and A. Arneth, 2010. Modelling burned area in Africa. Biogeosciences, 7:3199-3214.

Liu, J., S. Fan, L.W. Horowitz and H. Levy II, 2011. Evaluation of factors controlling long-range transport of black carbon to the Arctic. Journal of Geophysical Research, 116:D04307.

Lohmann, U. and J. Feichter, 2005. Global indirect aerosol effects: A review. Atmospheric Chemistry and Physics, 5:715-737.

Lohmann, U., J. Feichter, J. Penner and R. Leaitch, 2000. Indirect effect of sulfate and carbonaceous aerosols: A mechanistic treatment. Journal of Geophysical Research - Atmospheres, 105:12193-12206.

Lubin, D. and A.M. Vogelmann, 2006. A climatologically significant aerosol longwave indirect effect in the Arctic. Nature, 439:453-456.

Lucht, W., I.C. Prentice and R.B. Myneni, 2002. Climatic control of the high-latitude vegetation greening trend and Pinatubo effect. Science, 296:1687-1689.

Macias Fauria, M. and E.A. Johnson, 2008. Climate and wildfires in the North American boreal forest. Philosophical Transactions of the Royal Society B, 363:2315-2327.

Martins, J.V., P.V. Hobbs, R.E. Weiss and P. Artaxo, 1998. Sphericity and morphology of smoke particles from biomass burning in Brazil. Journal of Geophysical Research, 103:32051-32057.

Matsui, H., Y. Kondo, N. Moteki, N. Takegawa, L.K. Sahu, Y. Zhao, H.E. Fuelberg, W.R. Sessions, G. Diskin, D.R. Blake, A. Wisthaler and M. Krioke, 2011. Seasonal variation of the transport of black carbon aerosol from the Asian continent to the Arctic during the ARCTAS aircraft campaign. Journal of Geophysical Research, 116:D05202.

McCarty, J.L., C.O. Justice and S. Korontzi, 2007. Agricultural burning in the southeastern United States detected by MODIS. Remote Sensing of Environment, 108:151-162.

McConnell, J.R., 2010. New directions: Historical black carbon and other ice core aerosol records in the Arctic for GCM evaluation. Atmospheric Environment, 44:21-22.

McConnell, J.R., R. Edwards, G.L. Kok, M.G. Flanner, C.S. Zender, E.S. Saltzman, J.R. Banta, D.R. Pasteris, M.M. Carter and J.D.W. Kahl, 2007. 20th-century industrial black carbon emissions altered Arctic climate forcing. Science, 317:1381-1384.

Mitchell, M., 1957. Visual range in the polar regions with particular reference to the Alaskan Arctic. Journal of Atmospheric and Terrestrial Physics, Special Supplement:195-211.

Moteki, N., Y. Kondo, Y. Miyazaki, N. Takegawa, Y. Komazaki, G. Kurata, T. Shirai, D.R. Blake, T. Miyakawa and M. Koike, 2007. Evolution of mixing state of black carbon particles: Aircraft measurements over the western Pacific in March 2004. Geophysical Research Letters, 34:L11803.

Myhr, K.A., 2003. Støv i arbeidsmiljø og ytre miljø i Svea. Diploma Thesis, Faculty of Engineering and Technology, Norwegian University of Science and Technology.

Myhre, G., N. Bellouin, T.F. Berglen, T.K. Berntsen, O. Boucher, A. Grini, I.S.A. Isaksen, M. Johnsrud, M.I. Mishchenko, F. Stordal and D. Tanre, 2007. Comparison of the radiative properties and direct radiative effect of aerosols from a global aerosol model and remote sensing data over ocean. Tellus B, 59:115-129.

Nedelec, P., V. Thouret, J. Brioude, B. Sauvage, J.P. Cammas and A. Stohl, 2005. Extreme CO concentrations in the upper troposphere over northeast Asia in June 2003 from the in situ MOZAIC aircraft data. Geophysical Research Letters, 32:L14807.

Niinemets, Ü., R.K. Monson, A. Arneth, P. Ciccioli, J. Kesselmeier, U. Kuhn, S.M. Noe, J. Penuelas and M. Staudt, 2010. The emission factor of volatile isoprenoids: caveats, model algorithms, response shapes and scaling. Biogeosciences, 7:1809-1832.

NSIDC, 2007. Arctic sea ice shatters all previous record lows. National Snow and Ice Data Center, Arctic Sea Ice News, 1 October 2007.

NSIDC, 2010. Weather and feedbacks lead to third-lowest extent. National Snow and Ice Data Center, Arctic Sea Ice News and Analysis, 4 October 2010.

Overland, J.E. and M. Wang, 2010. Large-scale atmospheric circulation changes are associated with the recent loss of Arctic sea ice. Tellus, 62A:1-9.

Park, R.J., D.J. Jacob, P.I. Palmer, A.D. Clarke, R.J. Weber, M.A. Zondlo, F.L. Eisele, A.R. Bandy, D.C. Thornton, G.W. Sachse and T.C. Bond, 2005. Export efficiency of black carbon aerosol in continental outflow: Global implications. Journal of Geophysical Research, 110:D11205.

Parungo, F.P., C.T. Nagamoto, P.J. Sheridan and R.C. Schnell, 1990. Aerosol characteristics of Arctic haze sampled during AGASP 11. Atmospheric Environment, 24:937-949.

Pechony, O. and D. T. Shindell, 2010. Driving forces of global wildfires over the past millennium and the forthcoming century. Proceedings of the National Academy of Sciences, 107:19167-19170.

Pettus, A., 2009. Agricultural Fires and Arctic Climate Change: A Report for the Clean Air Task Force (CATF). www.catf.us.

Petzold, A., A. Dopelheuer, C.A. Brock and F. Schroder, 1999. In situ observations and model calculations of black carbon emission by aircraft at cruise altitude. Journal of Geophysical Research, 104:22171-22181.

Polissar, A.V., 1993. Measurements of the soot mass concentration and particle-size distribution of atmospheric aerosol in the eastern Arctic. Izv. Acad. Sci. USSR. Atmos. Oceanic Physics (English Translation), 29:66-73.

Polissar, A., P. Hopke, P. Paatero, Y. Kaufmann, D. Hall, B. Bodhaine, E.G. Dutton and J.M. Harris, 1999. The aerosol at Barrow, Alaska: Long-term trends and source locations. Atmospheric Environment, 33:2441-2458.

Polissar, A., P. Hopke and J. Harris, 2001. Source regions for atmospheric aerosol measured at Barrow, Alaska. Environmental Science and Technology, 35:4214-4226.

Pol'kin, V.V., L.P. Golobokova, V.S. Kozlov, V.B. Korobov, A.P. Lisitsyn, M.V. Panchenko, M.A. Peskova, T.V. Khodzher and V.P. Shevchenko, 2004. Estimation of correlation between microphysical properties and chemical composition of aerosol over the White Sea. Atmospheric and Oceanic Optics, 17:330-338.

Pol'kin, V.V., M.V. Panchenko, I.V. Grishchenko, V.B. Korobov, A.P. Lisitsyn and V.P. Shevchenko, 2008. Study of the disperse composition of the near-water aerosol over the White Sea in the end of summer, 2007. Atmospheric and Oceanic Optics, 21:725-729.

Pol'kin, V.V., M.V. Panchenko, L.P. Golobokova, U.G. Filippova, T.V. Khodzher, A.P. Lisitzin and V.P. Shevchenko, 2011. Aerosols in the marine boundary layer over the White and Kara seas in August – September 2007. Meteorological and Geophysical Researches, pp. 199-214. Paulsen, Moscow (in Russian).

Prinn, R.G., R.F. Weiss, B.R. Miller, J. Huang, F.N. Alyea, D.M. Cunnold, P.J. Fraser, D.E. Hartley and P.G. Simmonds, 1995. Atmospheric trends and lifetime of CH_3CCl_3 and global OH concentrations. Science, 269:187-189.

Quinn, P.K. and T.S. Bates, 2005. Regional aerosol properties: comparisons from ACE 1, ACE 2, Aerosols99, INDOEX, ACE Asia, TARFOX, and NEAQS. Journal of Geophysical Research, 110:D14202.

Quinn, P.K., G. Shaw, E. Andrews, E.G. Dutton, T. Ruoho-Airola and S.L. Gong, 2007. Arctic haze: Current trends and knowledge gaps. Tellus, 59B:99-114.

Quinn, P.K., T.S. Bates, E. Baum, N. Doubleday, A.M. Fiore, M. Flanner, A. Fridlind, T.J. Garrett, D. Koch, S. Menon, D. Shindell, A. Stohl and S.G. Warren, 2008. Short-lived pollutants in the Arctic: their climate impact and possible mitigation strategies. Atmospheric Chemistry and Physics, 8:1723-1735.

Quinn, P.K., T.S. Bates, K. Schulz and G.E. Shaw, 2009. Decadal trends in aerosol composition at Barrow, Alaska: 1976 – 2008. Atmospheric Chemistry and Physics, 9:8883-8888.

Ramanathan, V. and G. Carmichael, 2008. Global and regional climate changes due to black carbon. Nature Geoscience, 1:221-227.

Randerson, J.T., H. Lui, M.G. Flanner and 14 others, 2006. The impact of boreal forest fire on climate warming. Science, 314:1130-1132.

Rasch, P.J., M.C. Barth, J.T. Kiehl, S.E. Schwartz and C.M. Benkovitz, 2000. A description of the global sulfur cycle and its controlling processes in the National Center for Atmospheric Research Community Climate Model. Journal of Geophysical Research, 105:1367-1385.

Rasch, P.J., W.D. Collins and B.E. Eaton, 2001. Understanding the Indian Ocean Experiment (INDOEX) aerosol distributions with an aerosol assimilation. Journal of Geophysical Research, 106:7337-7355.

Rastigejev, Y., R. Park, M. Brenner and D. Jacob, 2010. Resolving intercontinental pollution plumes in global models of atmospheric transport. Journal of Geophysical Research, 115:D02302.

Rinne, J., J. Bäck and H. Hakola, 2009. Biogenic volatile organic compound emissions from the Eurasian taiga: current knowledge and future directions. Boreal Environment Research, 14:807-826.

Robock, A., 1983. Ice and snow feedbacks and the latitudinal and seasonal distribution of climate sensitivity. Journal of the Atmospheric Sciences, 40:986-997.

Roy, D.P., L. Boschetti, C.O. Justice and J. Ju, 2008. The collection 5 MODIS burned area product – Global evaluation by comparison with the MODIS active fire product. Remote Sensing of Environment, 112:3690-3707.

Rupp, T.S., A.M. Starfield, F.S. Chapin III and P. Duffy, 2002. Modeling the impact of black spruce on the fire regime of Alaskan boreal forest. Climatic Change, 55:213-233.

Rypdal, K., N. Rive, T.K. Berntsen, Z. Klimont, T.K. Mideksa, G. Myhre and R.B. Skeie, 2009. Costs and global impacts of black carbon abatement strategies. Tellus, 61B:625-641.

Sarofim, M.C., B.J. DeAngelo, D. Grano, D.L. Meitiv, L.W.H. Alnes, N. Rive, T. Berntsen, T.K. Mideksa, G. Myhre, R.B. Skeie, Z. Klimont, K.A. Weitz, A. Zapata, M.A. Bahner and B. Zaitchik, 2009. Current Policies, Emission Trends and Mitigation Options for Black Carbon in the Arctic Region. Draft White Paper by an Ad Hoc Working Group. Available at: www.iiasa.ac.at/rains/reports/DRAFTWhitePaper-BCArcticMitigation-280909.pdf

Schmid, H., L. Laskus, H.J. Abraham and 19 others, 2001. Results of the "carbon conference" international aerosol carbon round robin test stage 1. Atmospheric Environment, 35:2111-2121.

Schnaiter, M., M. Linke, O. Mohler, K.H. Naumann, H. Saathoff, R. Wagner, U. Schurath and B. Wehner, 2005. Absorption amplification of black carbon internally mixed with secondary organic aerosol. Journal of Geophysical Research, 110:D19204.

Schnell, R.C., 1984. Arctic haze and the Arctic Gas and Aerosol Sampling Program (AGASP). Geophysical Research Letters, 11:361-364.

Schnell, R.C. and W.E. Raatz, 1984. Vertical and Horizontal characteristics of Arctic haze during AGASP: Alaskan Arctic. Geophysical Research Letters, 11:369-372.

Schwarz, J.P., R.S. Gao, D.W. Fahey and 18 others, 2006. Single-particle measurement of mid latitude black carbon and light-scattering aerosols from the boundary layer to the lower stratosphere. Journal of Geophysical Research, 111:D16207.

Schwarz, J.P., R.S. Gao, J.R. Spackman and 13 others, 2008. Measurement of the mixing state, mass, and optical size of individual black carbon particles in urban and biomass burning emissions. Geophysical Research Letters, 35:L13810.

Serreze, M.C., M.M. Holland and J. Stroeve, 2007a. Perspectives on the Arctic's shrinking sea-ice cover. Science, 315:1533-1536.

Serreze, M.C., A.P. Barrett, A.G. Slater, M. Steele, J. Zhang and K.E. Trenberth, 2007b. The large-scale energy budget of the Arctic. Journal of Geophysical Research, 112:D11122.

Sharma, S., D. Lavoué, H. Cachier, L.A. Barrie and S.L. Gong, 2004. Long-term trends of the black carbon concentrations in the Canadian Arctic. Journal of Geophysical Research, 109:D15203.

Sharma, S., E. Andrews, L. Barrie, J. Ogren and D. Lavoué, 2006. Variations and sources of the equivalent black carbon in the high Arctic revealed by long-term observations at Alert and Barrow: 1989–2003. Journal of Geophysical Research, 111:D14208.

Shaw, G.E., 1986. Cloud condensation nuclei associated with Arctic Haze. Atmospheric Environment, 20:1453-1456.

Shaw, G.E. and K. Stamnes, 1980. Arctic haze: perturbation of the polar radiation budget. Annals of the New York Academy of Sciences, 338:533-539.

Shevchenko, V.P., N.V. Goryunova, A.N. Novigatsky, S.A. Popova, K.P. Koutsenogii, V.Yu. Kashchenko and A.S. Filippov, 2010. Distribution and composition of particulate matter in snow cover on ice in the Arctic. The International Polar Year Oslo Science Conference. Oslo, Norway, 6–12 June 2010. Abstract PS1-B.9.

Shindell, D., 2007. Local and remote contributions to Arctic warming. Geophysical Research Letters, 34:L14704.

Shindell, D. and G. Faluvegi, 2009. Climate response to regional radiative forcing during the twentieth century. Nature Geoscience, 2:294-300.

Shindell, D.T., M. Chin, F. Dentener and 31 others, 2008. A multi-model assessment of pollution transport to the Arctic. Atmospheric Chemistry and Physics, 8:5353-5372.

Shiraiwa, M., Y. Kondo, N. Moteki, N. Takegawa, L.K. Sahu, A. Takami, S. Hatakeyama, S. Yonemura and D.R. Blake, 2008. Radiative impact of mixing state of black carbon aerosol in Asian outflow. Journal of Geophysical Research, 113:D24210.

Skeie, R.B., T. Berntsen, G. Myhre, C.A. Pedersen, J. Ström, S. Gerland, J.A. Ogren, 2011. Black carbon in the atmosphere and snow, from pre-industrial times until present. Atmospheric Chemistry and Physics Discussions, 11:7469-7534.

Slowik, J.G., K. Stainken, P. Davidovits, L.R. Williams, J.T. Jayne, C.E. Kolb, D.R. Worsnop, Y. Rudich, P.F. DeCarlo and J.L. Jimenez, 2004. Particle morphology and density characterization by combined mobility and aerodynamic diameter measurements. Part 2: Application to combustion-generated soot aerosols as a function of fuel equivalence ratio. Aerosol Science and Technology, 38:1206-1222.

Smol, J.P., A.P. Wolfe, H.J.B. Birks and 23 others, 2005. Climate-driven regime shifts in the biological communities of Arctic lakes. Proceedings of the National Academy of Sciences, 102:4397-4402.

Sodemann, H., M. Pommier, S.R. Arnold and 12 others, 2010. Episodes of cross-polar transport in the Arctic troposphere during July 2008 as seen from models, satellite, and aircraft observations. Atmospheric Chemistry and Physics Discussions, 10:26361-26410.

Soja, A.J., W.R. Cofer, H.H. Shugart, A.I. Sukhinin, P.W. Stackhouse Jr., D.J. McRae and S.G. Conard, 2004. Estimating fire emissions and disparities in boreal Siberia (1998 – 2002). Journal of Geophysical Research, 109:D14S06.

Spackman, J.R., R.S. Gao, W.D. Neff, J.P. Schwarz, L.A. Watts, D.W. Fahey, J.S. Holloway, T.B. Ryerson, J. Peischl and C.A. Brock, 2010. Aircraft observations of enhancement and depletion of black carbon mass in the springtime Arctic. Atmospheric Chemistry and Physics, 10:9667-9680.

Stier, P., J.H. Seinfeld, S. Kinne, J. Feichter and O. Boucher, 2006. Impact of nonabsorbing anthropogenic aerosols on clear-sky atmospheric absorption. Journal of Geophysical Research, 111:D18201.

Stohl, A., 1998. Computation, accuracy and applications of trajectories - a review and bibliography. Atmospheric Environment, 32:947-966.

Stohl, A., 2006. Characteristics of atmospheric transport into the arctic troposphere. Journal of Geophysical Research, 111:D11306.

Stohl, A., E. Andrews, J.F. Burkhart and 15 others, 2006. Pan-arctic enhancements of light absorbing aerosol concentrations due to North American boreal forest fires during summer 2004. Journal of Geophysical Research, 111:D22214.

Stohl, A., T. Berg, J.F. Burkhart and 16 others, 2007. Arctic smoke - record high air pollution levels in the European Arctic due to agricultural fires in Eastern Europe. Atmospheric Chemistry and Physics, 7:511-534.

Stroeve, J.C., T. Markus, W.N. Meier and J. Miller, 2006. Recent changes in the Arctic melt season. Annals of Glaciology, 44:367-374.

Strunin, M.A., A.A. Postnov and M.Y. Mezrin, 1997. Meteorological potential for contamination of arctic troposphere: Boundary layer structure and turbulent diffusion characteristics. Atmospheric Research, 44:37-51.

Sundqvist, M.K., R.G. Björk and U. Molau, 2008. Establishment of boreal forest species in alpine dwarf-shrub heath in subarctic Sweden. Plant Ecology and Diversity, 1:67-75.

Swietlicki, E., H.C. Hansson, K. Hameri and 13 others, 2008. Hygroscopic properties of submicrometer atmospheric aerosol particles measured with H-TDMA instruments in various environments - a review. Tellus B, 60:432-469.

Textor, C., M. Schulz, S. Guibert and 36 others, 2007. The effect of harmonized emissions on aerosol properties in global models - an AeroCom experiment. Atmospheric Chemistry and Physics, 7:4489-4501.

Thonicke, K., A. Spessa, I.C. Prentice, S P. Harrison, L. Dong and C. Carmona-Moreno, 2010. The influence of vegetation, fire spread and fire behaviour on global biomass burning and trace gas emissions. Biogeosciences, 7:1991-2011.

Trenberth, K.E. and J.M. Caron, 2001. Estimates of meridional atmosphere and ocean heat transports. Journal of Climate, 14:3433-3443.

Tunved, P., H.-C. Hansson, V.-M. Kerminen, J. Ström, M. Dal Maso, H. Lihavainen, Y. Viisanen, P.P. Aalto, M. Komppula and M. Kulmala, 2006. High natural aerosol loading over boreal forests. Science, 312:261-263.

Turpin, B.J., R.A. Cary and J.J. Huntzicker, 1990. An in-situ time resolved analyzer for aerosol organic and elemental carbon. Aerosol Science and Technology, 12:161-171.

Turquety, S., J.A. Logan, D.J. Jacob, R.C. Hudman, F.Y. Leung, C.L. Heald, R.M. Yantosca, S. Wu, L.K. Emmons, D.P. Edwards and G.W Sachse, 2007. Inventory of boreal fire emissions for North America in 2004: Importance of peat burning and pyroconvective injection. Journal of Geophysical Research, 112:D12S03.

Twomey, S., 1977. The influence of pollution on the shortwave albedo of clouds. Journal of Atmospheric Sciences, 34:1149-1152.

Van der Werf, G., J.T. Randerson, L. Giglio, G.J. Collatz, P.S. Kasibhatla and A.F. Arellano Jr., 2006. Interannual variability in global biomass burning emissions from 1997 to 2004. Atmospheric Chemistry and Physics, 6:3423-3441.

Van der Werf, G., J.T. Randerson, L. Giglio, G.J. Collatz, M. Mu, P.S. Kasibhatla, D.C. Morton, R.S. DeFries, Y. Jin and T.T. van Leeuwen, 2010. Global fire emissions and the contribution of deforestation, savanna, forest, agricultural, and peat fires (1997-2009). Atmospheric Chemistry and Physics Discussions, 10:16153-16230.

Vestreng, V., E. Økstad and R. Kallenborn, 2009. Climate influencing emissions, scenarios and mitigation options at Svalbard. Klif report, TA 2552/2009.

Vignati, E., M. Karl, M. Krol, J. Wilson, P. Stier and F. Cavalli, 2010. Sources of uncertainties in modelling black carbon at the global scale. Atmospheric Chemistry and Physics, 10:2595-2611.

Virkkula, A., N.C. Ahlquist, D.S. Covert, W.P. Arnott, P.J. Sheridan, P.K. Quinn and D.J. Coffman, 2005. Modification, calibration, and a field test of an instrument for measuring light absorption by particles. Aerosol Science and Technology, 39:68-73.

Von Schneidemesser, E., J.J. Schauer, G.S.W. Hagler and M.H. Bergin, 2009. Concentrations and sources of carbonaceous aerosol in the atmosphere of Summit, Greenland. Atmospheric Environment, 43:4155-4162.

Walker, M.D., C.H. Wahren, R.D. Hollister and 24 others, 2006. Plant community responses to experimental warming across the tundra biome. Proceedings of the National Academy of Sciences, 103:1342-1346.

Warneke, C., R. Bahreini, J. Brioude and 14 others, 2009. Biomass burning in Siberia and Kazakhstan as an important source for haze over the Alaskan Arctic in April 2008. Geophysical Research Letters, 36:L02813.

Warneke, C., K.D. Froyd, J. Brioude and 13 others, 2010. An important contribution to springtime Arctic aerosol from biomass burning in Russia. Geophysical Research Letters, 37:L01801.

Warren, S. and W. Wiscombe, 1980. A model for the spectral albedo of snow. II: Snow containing atmospheric aerosols. Journal of the Atmospheric Sciences, 37:2734-2745.

Westerling, A.L., H.G. Hidalgo, D.R. Cayan and T.W. Swetnam, 2006. Warming and earlier spring increase western U.S. forest wildfire activity. Science, 313:940-943.

Winther, M. and O.-K. Nielsen, 2011. Technology dependent BC and OC emissions for Denmark, Greenland and the Faroe Islands calculated for the time period 1990-2030. Atmospheric Environment, 45:5880-5895.

Wiscombe, W.J. and S.G. Warren, 1980. A model for the spectral albedo of snow. I: Pure snow. Journal of the Atmospheric Sciences, 37:2712-2733.

Wuebbles, D.J. and K. Hayhoe, 2002. Atmospheric methane and global change. Earth-Science Reviews, 57:177-210.

Young, P.J., A. Arneth, G. Schurgers, G. Zeng and J. Pyle, 2009. The CO_2 inhibition of terrestrial isoprene emission significantly affects future ozone projections. Atmospheric Chemistry and Physics, 9:2793-2803.

Zarzycki, C.M. and T.C. Bond, 2010. How much can the vertical distribution of black carbon affect its global direct radiative forcing? Geophysical Research Letters, 37:L20807.

Zhang, R., A.F. Khalizov, J. Pagels, D. Zhang, H. Xue and P.H. McMurry, 2008. Variability in morphology, hygroscopicity, and optical properties of soot aerosols during atmospheric processing. Proceedings of the National Academy of Sciences, USA, 105:10291-10296.

Zwally, H.J., W. Abdalati, T. Herring, K. Larson, J. Saba and K. Steffen, 2002. Surface melt-induced acceleration of Greenland ice-sheet flow. Science, 297:218-222.

Abbreviations

ACIA	Arctic Climate Impact Assessment
ACTFSLCF	Arctic Council Task Force on Short-Lived Climate Forcers
AGASP	Arctic Gas and Aerosol Sampling Programs
AMAP	The Arctic Monitoring and Assessment Program
AO	Arctic Oscillation
ARCPAC	Aerosol, Radiation, and Cloud Processes affecting Arctic Climate, an IPY program
ARCTAS	Arctic Research of the Composition of the Troposphere from Aircraft and Satellites
BAU	Business-as-usual
BC	Black Carbon
BVOC	Biogenic volatile organic carbon
CAM	Community Atmosphere Model
CCM	Chemistry Climate Models
CNG	Compressed natural gas
CTM	Chemistry Transport Models
DEHM	Danish Eulerian Hemispheric Model
EC	Elemental carbon
ECMWF	European Center for Medium Range Weather Forecast
EDGAR	Emission Database for Global Atmospheric Research
ENSO	El Niño Southern Oscillation
GAINS	Greenhouse Gas and Air Pollution Interactions and Synergies model
GCM	Global Climate Model
GEIA	Global Emissions Inventory Activity
GFED	Global Fire Emission Database
GHG	Greenhouse gas
GISS	ModelE NASA-GISS GCM
IEA	International Energy Agency
IIASA	International Institute for Applied Systems Analysis
ISSW	Integrating-Sandwich/Integrating Sphere
IPCC	Intergovernmental Panel on Climate Change
IPY	International Polar Year
LNG	Liquefied natural gas
MAC	Mass Absorption Cross section
MARPOL	Marine Pollution
MFR	Maximum Feasible Reduction
MODIS	Moderate Resolution Imaging Spectroradiometer
NAO	North Atlantic Oscillation
NASA GISS	National Aeronautics and Space Administration Goddard Institute for Space Studies
NCAR	National Center for Atmospheric Research
CCSM	Community Climate System Model
NEP	Northeast Passage
NOAA	National Oceanic and Atmospheric Administration
NorESM	Norwegian Earth System Model
NSIDC	National Snow and Ice Data Center
NWP	Northwest Passage
OC	Organic Carbon
OECD	Organisation for Economic Co-operation and Development
PAS	Photoacoustic spectrometer
PD1	Present-day control simulation
PDO	Pacific Decadal Oscillation
POLARCAT	Polar Study using Aircraft, Remote Sensing, Surface Measurements and Models, of Climate, Chemistry, Aerosols, and Transport
PSAP	Particle Soot Absorption Photometer
pyro-Cbs	Pyro cumulonimbus clouds produced from large fires that produce deep convective columns
RCP	Representative Concentration Pathways
RF	Radiative forcing
ROW	"Rest Of the World" (i.e. regions outside the Arctic nations)
SLCF	Short-Lived Climate Forcers
SOA	Secondary organic aerosol
SP2	Single Particle Soot Photometer
SPEW	Special Pollutant Emission Wizard
TC	Total carbon (= OC + EC)
TM5 model	A 3D atmospheric chemistry-transport model
TOA	Top of the atmosphere
vd	Deposition velocity